The patterns and drivers of recent outlet glacier change in East Antarctica

MILES, ALBERT,WILLIAM,JOHN

Abstract

West Antarctica and Greenland have made substantial contributions to global sea level rise over the past two decades. In contrast, the East Antarctic Ice Sheet (EAIS) has largely been in balance or slightly gaining mass over the past two decades. This is consistent with the long-standing view that the EAIS is relatively immune to global warming. However, several recent reports have highlighted instabilities in the EAIS in the past, and some numerical models now predict near-future sea level contributions from the ice sheet, albeit with large uncertainties surrounding the rates of mass loss. Using primarily remote sensing methods, this thesis aims to determine spatial and temporal patterns of outlet glacier change in the EAIS and assess the drivers and mechanisms of any changes in their dynamics. In doing so, it will also explore the wider debate surrounding the potential vulnerability of the ice sheet in the coming decades to centuries.

Pan-ice sheet terminus mapping in 1974, 1990, 2000 and 2012 reveals significant decadal variability in the behaviour of the EAIS. The majority of outlet glaciers retreated between 1974 and 1990, before switching to a dominant advance phase from 1990-2000. This trend of outlet glacier advance largely continued between 2000 and 2012, with the exception of Wilkes Land, where 74% of glaciers retreated. It is hypothesized that this anomalous retreat is linked to a reduction in sea ice and associated impacts on ocean stratification.

A more detailed examination of six glaciers in Porpoise Bay, Wilkes Land, reveals that large simultaneous calving events in January 2007 and March 2016, totalling ~2,900 km^2 and 2,200 km^2, were driven by the break-up of the multi-year landfast sea ice which usually occupies Porpoise Bay. However, these break-up events were driven by contrasting mechanisms. The 2007 break-up event is linked to an exceptionally warm December 2005 weakening the band of multi-year sea ice prior to its eventual break-up in the following summer. Whereas, the 2016 event is linked to the terminus advance of Holmes (West) Glacier pushing the multi-year sea ice further into the open ocean, making it more vulnerable to break-up.

In order to examine how changes at the terminus of glaciers might impact on their inland velocity, this thesis then analyses Cook Glacier, which is a major outlet glacier which drains a large proportion of the Wilkes Subglacial Basin. Analysis of ice-front positon change from 1947-2017, glacier velocity from 1973-2017 and ice shelf thickness from 1994-2012, reveals dynamic instability in the recent past. Cook West Ice Shelf retreated to its grounding line between 1973 and 1989, resulting the doubling of its velocity. Cook East Ice Shelf did not show a similar retreat pattern, but its ice shelf thinned rapidly between

1998 and 2002, which coincided with an increase of its velocity of ~10%. This rapid thinning is linked to periodic intrusions of warm mCDW. If these intrusions become more persistent in the future, Cook Glacier has the potential to contribute to sea level rise in the future.

In a wider context the results from this thesis highlight some key issues which need to be considered when predicting the response of the EAIS to future climate warming: i) The sensitivity of the EAIS to decadal variations in climate. ii) The potential for future changes in the location and persistency of landfast sea ice to alter outlet glacier dynamics. iii) The potential for rapid thinning of those ice shelves with a low steady-state basal melt rate.

The patterns and drivers of recent outlet glacier change in East Antarctica

Bertie Miles

Thesis submitted for the degree of Doctor of Philosophy

Department of Geography

Durham University

July, 2017

Table of Contents

List of Tables

List of Figures

Declaration and statement of copyright

Bertie Miles

Acknowledgements

I would like to thank my supervisors Chris Stokes and Stewart Jamieson for providing help and support with this project. This is in addition to understanding my necessity to keep up to date with the BBC Sport page at regular intervals throughout the day and my dubious alarm clock.

I would also like to thank the European Space Agency and USGS Earth Resources Observations Science Centre for granting me access to the data required to complete this project. Additionally, I would also like to thank the DigitalGlobe Foundation for proving satellite imagery free of charge. I am grateful to M. van den Broke and F. Paolo for providing data and assistance on RACMO and ice shelf thickness changes respectively. I would also like to thank the many scientists from other institutions who have taken the time to provide input on conference presentations or papers.

Finally, I would like to thank all those connected with the Geography department for making this PhD highly enjoyable. In particular, I would like to thank all those who I have spent an estimated ~1,400 hours and consumed ~1,600 cups of tea with in the Manley Room throughout the course of this PhD, not to mention the GIS LAB. I would also like to thank my family for their continued support and showing interest. Although I am still not 100% sure they understand what an iceberg is, despite several explanations.

Chapter 1: Introduction and research aims

1.1 Research context

The Greenland (~7.3 m of sea level of equivalent: SLE), West Antarctic (~4.3 m SLE) and East Antarctic (~53 m SLE) Ice Sheets contain enough freshwater to raise global sea level by ~65 m. In recent decades there has been a shift in our understanding as to how these ice sheets will respond to a warming climate. The first IPCC report (1991) highlighted the potential instabilities of the Greenland (GrIS) and West Antarctic Ice Sheets (WAIS) over longer timescales, but suggested that they could only make minor contributions to global sea level on decadal timescales, and predicted that Antarctica as a whole would gain mass. Since then, there have been vast improvements in our understanding of past ice sheet behaviour (e.g. Young et al., 2011; Cook et al., 2014) and modern-day satellites have enabled ice-sheet-wide observations (e.g. Pritchard et al., 2009; Rignot et al., 2013). Taking this into account, the most recent IPCC report (2013) predicted that both Greenland and West Antarctica will make significant contributions (0.03 – 0.20 m) to global sea level over the coming decades and that there is potential for mass loss in some of the marine sectors of East Antarctica. Essentially, it is now certain that the Earths ice sheets will contribute to global sea level in future decades; but uncertainties still exist as to the rate of acceleration of mass loss from Greenland and West Antarctica, with by far the largest uncertainties for the East Antarctic Ice Sheet (EAIS). An example of this uncertainty is illustrated in numerical models which predict the future contribution of Antarctica (both WAIS and EAIS) to global sea level by 2100, where estimates range from 0.10 to 1.05 m (Golledge et al., 2015; Ritz et al., 2015; DeConto and Pollard, 2016). Given that an estimated 625 million people inhabit low lying coastal zones (Neumann et al., 2015), it is of undoubted societal interest to constrain model predictions of sea level rise.

Greenland was losing 263 ±30 Gt of ice per year for the period 2005 to 2010 (Shepherd et al., 2012) and there is a growing trend of acceleration (Howat et al., 2007), thinning (Pritchard et al., 2009) and retreat (Moon and Joughin, 2008) of its major outlet glaciers. This is thought to be driven by a combination of both atmospheric warming driving surface melt and oceanic-driven basal melt of its outlet glaciers (e.g. Rignot and Kanagaratnam, 2006; Holland et al., 2008). The WAIS is also out of balance and lost 102 ±18 Gt of ice per year for the period 2005 to 2010 (Shepherd et al., 2012). This is thought to be driven by incursions of warm modified Circumpolar Deep Water (mCDW) onto the continental shelves driving rapid basal melt. Because large sections of the WAIS are grounded below sea level there is the potential for marine ice sheet instability (e.g. Joughin et al., 2014) and

it could lead to rapid increases in ice discharge rates. It is near-certain that both of these ice sheets will continue to lose mass and accelerate throughout this century.

In contrast, the EAIS (Fig. 1.1) is thought to be in balance or slightly gaining mass (e.g. Shepherd et al., 2012; King et al., 2012), with snowfall-driven growth in Dronning Maud Land counteracting ocean-driven mass loss in Wilkes Land (King et al., 2012). The apparent lack of mass loss and dynamic change over recent years in comparison to the WAIS and GrIS, combined with some arguments for a stable EAIS during past warm periods (e.g. Barrett, 2013), suggests it could be relatively stable in a warming climate. On the other hand, there are large sections of the EAIS which are grounded well below sea level (Fretwell et al., 2013) and which are thought to be vulnerable to marine ice sheet instability, perhaps in a similar manner to the WAIS. This, combined with some studies reporting an unstable EAIS during past warm periods (e.g. Young et al., 2011; Cook et al., 2013), raises the prospect of instability in a warming climate and a potentially rapid sea level contribution. These competing ideas have led to large uncertainties surrounding the future behaviour of the EAIS. This thesis is primarily aimed at narrowing down some of these uncertainties by analysing recent changes in outlet glacier behaviour in the EAIS and the mechanisms driving any changes.

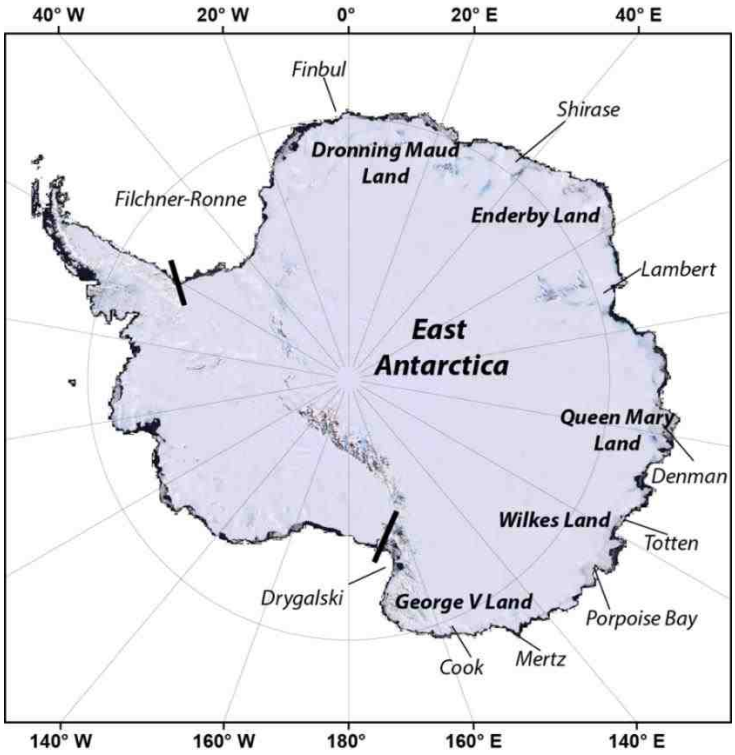

Figure 1.1: Landsat image mosaic (LIMA) of Antarctica showing the location of East Antarctica which is delineated by the two black lines.

1.2 Research aims and objectives

The overall aim of this thesis is to assess the patterns, drivers and mechanisms of recent outlet glacier change in East Antarctica, and how this relates to wider debates regarding the potential vulnerability of the ice sheet in the coming decades to centuries. To address this aim, this work will be conducted through three specific research objectives:

- To determine the spatial and temporal patterns of decadal-scale glacier change in East Antarctica and the potential drivers of those changes.

- To investigate the frontal position change of a smaller sample of glaciers at a higher sub-annual temporal resolution to understand the controls on their behaviour.

- To undertake a detailed study of a major East Antarctic outlet glacier in order to understand how frontal changes might impact on inland ice dynamics.

1.3 Thesis structure

Chapter 2 provides an overview of the past, present and future stability of the EAIS based on previously published literature. Following this, Chapter's 3-5 are composed of a series of research papers that have been published or prepared for publication in peer-reviewed journals. An introduction to each chapter is given below. The papers have been edited for consistency within the thesis. In some cases this resulted in supplementary information from the published manuscript being incorporated into the chapters and some light editing to ensure a consistent style throughout this thesis. Because the methods used are specific to each chapter, they are included throughout the thesis rather than as a separate section. Chapter 6 presents a wider discussion of the collective results of this research project and details how these results relate to the wider debate of the stability of the EAIS in a warming world.

1.3.1 Chapter 2

An overview of the links between past, present and future changes in the East Antarctic Ice Sheet

This chapter provides an overview of the past, present and future stability of the EAIS. It begins by exploring the debate regarding the stability of the EAIS during warm periods of

the Pliocene. It then goes on to provide an overview of recent ice-sheet wide observations of ice sheet dynamics, before examining the predicted sea-level contributions from the EAIS in the coming decades and centuries. It concludes by highlighting some key uncertainties, which are limiting the accuracy of predictions of the ice sheets future behaviour.

1.3.2 Chapter 3

*Miles, B.W.J., Stokes, C.R. & Jamieson, S.S.R. (2016). Pan–ice-sheet glacier terminus change in East Antarctica reveals sensitivity of Wilkes Land to sea ice changes. Science Advances **2**(5): e1501350.*

The dynamics of ocean-terminating outlet glaciers are an important component of ice sheet mass balance. This paper uses satellite imagery over the past 40 years to compile an approximately decadal record of outlet glacier terminus position change around the entire EAIS marine margin. The majority of outlet glaciers retreated during the period 1974-1990, before switching to advance in every drainage basin during the two most recent decades: 1990-2000 and 2000-2012. The only exception to this trend was in Wilkes Land, where the majority of glaciers (74%) retreated between 2000 and 2012. It is hypothesized that this anomalous retreat is linked to a reduction in sea ice and associated impacts upon ocean stratification, which increases the incursion of warm deep water towards glacier termini. Because Wilkes Land overlies a large marine basin, it raises the possibility of a future sea level contribution from this sector of East Antarctica.

In this paper, BWJM undertook the data collection and analysis; wrote the manuscript; and drew the figures. All authors contributed ideas and edited the text. The paper has been published in *Science Advances* and the supplementary information from that paper has been incorporated into the main text of this thesis.

1.3.3 Chapter 4

Miles, B.W.J., Stokes, C.R. & Jamieson, S.S.R. 2017. Simultaneous disintegration of outlet glaciers in Porpoise Bay (Wilkes Land), East Antarctica, driven by sea ice break-up. Cryosphere, 10.5194/tc-11-427- 2017.

This chapter builds on the results of Chapter 3 which pinpointed Wilkes Land as the only major drainage basin where most glaciers were retreating. The paper uses ENVISAT ASAR wide swath mode imagery to investigate monthly glacier terminus change across six marine-terminating outlet glaciers in Porpoise Bay (-76°S, 128°E), Wilkes Land, between November 2002 and March 2012. This reveals a large near-simultaneous calving event in January 2007, resulting in a total of ~2,900 km^2 of ice being removed from glacier tongues. It also reports on the start of a similar large near-simultaneous calving event in March 2016. The observations suggest that both of these large calving events were driven by the break-up of the multi-year sea ice which usually occupies Porpoise Bay. In the context of predicted future warming and the sensitivity of sea ice to changes in climate, these results highlight the importance of interactions between landfast sea ice and glacier tongue stability in East Antarctica.

In this paper, BWJM undertook the data collection and analysis; wrote the manuscript; and drew the figures. All authors contributed ideas and edited the text. The paper has been published in *The Cryosphere*.

1.3.4 Chapter 5

Miles, B.W.J., Stokes, C.R. & Jamieson, S.S.R. 2017. Dynamic instabilities at the Cook Glacier in the recent past. To be submitted

Cook Glacier drains a large proportion of the Wilkes Subglacial Basin, which may be vulnerable to marine ice sheet instability and may have made substantial sea level contributions during past warm periods (Cook et al., 2013). Through analysing glacier velocity from 1973-2017, together with the rates of ice shelf thickness changes from 1994-2012 and ice-front position from 1947-2017, it is shown that there have been dynamic instabilities in the recent past. More specifically, Cook West Ice Shelf retreated to near its present grounding line between 1974 and 1989, which was manifested a doubling in the velocity of the ice which the former ice shelf buttressed. The remaining and larger Cook East ice shelf rapidly thinned at 7.5 m yr^{-1} between 1998 and 2002, which is linked to a stepped increase in its velocity of ~10% during the same time period. These instabilities are linked to periodic intrusions of warm water, which have the potential to rapidly thin the Cook East Ice Shelf because of its low steady-state basal melt rate.

In this paper, BWJM undertook the data collection and analysis; wrote the manuscript; and drew the figures. All authors contributed ideas and edited the text. The paper will be prepared to be submitted to a peer-reviewed journal.

1.3.5 Chapter 6

This chapter presents a discussion of the key results presented in Chapters 3, 4 and 5. Section 6.1 discusses the importance of pan-ice sheet decadal variability in terminus in terms of the behaviour of the EAIS in the recent past and in the future. This highlights the potential importance of including decadal variability in numerical models which predict future change in the EAIS. Section 6.2 provides a wider discussion into the importance of sea ice in driving changes in ice-front positon and highlights the importance of the response of landfast sea ice to predicted future warming. Section 6.3 discusses the potential for Cook Glacier to make sea level contributions in the future and argues that it's potential to thin rapidly prime candidate for future sea level contributions. This chapter is concluded by outlining some future research priorities (section 6.4).

1.3.6. Chapter 7

The thesis ends with a concise chapter on the key conclusions.

Chapter 2: An overview of the links between past, present and future changes in the East Antarctic Ice Sheet (EAIS)

2.1 Introduction

The EAIS is the world's largest ice sheet and contains enough ice to raise global sea levels by 53 m (Fretwell et al., 2013). This is in comparison to the much smaller Greenland and West Antarctic Ice Sheets which have a sea level potential of 7.3 m (Bamber et al., 2013) and 4.3 m (Fretwell et al., 2013), respectively. Despite being much larger, the EAIS has received comparatively less scientific interest than Greenland and West Antarctica, with both of these ice sheets receiving over double the amount of peer-reviewed scientific articles since 2000 in comparison to the EAIS (Fig. 2.1). This can be attributed to relatively simpler logistics of undertaking field studies in Greenland and, to an extent, West Antarctica, in contrast to the more remote EAIS; along with the traditional view that the EAIS was stable and largely insensitive to predicted future warming (e.g. Sugden et al., 1993; Denton et al., 1993). However, several recent studies have suggested that the EAIS is more vulnerable than previously recognised (e.g. Pritchard et al., 2009; Miles et al., 2013; Rignot et al., 2013; Mengel and Levermann, 2014; Li et al., 2015; Rintoul et al., 2016), and improvements in numerical modelling, geophysical techniques, and remote sensing now suggest that the EAIS is likely to contribute to future sea level rise from decadal to centennial timescales, albeit with large uncertainties (e.g. Ritz et al., 2015; Golledge et al., 2015; DeConto and Pollard, 2016).

This review explores the reasoning behind the initial consensus of a stable EAIS and how this has evolved towards the view that the EAIS marine basins could make significant contributions to global sea level in the context of future warming. First, the marine ice sheet instability hypothesis and its potential role in the EAIS is explored (Section 2.2), before reviewing the debate regarding the stability of EAIS during past warm periods (Section 2.3). The chapter then reviews present-day changes in the ice sheet in terms of mass balance and changes in the extent and thickness of the floating ice shelves (Section 2.4). Predictions of future sea level contributions from the EAIS are then examined (Section 2.5), before highlighting some key research priorities which are needed to constrain future predictions (Section 2.6).

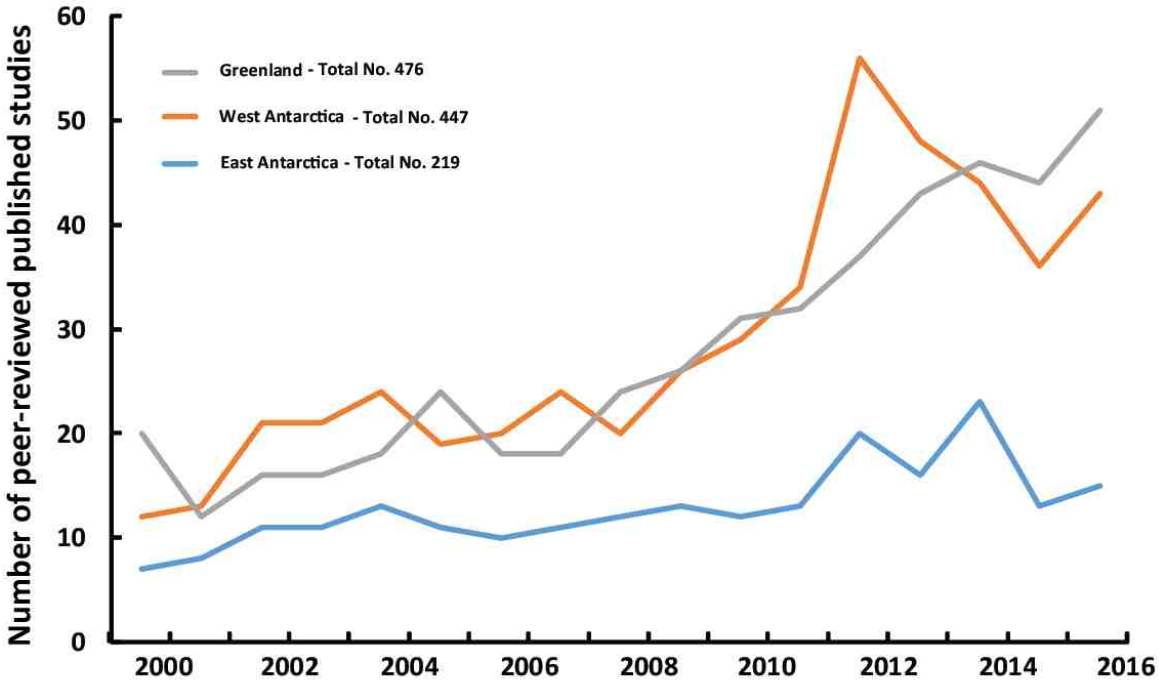

Figure 2.1: Number of peer-reviewed published studies per year related to the Greenland, West Antarctic and East Antarctic ice sheets. Note West Antarctica also includes studies related to the Antarctic Peninsula. Search Criteria: all articles must include at least one of the following words in the title 'Glacier(s)', 'Ice Shelf', 'Velocity', 'Dynamic'; in addition to a word relating to Greenland (e.g. Jakobshavn, Hellheim, Greenland, etc.), West Antarctica (e.g. West Antarctica, Pine Island, Thwaites, etc.) or East Antarctica (e.g. East Antarctica, Totten, Dronning Maud, etc.). All searchers were performed in the Web of Science database in April, 2017 and were manually checked to filter erroneous studies.

2.2 The marine ice sheet instability hypothesis

Ice which is grounded deep below sea level on a reverse bed slope is thought to be inherently vulnerable to even just a small perturbation in external forcing. This is because an initial grounding line retreat into deeper water creates an unstable and self-sustained feedback leading to increased ice discharge and inland thinning (Weertman, 1974; Mercer et al., 1978; Thomas, 1979). This means that there is a highly non-linear response to the initial forcing of grounding line retreat, resulting in the potential for rapid sea level contributions (Schoof et al., 2007; Jamieson et al., 2012; Jones et al., 2015). The configuration of the WAIS is thought to be particularly vulnerable to this process (Mercer et al., 1978; Schoof et al., 2007) and marine ice sheet instability may already be underway in the Thwaites Glacier basin (Joughin et al., 2014). However, there is a much bigger sea-level equivalent of 19 m of ice grounded well below present day sea level in East Antarctica (Fretwell et al., 2013), where the Aurora, Recovery and Wilkes marine basins

might also be vulnerable to marine ice sheet instability (Fig. 2.2). In particular, modelling studies from Mengel and Levermann (2014) have shown that the present day coastal configuration of the Wilkes subglacial basin is potentially vulnerable. They showed that the removal of a small amount of buttressing coastal ice resulted in the self-sustained discharge of the entire basin, eventually resulting in a 3-4 m sea level contribution over centennial to millennial time-scales. However, the magnitude of climate forcing required to initially destabilize coastal ice is unknown. One way to constrain this is too look at past warm periods and reconstruct the configuration the EAIS marine basins.

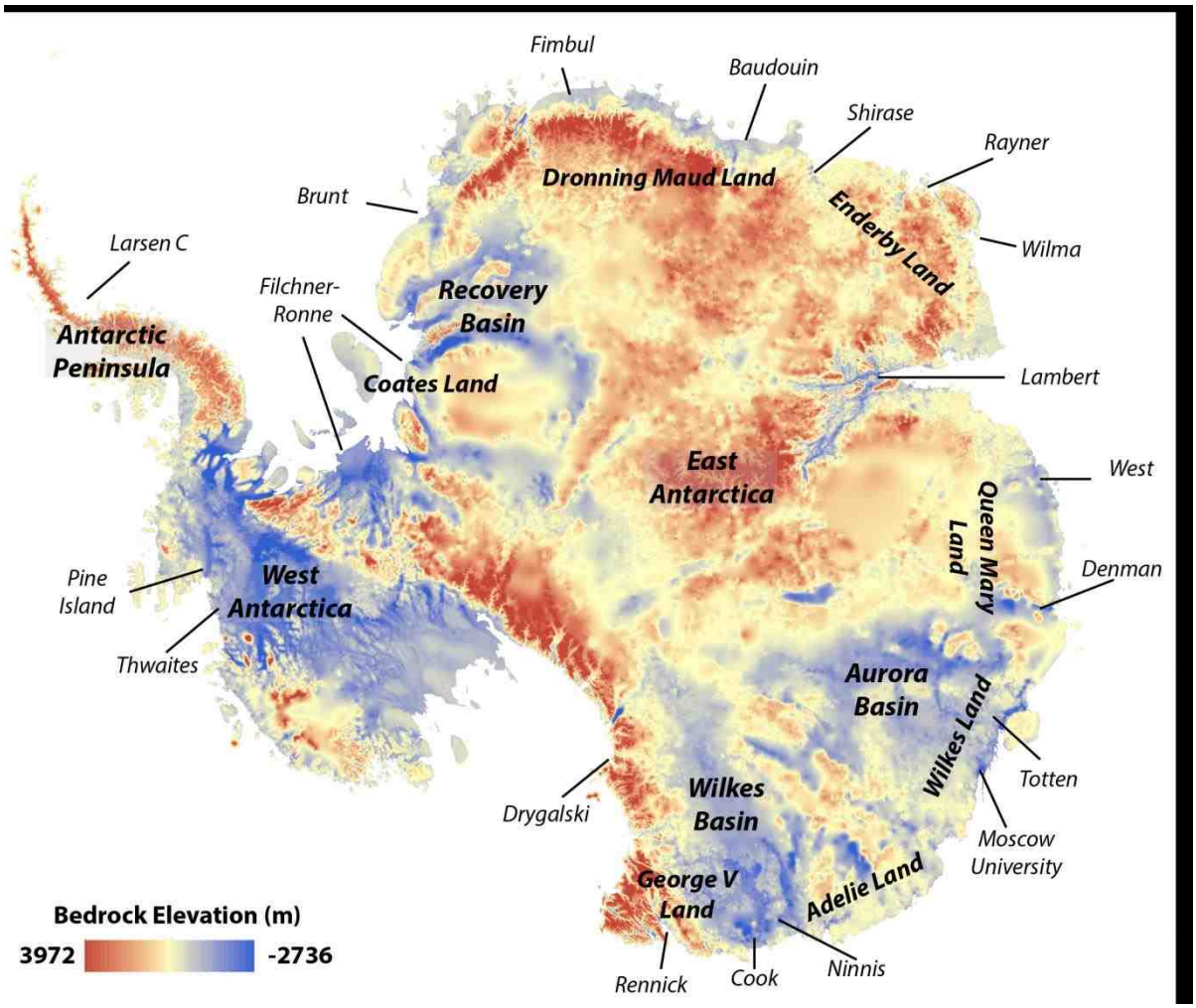

Figure 2.2: Bedmap2 bedrock elevations (Fretwell et al., 2013). Note the low lying topography in the Wilkes, Aurora and Recovery subglacial basins.

2.3 An unstable East Antarctic Ice Sheet during the Pliocene?

The potential instability of the major marine basins in the EAIS (Fig. 2.2 & 2.3) during the warm periods of the Pliocene (5.33 – 2.58 Million years ago) is of great scientific and societal interest. This is because these warm periods are thought to be appropriate

analogues for future climate conditions, with CO_2 values during the Pliocene similar to today's values (~400 ppm), but with temperatures a few degrees higher (Haywood et al., 2013). As such, the potential sea level contribution of the EAIS during these warm periods is important because it may represent our best analogue for future sea level change in the coming centuries. However, the stability of the EAIS has been a contentious issue (Miller and Mabin, 1998), with early arguments ranging from a stable, persistent and cold based EAIS (Sugden et al., 1993; Denton et al., 1993) to a highly variable and dynamic EAIS (Webb et al., 1984, 1991; Harwood et al., 1998).

This debate was originally focused on the origin and interpretation marine diatoms extracted from tillites in the Transantarctic Mountains. Webb et al. (1984) argued that these diatoms accumulated in subglacial basins of the EAIS, before ice-sheet advance subsequently transported the sediments to the Transantarctic Mountains. This suggested the presence of interior seaways within the EAIS and a major retreat of the Wilkes, Aurora and Recovery marine basins during at least one warm period of the Pliocene. However, the discovery of marine and non-marine diatoms in multiple regions in Antarctica, despite an absence of local sources, suggested that these diatoms were deposited by winds (Kellogg and Kellogg, 1996). Further examination of the deposits in the Transantarctic Mountains showed that most of the diatoms of Pliocene age were concentrated on the outer layers and not evenly distributed throughout the diamicton (Stroeven et al., 1996; 1998). This is consistent with these diatoms being deposited by aeolian transport (e.g. Kellogg and Kellogg, 1996) and challenged Webb et al.'s (1984) original hypothesis. However, whilst Webb et al.'s (1984) interpretation of the marine diatoms in the Transantarctic Mountains has been largely refuted, it does not rule out the possibility of major recession in some of East Antarctica's marine basins during the Pliocene (Scherer et al., 2016). Nevertheless, the refutation of this hypothesis, combined with the inability of early ice sheet models to simulate major EAIS retreat under realistic Pliocene conditions (e.g. Huybrechts, 1993; Pollard and DeConto, 2005), led to the early consensus of a stable EAIS during the Pliocene (e.g. Barrett, 2013).

Despite the traditional view of a stable EAIS, estimates of Pliocene sea levels vary between 15 m (Krantz, 1991) and 35 m (Dowsett and Cronin, 1990), and have been widely cited at ~25 m above present (e.g. Raymo et al., 2011; Miller et al., 2012). Because the complete melting of Greenland and West Antarctica's ice sheets could only account for ~12 m (Bamber et al., 2013; Fretwell et al., 2013), this would indicate that most sea level estimates for the Pliocene require a significant contribution from the EAIS. In addition,

recent evidence from the geological record has provided observational evidence of significant retreat of the Aurora and Wilkes subglacial basins. Williams et al. (2010) interpreted layers of ice-rafted debris (IRD) offshore of Lambert Glacier as evidence of large iceberg armadas dated during the Pliocene. Such large iceberg armadas are indicative of ice-sheet instability and, based on the geochemical signature of the IRD, Williams et al. (2010) suggested they reflected instability in the Wilkes Basin during the Pliocene. Cook et al. (2013) also analysed marine sediments recovered of the coast of Adelie Land. Similarly, the provenance of the detrital material suggested active erosion of continental bedrock with the Wilkes Basin during the Pliocene, which also indicated instability. Using geophysical techniques both Young et al. (2011) and Aitken et al. (2016) were also able to show evidence of landscape evolution within the Aurora basin that might indicate ice sheet configurations smaller than present. Young et al. (2011) identified a fjord landscape buried beneath the ice and revealed a succession of different ice-sheet configurations and suggested the switch between these configurations could have been driven by marine ice sheet instability. In addition, Aitken et al. (2016) interpreted evidence of ice-sheet erosion patterns as evidence for multiple large scale retreats of the Totten Glacier of up to 250 km from its present position. These studies are important because they provide indirect evidence of the vulnerability of the marine basins in the EAIS. This geological evidence can also act as a constraint in numerical models for the potential retreat of these glaciers in the future under climate forcing scenarios.

Early ice sheet models could not replicate the geologically-inferred retreat of subglacial basins without unrealistic atmospheric forcing's of ~20 °C (Huybrechts, 1993) or 4-9 x pre-industrial CO_2 concentrations (Pollard and DeConto, 2005). Models which also included some representation of ocean forcing were also unable to simulate significant EAIS grounding line retreat, even with substantial oceanic warming (e.g. Ritz et al., 2001; Huybrechts, 2002; Pollard and DeConto, 2009). However, more recent and more sophisticated models were able to produce significant retreat of the present day configuration of the Wilkes subglacial basin, driven by oceanic warming (Mengel and Levermann, 2014). Moreover, the inclusion of additional physical processes of surface melt induced hydro-fracture and ice-cliff failure (Pollard et al. 2015) have resulted in simulations of substantial retreat of EAIS marine basins, based on a warmer climate than present day conditions. Using a similar model, DeConto and Pollard (2016) were able to simulate major retreat of the EAIS's marine basins and an 11.3 m sea level contribution under Pliocene conditions (Fig. 2.3). This is important, because it represents the first time a numerical model was able to simulate a Pliocene based EAIS configuration, consistent

with both the geological record and sea-level reconstructions; and thereby supporting the notion of a dynamic EAIS during the Pliocene.

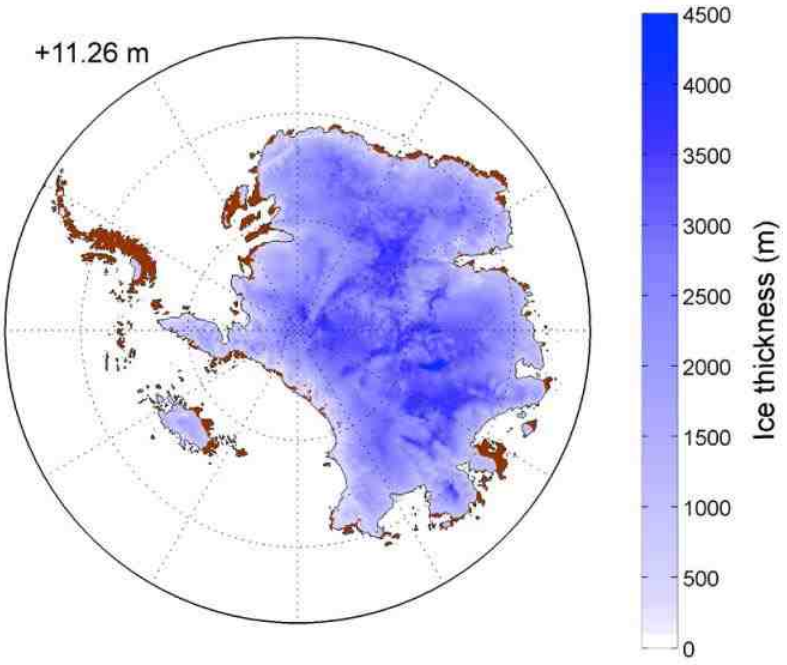

Figure 2.3: Simulated Pliocene ice sheet configuration (DeConto and Pollard, 2016). Note the significant retreat of the EAIS marine basins (e.g. compare with Fig. 2.2).

The retreated configuration of the EAIS during the Pliocene (e.g. Fig. 2.3) may also explain the presence of marine diatoms in the Transantarctic Mountains, the interpretation of which was the main focus of the original 'stable' versus 'dynamic' EAIS debate (e.g. Webb et al., 1984; Sugden et al., 1993). Atmospheric modelling suggests that prevailing mid-latitude winds transported diatoms from open seaways in the Aurora basin towards the Transantarctic Mountains (Scherer et al., 2016). This effectively unifies the original competing theories for the origin of the diatoms, in that they appear to indicate a vulnerable and dynamic EAIS (e.g. Webb et al., 1984), but they are also deposited by aeolian transport (e.g. Kellogg and Kellogg, 1996).

To summarise, recent evidence from the geological record and improvements in numerical modelling have challenged the long standing view of a stable EAIS to the point where its marine basins are considered vulnerable to both past and future warming. This has led to a renewed effort to quantify recent changes in the EAIS and the mechanisms driving these changes, which is important in the context of estimating future sea level contribution from the EAIS.

2.4 Recent measurements of the East Antarctic Ice Sheet

2.4.1 Mass balance

There are three principal methods of estimating ice sheet mass balance: (i) satellite altimetry (e.g. Davis et al., 2005; Shepherd et al., 2007; McMillan et al., 2014; Helm et al., 2014), (ii) gravimetry (e.g. King et al., 2012 (see Fig.4); Sasgen et al., 2013; Williams et al., 2014) and (iii) estimating the difference between ice sheet surface mass balance and glacier discharge (often referred to as the 'Input Output Method'; e.g. Rignot et al., 2011a). In attempting to reconcile all three of these methods, Shepherd et al. (2012) estimated an EAIS mass balance of 14 ±43 Gt yr^{-1} between 1992 and 2011 and 58 ±31 Gt yr^{-1} between 2005 and 2010. This estimate is consistent with recent independent studies using gravimetry, which estimated a positive mass balance trend between the early 2000s and early 2010s, varying from 26 ±13 to 97 ±13 (e.g. Sasgen et al., 2012; Williams et al., 2014). However, using satellite altimetry, Zwally et al. (2015) estimated a positive mass balance of 136 ±28 Gt yr^{-1} between 1992-2001 and 2003-2008. This was based on the assumption of dynamic thickening in response to a long-term increase in snowfall since the start of the Holocene in the ice sheet interior, and represents a substantially larger positive mass trend than other studies during a similar time period (e.g. Davis et al., 2005; Shepherd et al., 2007). Indeed, using both gravimetry and altimetry, Martin-Espanol et al. (2017) failed to reproduce the magnitude of mass gain of Zwally et al. (2015), even when taking into account dynamic thickening of the ice sheet interior. They concluded that in order to reproduce the values of Zwally et al. (2015), a GIA correction of more than an order of magnitude lower than the lowest published estimate would be required.

The recent slightly positive trend in EAIS mass balance is thought to have been driven by snowfall-driven growth (Davis et al., 2005; Shepherd et al., 2012), which has outweighed mass loss in the coastal sections of Wilkes and George V Land (e.g. Fig. 2.4). Snowfall-driven growth has largely been concentrated in Dronning Maud Laud (See Fig. 2.2 for location) where, in 2009, exceptional snowfall deposited 200 Gt in the first 6 months of the year. This represents a significant proportion of the total EAIS mass gain throughout the satellite era (Shepherd et al., 2012). It is uncertain if this snowfall anomaly was driven by atmospheric warming or falls within the bounds of natural variation, although a recent study confirmed that it was unprecedented since at least 1979 (Lenaerts et al., 2013).

Mass loss in Wilkes Land and George V Land has been driven by ice dynamics (e.g. Pritchard et al., 2009; Flament and Remy, 2012). Inland thinning and grounding line retreat

has been observed in Wilkes Land (Pritchard et al., 2009; Flament and Remy, 2012; Li et al., 2015), centred around the Totten Glacier which is currently losing mass (~7Gt yr^{-1} between 1989 and 2015; Li et al., 2016). There is also the possibility mass loss in George V Land, where Shepherd et al. (2007) observed inland thinning of the Cook Glacier. However, any such thinning may have abated in recent years (Shepherd et al., 2012; McMillan et al., 2014). It is notable that the regions of the EAIS which show potential dynamical mass loss are the coastal sectors of marine basins (Fig. 2.2). As such, they have the potential to increase their rate of mass loss rapidly (see Section 2.2). Indeed, more recent studies based on Cryosat-2 data between 2011 and 2014 estimate a decrease in the mass gain of the EAIS at -3 ±36 or -15 ±60 Gt yr^{-1} (McMillan et al., 2014; Helm et al., 2014) . This was largely attributed to increased mass loss in Wilkes Land, where intrusions of warm water are thought to be driving dynamic changes (e.g. Rintoul et al., 2016).

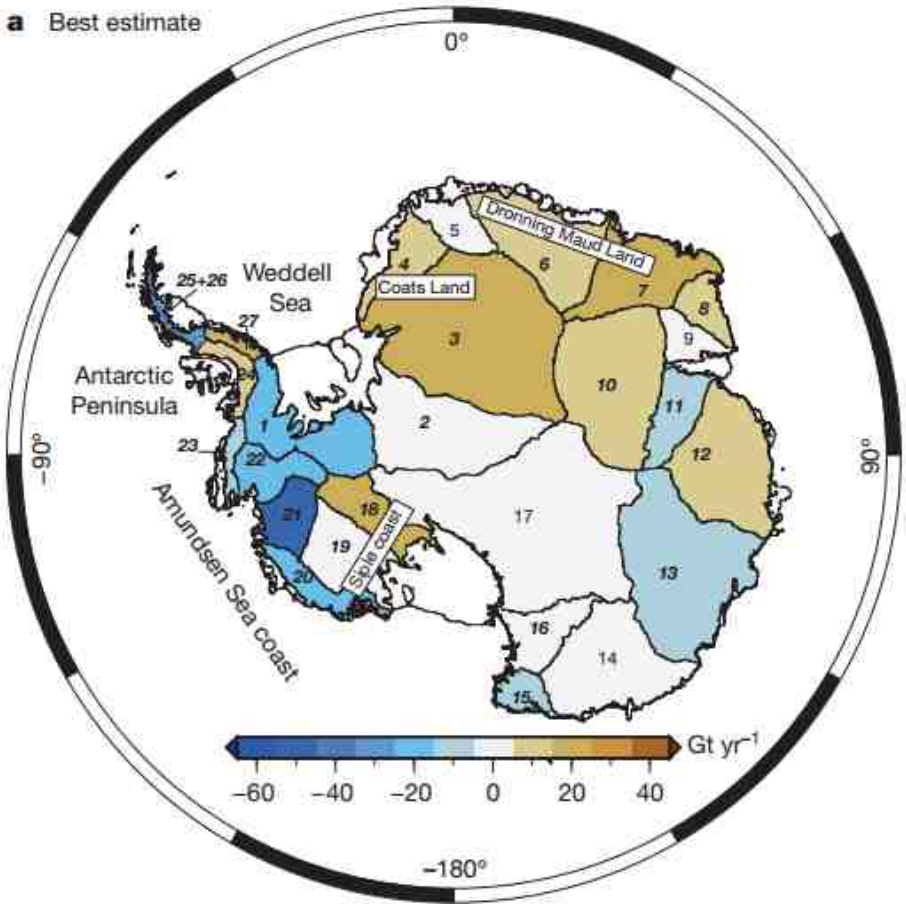

Figure 2.4: Mass change rates by drainage basin derived from Gravimetry (King et al., 2012). Note the mass gain in Droning Maud Land and the mass loss in Drainage basin 13 (Wilkes Land) and 15 (George V Land).

2.4.2 Ice shelves

The ice shelves and floating ice tongues which fringe East Antarctica are important because they can act to buttress ice flow from the ice sheet interior. Observed changes to the extent and thickness of these ice shelves and floating tongues in the WAIS and the Antarctic Peninsula has resulted in accelerated glacier discharge into the ocean (e.g. De Angelis and Skvarca, 2003; Scambos et al., 2004; Joughin et al., 2012). Paolo et al. (2015) calculated the volume change of Antarctic ice shelves between 1994 and 2012 (Fig. 2.5). Overall, ice shelves which fringed the EAIS slightly gained mass (i.e. thickened) between 1994 and 2003 before slightly losing mass between 2003 and 2012. However, there are strong spatial variations with strong thinning trends detected on Dibble (DIB) and Rennick (REN) Ice Shelves; whereas in Queen Maud Land there was a thickening trend, most notably in the Brunt (BRU), Fimbul (FIM), Baudouin (BAU), and Prince Harald (PRI) Ice Shelves, which thickened by up to 10 m per decade (Fig. 2.5). Moreover, in some of the major East Antarctic ice shelves there is substantial temporal variation in the rate of thickness change. For example, throughout the observational periods (1994-2012), there was little change in thickness of Cook (COO) Ice Shelf (-0.1 ± 3.9 m per decade). However, the local minimum in thickness change throughout these same periods was -22.9 ± 4 m per decade, which is comparable to the local minimum of some of the most rapidly thinning ice shelves in West Antarctica (e.g. Pine Island, 34.7 ± 4.7 m per decade). Therefore, even though some ice shelves may display little change in average ice shelf thickness over the long-term record, ice-climate-ocean interactions have the potential to drive rapid thinning at short time-scales.

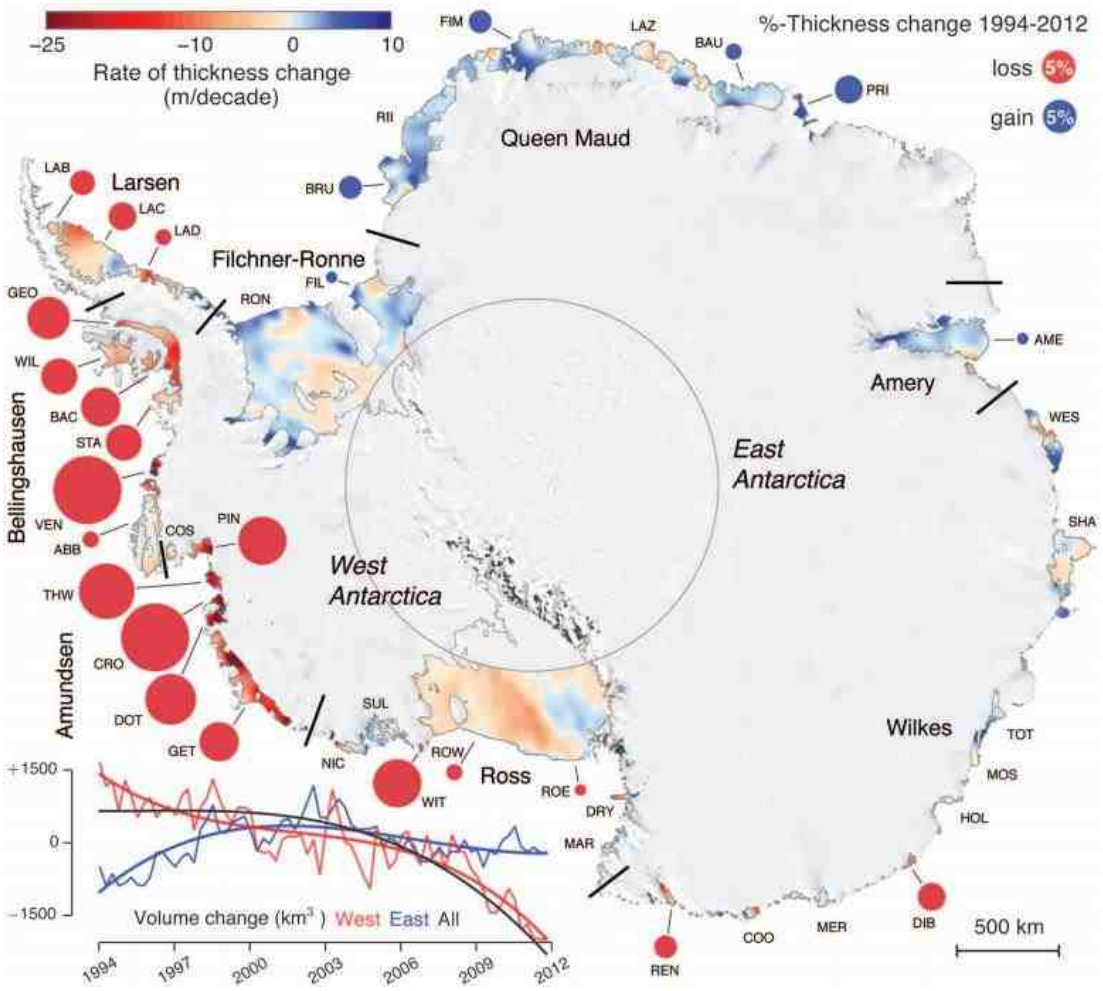

Figure 2.5: Rates of thickness change of Antarctic Ice Shelves (Paolo et al., 2015).

2.4.2.1 Basal melting of ice shelves

Ice shelves and ice tongues gain mass from the influx of ice across the grounding line, snowfall onto the ice shelf surface, and marine ice accretion beneath the ice shelf. They lose mass from basal melt, iceberg calving and surface melt. Antarctic-wide estimates suggest that the contribution of calving and basal melt are approximately equal (Depoorter et al., 2013), but perhaps with a slightly greater contribution from basal melt (Rignot et al., 2013), and with a negligible contribution from surface melt. However, these patterns are not spatially consistent, with the proportion of basal melt ranging between 10 and 90% of the annual mass loss for individual ice shelves or ice tongues (Fig. 2.6). This is important because basal mass loss is an important indicator of ice shelf vulnerability. The rate of basal melting is determined by the amount of relatively warm water able to reach ice shelf cavities. Three principle modes of basal melting are known (Silvano et al., 2016). Mode 1 is driven by brine rejection from sea ice formation that generates cold, saline water which

sinks to the seafloor forming Dense Shelf Water (DSW). The spread of DSW to deep grounding lines can influence basal melting because DSW is relatively warmer than the local freezing point, which decreases with depth and is typical in 'cold cavity' ice shelves e.g. Amery (Herraiz-Borreguero et al., 2016). The second mode is due to incursions of warm and relatively dense modified Circumpolar Deep Water (mCDW) spreading across the continental shelf and accessing ice shelf cavities; this mode is thought to drive the most rapid basal melting e.g. Amundsen Sea sector (Jenkins et al., 2010). The third mode is driven by atmospheric heating of surface waters during the summer months, which are then transported to the calving fronts of ice shelves (Silvano et al., 2016). This mechanism is particularly important in the Ronne-Filchner and Fimbul Ice Shelves (Makinson and Nicholls, 1999; Joughin and Padman, 2003). It is important to note that these modes of basal melt are not temporally or spatially consistent. For example, there are strong inter-annual variations in the melt rate of Pine Island (Dutrieux et al., 2014) and Totten Glacier (Khazendar et al., 2013), which have been linked to atmospheric forcing (Dutrieux et al., 2014) and sea ice conditions (Khazendar et al., 2013; Gwyther et al. 2014, Webber et al., 2017). Therefore, the interaction between the ocean and the atmospheric processes can also be important in determining variations in basal melt rates.

In East Antarctica, satellite-based estimates show high basal melt rates (>2 m yr^{-1} – 11 m yr^{-1}) in Wilkes Land (e.g. Totten, Moscow University, Shackleton, Dibble, Holmes and Vanderford Glaciers) that are comparable to basal melt rates in the Amundsen Sea sector (Fig. 2.6) of the WAIS (Depoorter et al., 2013; Rignot et al., 2013). These rates are likely to have been driven by mCDW which has been shown to occupy the continental shelf close to the Moscow University and Totten Glaciers (Silvano et al., 2017). Additionally, satellite-based estimates also show very high basal melt rates (>10 m yr^{-1}) on a selection of small glaciers in Enderby Land (e.g. Wilma, Edward VIII and Rayner Glaciers) and high rates (>2 m yr^{-1}) on the Drygalski, Rennick and Lille Glaciers in Victoria Land (Depoorter et al., 2013; Rignot et al., 2013), although there have been no direct oceanic observations from these regions. All other ice shelves in East Antarctica have basal melt rate estimates of <2 m yr^{-1} (Depoorter et al., 2013; Rignot et al., 2013). However, an important derivative of the basal melt equation from Rignot et al. (2013) and Depoorter et al. (2013) is the non-steady state changes in ice shelf thickness, of which both studies use data from 2003-08 derived from Pritchard et al. (2012). Because this record is short, it is possible that, for some ice shelves, the basal melt estimates do not represent the long-term trend or potential for melt, especially given the interannual/decadal variability of ice shelf thickness in the longer term eighteen year record of Paolo et al. (2015). This could result in a different

interpretation of the vulnerability/stability of some glaciers and interpretations of the mode of basal melt in regions with no subsurface ocean observations.

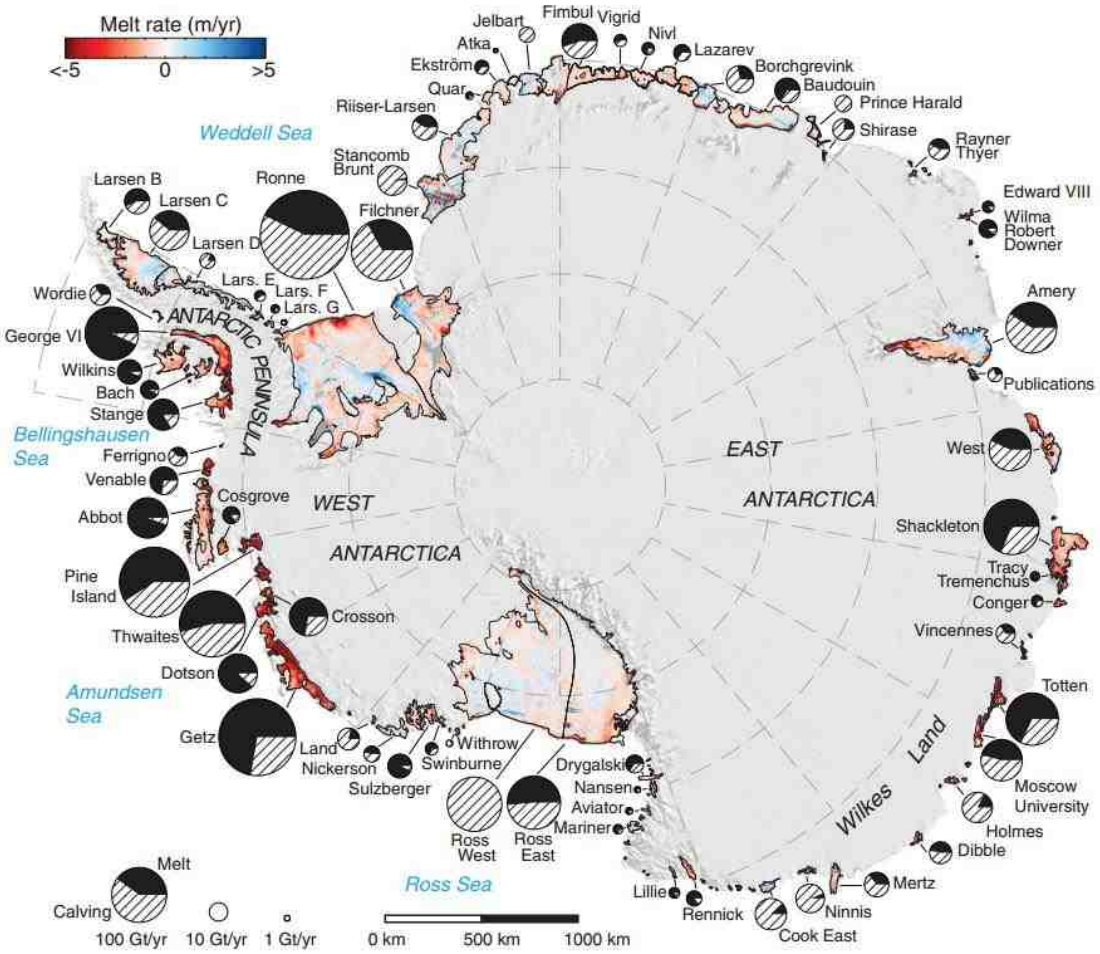

Figure 2.6: Basal melt rates for ice shelves in Antarctica (Rignot et al., 2013). Each ice shelf is colour coded based on its basal melt rate. The proportion of mass lost from either calving (hatched) or basal melt (black fill) is represented in each circle. Note the high basal melt rates in Wilkes Land in comparison to the rest of East Antarctica.

2.4.2.2 Ice shelf extent and calving

The extent of ice shelves and floating tongues is also important in determining the amount of buttressing provided to the ice upstream (Dupont and Alley, 2005; Gagliardini et al., 2010). In general, however, the floating ice closer to the grounding line exerts a greater amount of buttressing than floating ice at the seaward edge of ice shelves. Indeed, parts of some ice shelves and floating tongues are thought to be passive and can be removed without exerting any dynamic influence on ice flow upstream (Furst et al., 2016). Therefore, those ice shelves or floating tongues with a smaller proportion of passive ice are more vulnerable to terminus retreat than those ice shelves or floating tongues with a greater

proportion of passive ice. Furst et al. (2016) estimated the proportion of passive ice in ice shelves across Antarctica (Fig. 2.7). The eastern part of the Ross Sea sector has the lowest average proportion of passive ice at 14.7% (Fig. 2.7). The East Indian sector has an average passive ice proportion of 25.2%, although there are strong local variations with Totten and Moscow University having passive proportions of 4.2% and 6.7%, respectively; whereas Mertz Glacier has a passive proportion of 52.5% (Fig. 2.7). The West Indian and Eastern Weddell Sea sectors have a passive proportion of 19.6% and 20.5%, respectively.

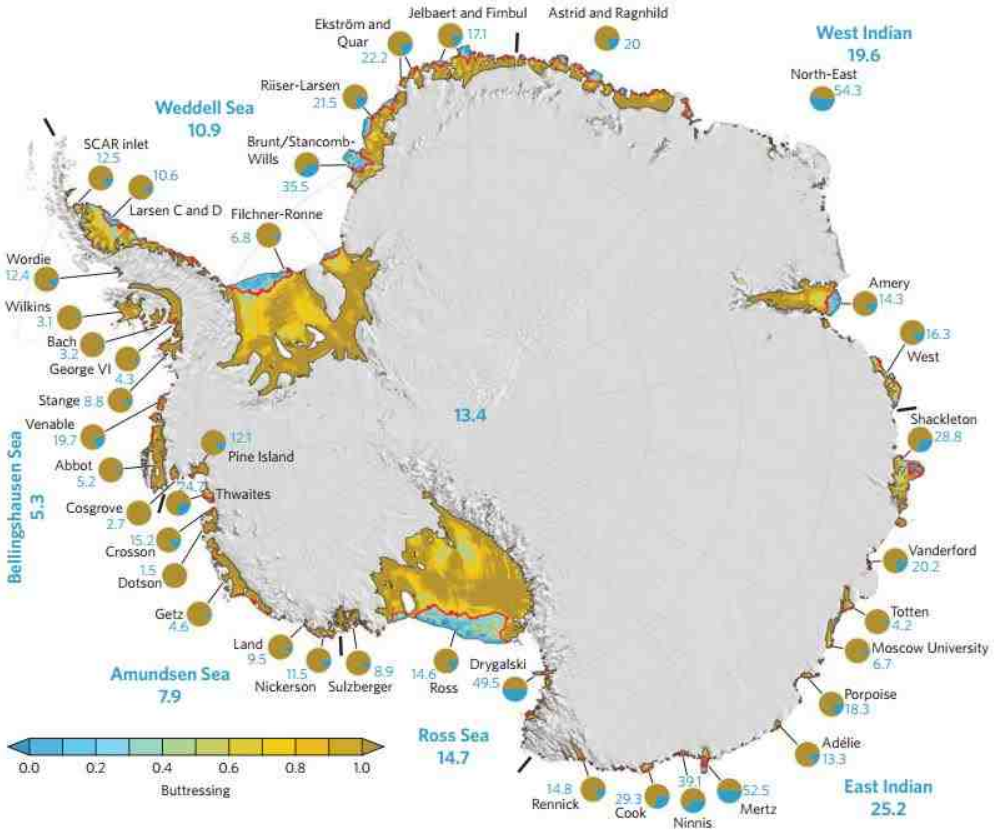

Figure 2.7: Maximum buttressing of Antarctic ice shelves, with the relative proportion of passive ice recorded for each ice shelf (Furst et al., 2016). Note the strong variability passive ice proportions in Wilkes Land.

The rate of iceberg calving is another important factor in determining the stability of floating ice shelves. Early studies used satellite imagery and aerial photography to analyse terminus position changes of ice shelves and ice tongues between the 1940s and the mid-1990s in a small selection of outlet glaciers in East Antarctica (Frezzotti, 1997; Frezzotti et al., 1998; Frezzotti and Polizzi, 2002). These results showed some evidence of cyclic behaviour and stochastic calving from ice shelves, but there were no obvious trends or change to their total area. A more comprehensive study by Miles et al. (2013) used satellite imagery to analyse the terminus position of all floating glaciers and ice shelves between

the Ross Ice Shelf and the Shackleton Ice Shelf at four epochs: 1974, 1990, 2000 and 2010. This revealed that 63% of glaciers retreated between 1974 and 1990 before switching to 72% advance from 1990-2000, and then 58% of glaciers advancing between 2000 and 2010 (Fig. 2.8). These trends were most pronounced along the warmer South Pacific coast, where Miles et al. (2013) linked statistically significant changes in glacier terminus position to significant changes in summer air temperatures. Furthermore, the decadal-scale switches in air temperature were linked to a rapid shift towards a positive phase of the Southern Annular Mode (SAM) in the 1990s, which may be linked to ozone depletion (Thompson and Solomon, 2002; Turner et al., 2009; Thompson et al., 2011). In contrast, there was little variation in median glacier terminus position between epochs in the Ross Sea, which coincides with much colder and negligible changes in air temperature, resulting in the conclusion that these glaciers are mostly stable (e.g. Miles et al., 2013; Lovell et al., 2017). The correlation between glacier terminus position and air temperatures is important because it suggests that despite some stochasticity, the rate of calving may be influenced by climate change. Moreover, the observed decadal-scale variability in terminus extent, suggests that the trends which are calculated using modern satellite techniques (e.g. altimetry or InSAR, which are typically limited to the mid-1990s or early 2000s), may not be representative longer-term outlet glacier/ice shelf behaviour. Despite this, there has yet to be a comprehensive assessment of terminus position change across the entire EAIS and the potential mechanisms driving any such changes, which partly motivates the work presented in this thesis.

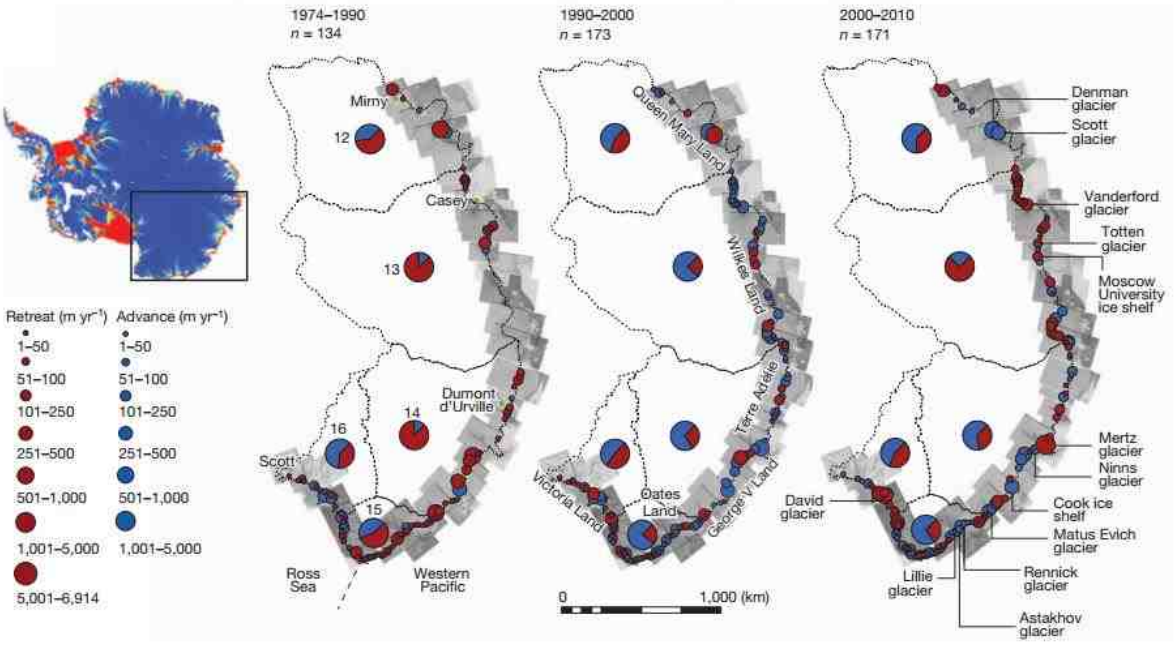

Figure 2.8: Spatial and temporal variations in EAIS glacier terminus position (Miles et al., 2013). The majority of glacier retreated between 1974 and 1990, before switching to advance in 1990-2000. This advance continued from 2000-2010, with the exception of glaciers in Wilkes Land (DB 13).

2.5 Predictions of future sea level contributions from East Antarctica

Recent predictions of the future sea level contribution from Antarctica all suggest that significant contributions are possible, but disagree on the timing and magnitude of these contributions (e.g. Ritz et al., 2015; Golledge et al., 2015; DeConto and Pollard, 2016). Ritz et al. (2015) estimated a maximum sea level contribution of the Antarctic Ice Sheet of 0.30 m by 2100 and 0.72 m by 2200 (Table 2.1a). Contributions from the Amundsen Sector dominate this sea level input, with small contributions from the Aurora (Totten and Moscow University) and Wilkes (Cook and Ninnis) subglacial basins, along with Dronning Maud Land (Fig. 2.9). They concluded that upper bound estimates from other models simulating sea-level contributions of up to 1 m by 2100 are implausible given our current understanding of physical mechanisms acting at ice sheet grounding lines. Ritz et al.'s (2015) predictions were estimated through statistical modelling of the probabilities of grounding line retreat which were calibrated using present-day observations of grounding line retreat and thinning, and projected ice shelf basal and surface melt rates. It is important to note, however, that these observations of surface thinning are based on just 5 years of data from Pritchard et al. (2009) and may not represent longer-term trends.

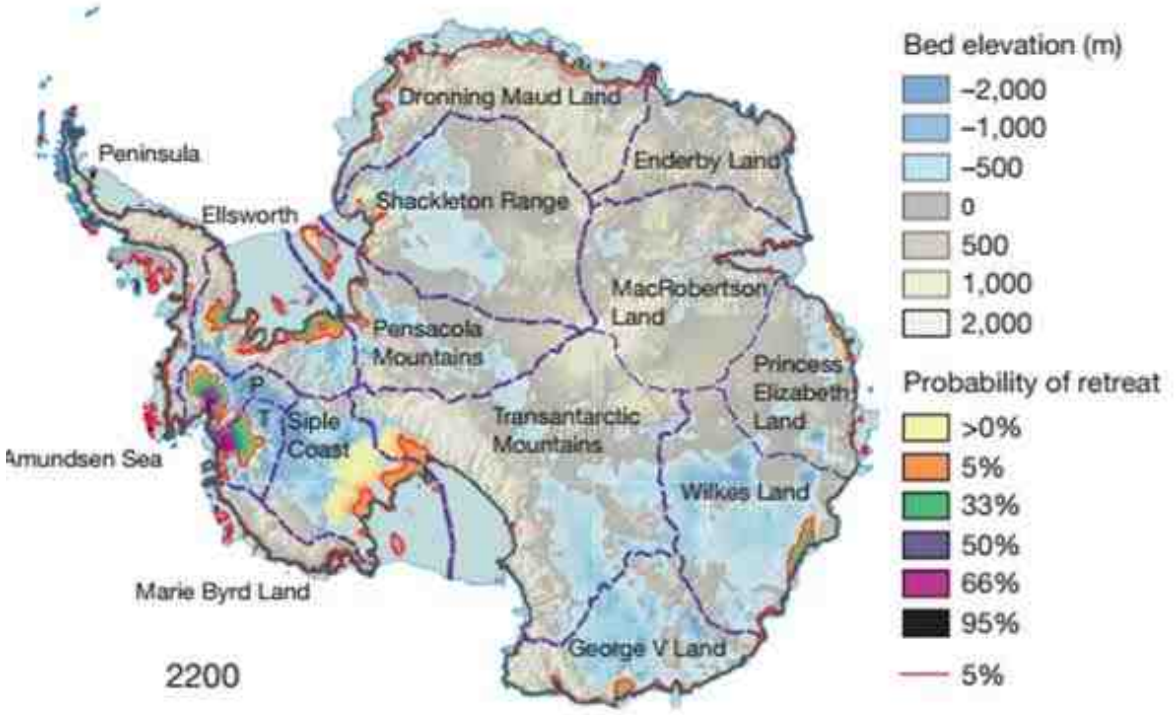

Figure 2.9: Probability density estimates of grounding line retreat at 2200 (Ritz et al., 2015). Red lines show 0.05 contour, which is an estimated 95% probability that retreat will be less extensive than this. Note the possibility of significant grounding line retreat in George V Land (Cook Glacier; Chapter 5) and Wilkes Land, along with the potential for a smaller retreat in Dronning Maud Land.

Golledge et al. (2015) used a lower resolution coupled ice-sheet/ice-shelf model to predict a sea level contribution from Antarctica of 0.1-0.39 m by 2100 and 0.6-3 m by 2300, with the bounds of the predictions determined by the IPCC's Representative Concentration Pathways (RCP) scenarios (Table 2.1b). This sea level contribution is driven by reducing the area of floating ice shelves, leading to a dynamic increase in ice discharge. Oceanic warming is the dominant driver in the short term, before atmospheric warming drives further retreat. As a result of these irreversible changes in ice shelf stability, it commits between 0.38 and 5.2 m of sea level contribution by the year 5000 (Fig. 2.10), with the upper bound estimate including large contributions from the Recovery, Aurora and Wilkes subglacial basins in East Antarctica. The large range in possible sea level contribution highlights the importance between the lower and upper bound emission scenarios. The aggressive mitigation scenario (RCP 2.5) results in little sea level contribution by the year

5000; whereas under the highest greenhouse gas emission scenario (RCP 8.5) Antarctic contributes significantly to global sea level by 5000.

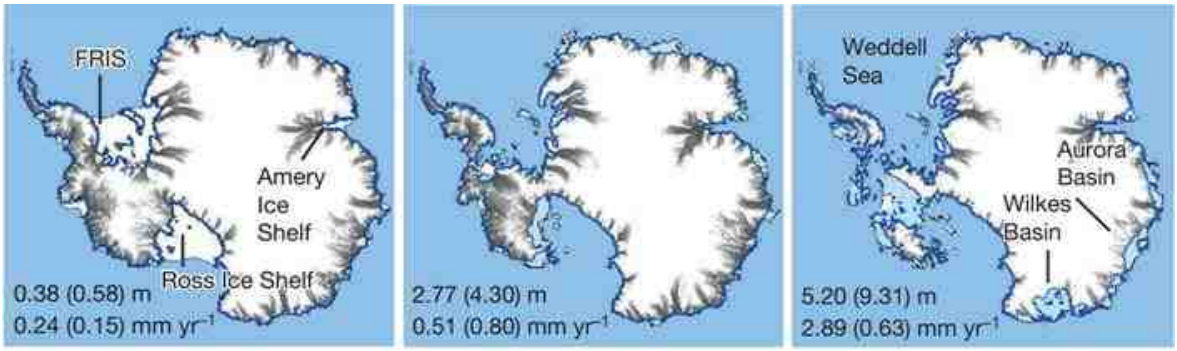

Figure 2.10: Total sea level commitment by 5000 based on emissions forced climate warming: left RCP 2.5, centre RCP 4.5 and right RCP 8.5. Magnitudes and rates of sea level contributions are shown on each panel (Golledge et al., 2015). Note large differences between the lower RCP scenario (left) and upper RCP scenario (right)

DeConto and Pollard (2016) used estimates of past sea level from the last interglacial and Pliocene period to constrain future sea level contributions of the Antarctic Ice Sheet. They use a model which includes processes related to surface melt induced hydrofracture and the structural collapse of marine ice cliffs. Their estimates of future sea-level contributions are strongly dependent on the RPC scenario used, with a smaller dependency on which Pliocene sea-level target is used as a constraint. By 2100, predictions range from 0.02 ± 0.13 m under low Pliocene sea level estimates (LP) RCP 2.5 to 1.05 ± 0.30 m under high Pliocene sea level estimates (HP) RCP 8.5, with these losses driven by oceanic warming. However, by 2500 they predict a 0.25 ± 0.23 m, 5.69 ± 1.00 m, and a 15.65 ± 2.00 m sea level contribution under the respective HP RCP 2.5, 4.5 and 8.5 scenarios (Fig. 2.11; Table 2.1c). Sea-level contributions up to 2100 are primarily driven by ocean warming, but after 2100 by the onset of atmospheric warming. Importantly, the moderate and high scenarios represent a significantly larger sea level contribution in a much shorter time scale than other studies (e.g. Ritz et al., 2015; Golledge et al., 2015). These RCP 4.5 and 8.5 scenario-based predictions result in large contributions from East Antarctica, with the initial retreat of the Wilkes Basin (~2200), followed by the Recovery (~2300) and Aurora (~2400) Basins.

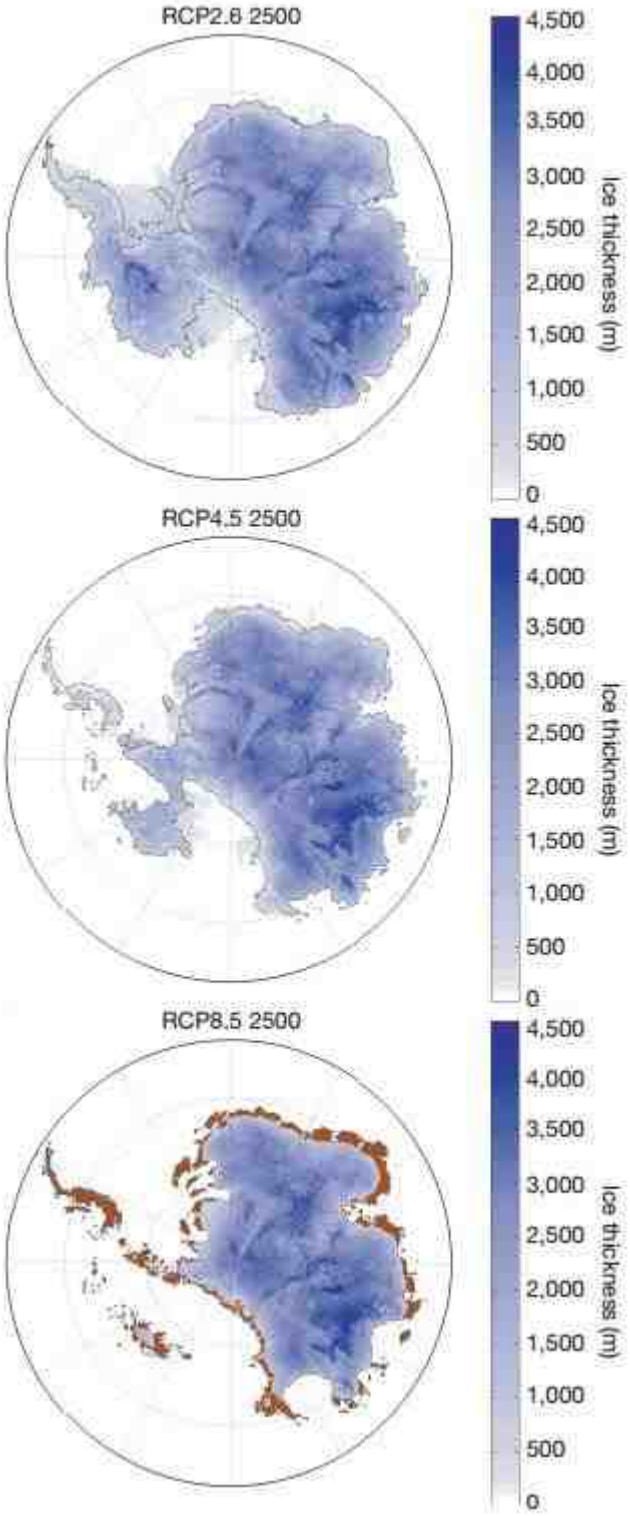

Figure 2.11: Simulated ice-sheet configuration at 2500 based on emissions scenarios: top: RCP 2.5, middle RCP 4.5, bottom RCP 8.5. Ice-free land surfaces are shown in brown. (DeConto and Pollard, 2016). Note the extensive retreats of the Aurora, Recovery and Wilkes Subglacial Basins under RCP 4.5 (middle) and RCP 8.5 (bottom).

Table 2.1: Predicted future Antarctic sea-level contributions (in metres). **A)** Predictions from Ritz et al. (2015) constrained from observations. **B)** Predictions from Golledge et al. (2015) using a coupled ice sheet/ice shelf model forced by RCP emissions scenarios. **C)** Predictions from DeConto and Pollard constrained with Pliocene sea-level estimates and forced by RCP emissions scenarios.

A	Ritz et al.	
Year	**2100**	**2200**
Contribution	0.30	0.72

B	Golledge et al.		
RCP	**2100**	**2300**	**5000**
2.5	0.10	0.23	0.58
4.5	0.19	0.95	4.30
8.5	0.39	2.96	9.31

C	DeConto and Pollard			
RCP	**2100(LP)**	**2100 (HP)**	**2500 (LP)**	**2500 (HP)**
2.5	0.02	0.11	0.19	0.25
4.5	0.26	0.49	3.97	5.69
8.5	0.64	1.05	13.11	15.65

Future predications of the sea level contribution of the EAIS can only be quantified from numerical models. Despite using different numerical modelling methods, recent studies all predict some contribution of the EAIS to future sea level change in the coming decades, centuries and millennia (Ritz et al., 2015; Golledge et al., 2015; DeConto and Pollard, 2016). However, there are large discrepancies on the timing and magnitude of any future sea level contributions from the EAIS. That said, most agree that oceanic warming is likely to drive mass loss on the short term (e.g. 2100-2300) before a switch to a dominant contribution of atmospheric warming in the long term. Predictions from numerical models are initially dependent on observations to provide initial calibration datasets, insight into the mechanisms driving glacier change, or the observed spatial pattern of recent glacier change. However, some of the mechanisms remain poorly understood and there are significant temporal gaps in the observations record, particularly in East Antarctica where there has been a comparative lack of studies to other regions e.g. West Antarctica and Greenland (Fig. 2.1). It is the relative interpretation of the uncertainties surrounding these mechanisms into numerical models which largely drives the current discrepancies in predicting the future sea level contribution from the EAIS. Future research priorities need

to be dedicated to narrowing down some of the key observational uncertainties, some of which are detailed in the next section.

2.6 Key uncertainties

2.6.1 Calving mechanisms and glacier frontal position change

Miles et al. (2013) linked decadal trends in outlet glacier terminus position along a section of the margin of the EAIS to climatic forcing. However, it remains unclear what mechanism(s) have driven these changes e.g. air temperatures or ocean temperatures. This is important in the context of predicting future changes in ice shelf area. It is also unclear if these trends persist across the whole ice sheet and whether the decadal trends also persist in velocity and mass balance. Furthermore, the rapid retreat of unstable ice cliffs has been proposed as a potentially important mechanism in the retreat of subglacial basins in East Antarctica (Pollard and DeConto, 2015). However, there is little observational evidence of the stability of such ice cliffs to constrain modelled retreat rates. In Greenland, sea ice melange is important in determining the stability of the calving front (e.g. Amundson et al., 2010; Todd and Christoffersen, 2014; Robel et al., 2017) and is therefore important in the long term evolution of glaciers. However, it is not clear if this is an important mechanism for East Antarctica where glacier tongues are typically not constrained by fjord walls.

2.6.2 Ice-ocean interactions

At present there are very few sub-surface ocean observations in the vicinity of outlet glaciers in East Antarctica. This results in large uncertainties regarding the type of water masses able to reach the grounding line of key outlet glaciers. This, in turn, is reflected in models where basal melt rates are thought to be most important in predicting sea level contributions, at least in the short term. Current satellite-based basal melt rates are a useful indicator of melt at a particular time period (e.g. Depoorter et al., 2013; Rignot et al., 2013), but they do not represent the spatial variation of basal melt rates across the ice shelf very well, particularly close to the grounding line where basal melt rates are likely to be significantly higher (e.g. Dutrieux et al., 2013; Berger et al., 2017). Furthermore, they do not currently capture temporal variations. There are also large uncertainties around the mechanisms driving basal melt. For example, sea ice production has been linked to variations in basal melt in Totten Glacier (Khazendar et al., 2013; Gwyther et al., 2014),

but it is unclear if this relationship persists elsewhere and how future changes in sea ice may influence basal melt rates.

There is little potential to increase basal melt rates for glaciers already floating in warm water (Timmermann and Hellmer, 2013), e.g. Totten Glacier. Instead, the greatest potential lies in those glaciers which currently have low steady state basal melt rates. The delivery of relatively warm water to these glaciers could drive rapid thinning and subsequent instabilities. This is predicted to happen in the Filcher-Ronne Ice Shelf by the end of the century (Hellmer et al., 2012). However, there are large uncertainties for other regions of East Antarctica. In short, without a better understanding of the present day ice-ocean interaction around East Antarctica it is very difficult to accurately predicted future basal melt rates.

2.6.3 Surface melt, hydrology and basal conditions

In Greenland, surface melt currently contributes to around 50% of the annual mass imbalance (Van den Broeke et al., 2009). The transport of surface melt towards the bed of the ice sheet also plays an important role in observed changes in outlet glacier dynamics at both seasonal (e.g. Moon et al., 2014) and decadal timescales (Tedstone et al., 2015). In East Antarctica, there is comparatively less melt, but there is emerging evidence of surface melt on the ice sheet (e.g. Phillips et al., 1998; Miles et al., 2013; Langley et al., 2016). However, it is not known if present-day surface melt influences ice dynamics and how important it is in determining ice shelf stability (e.g. Larsen B hydrofracture, Scambos et al., 2003), but there is evidence linking subglacial flood events to short-lived increases in glacier velocity through perturbing basal conditions (e.g. Stearns et al., 2008). Despite cooling over the past 50 years (Marshall et al., 2013), atmospheric warming is predicted in the EAIS over the coming decades to centuries with a corresponding increase in surface melt (Trusel et al., 2015). Without understanding how the present-day surface melt influence ice dynamics it is difficult represent predicted future increase in surface melt in numerical models.

2.6.4 Bed topography

The retreat of glaciers into overdeepenings can drive unstable non-linear retreat in relation to initial climatic forcing (Jamieson et al., 2012; Favier et al., 2014). For example, Jones et

al. (2015) showed that the rapid thinning of Mackay Glacier, East Antarctica, during the Holocene was driven by the retreat of its grounding line into deeper water, despite the absence of significant environmental forcing's. Therefore, in order to predict the behaviour of EAIS outlet glaciers in the future, high resolution bed topography is crucial. However, only 34% of cells in Bedmap2 currently have data within them, with some cells around 230 km away from the nearest data point (Fretwell et al., 2013). This could result in significant large and small scale features being unrepresented. To illustrate the potential for this, Jamieson et al. (2016) recently discovered an extensive 1 km deep canyon in Princess Elizabeth Land which extended over 1000 km. It is possible that uncertainties related to the elevation of the bedrock underneath Antarctica may be some of the largest sources of errors in terms of predicting future changes to the ice sheet.

2.7 Summary

Sea level reconstructions, geological records and models all point towards a major retreat of East Antarctica's marine basins during the Pliocene. This is important because climatic conditions during the warm periods of the Pliocene were similar to today or a near-future climate, suggesting a vulnerability of the EAIS in the coming decades to centuries. Presently, however, the mass balance of the EAIS indicates that the ice sheet is largely in balance or slightly gaining mass. However, it is notable that the regions which are currently losing mass in East Antarctica are concentrated in the vicinity of marine basins, which have the potential for marine ice sheet instability. Crucial to the future behaviour of the EAIS is the stability of its buttressing ice shelves. Observational records suggest that there is little overall change in ice shelf thickness, although some are thinning and there is evidence of considerable inter-annual variability in the rates of ice shelf thickness change. In addition, there remains large uncertainty around the potential rates of basal melt in regions where there have been no sub-surface ocean measurements. Fluctuations in ice front position of floating ice shelves can be forced by climate, but there is still some evidence of stochasticity. However, there are currently large uncertainties about the precise mechanisms driving ice front position change and how this would be reflected in a predicted warmer climate. As such, there are large uncertainties about the contribution to sea level change East Antarctica might make in the coming decades and centuries. Some of these uncertainties can be reduced by increasing are understanding of key physical processes and improving datasets through observations. With this in mind, this thesis aims

primarily address uncertainties surrounding calving mechanisms and glacier frontal change, and ice-ocean interactions, addressing the following research questions:

- What are the decadal spatial and temporal trends on outlet glacier frontal position and are any basins retreating and showing signs of instability?

- What processes are driving changes in the frontal position of outlet glaciers in East Antarctica?

- How are changes in the extent of floating ice shelves linked to glacier dynamics and what does this mean for long-term glacier stability?

Chapter 3: Pan-ice sheet glacier terminus change in East Antarctica reveals sensitivity of Wilkes Land to sea ice changes

Miles, B.W.J., Stokes, C.R. & Jamieson, S.S.R. (2016). Pan–ice-sheet glacier terminus change in East Antarctica reveals sensitivity of Wilkes Land to sea ice changes. *Science Advances* **2**(5): e1501350.

Abstract: The dynamics of ocean-terminating outlet glaciers are an important component of ice sheet mass balance. Using satellite imagery over the past 40 years we compile an approximately decadal record of outlet glacier terminus position change around the entire East Antarctic Ice Sheet (EAIS) marine margin. We find that the majority of outlet glaciers retreated during the period 1974-1990, before switching to advance in every drainage basin during the two most recent decades 1990-2000 and 2000-2012. The only exception to this trend was in Wilkes Land, where the majority of glaciers (74%) retreated between 2000 and 2012. We hypothesize that this anomalous retreat is linked to a reduction in sea ice and associated impacts upon ocean stratification, which increases the incursion of warm deep water towards glacier termini. Because Wilkes Land overlies a large marine basin, it raises the possibility of a future sea level contribution from this sector of East Antarctica.

3.1 Introduction

A growing body of evidence suggests that large marine basins in the EAIS have made significant contributions to sea level under periods of past climate when global CO_2 concentrations were comparable to today's values (Young et al., 2015; Cook et al., 2014; Dutton et al., 2015). Despite this, recent estimates suggest that the current mass balance of the EAIS has been in equilibrium or slightly positive over the past decade (King et al., 2012; Sasgen et al., 2013; Mcmillan et al., 2014). However, there are clear regional variations, with mass gained in Dronning Maud and Enderby Land, and a clear signal of mass loss in Wilkes Land (King et al., 2012; Sasgen et al., 2013; Mcmillan et al., 2014). This is significant because Wilkes Land overlies the Aurora subglacial basin. Due to its reverse bed slope and deep troughs (Young et al., 2011), this basin may have promoted a marine instability in the past (Cook et al., 2014), similar to that being proposed for West Antarctica (Hughes, 1981; Joughin et al., 2011).

Critical to marine ice sheet instability are ice shelves and the floating extension of outlet glaciers, which may act to buttress ice flow from the interior of the ice sheet (Dupont and

Alley, 2005). Recent modelling studies have suggested that changes in the extent the extent of floating termini are an important control on the stability of the EAIS (Pollard et al., 2015). However, despite recent reports of the heightened sensitivity of some East Antarctic outlet glaciers to changes in the ocean-climate system (Miles et al., 2013), there has yet to be a comprehensive analysis of outlet glacier terminus position changes around the whole East Antarctic ice sheet marine margin in relation to changes in mass balance and potential ocean or atmosphere forcings. We address this by compiling a pan-ice sheet record of outlet glacier terminus change over the past 40 years.

3.2 Methods

3.2.1 Glacier terminus mapping

We used Landsat imagery from the MS, TM and ETM+ satellites to map the terminus position of 176 outlet glaciers along the coast of East Antarctica across four approximate time steps: 1974, 1990, 2000 and 2012, stretching from Queen Mary Land to the Ronnie Ice shelf (Fig. 3.1). This adds 176 ocean terminating outlet glaciers to the previously published record of Miles et al. (2013). In total, 351 outlet glaciers, spanning the entire EAIS marine margin are included in our estimates. The change in glacier terminus position was calculated as the area change at each time step divided by the width, which was obtained by a reference box which approximately delineated the sides of the glacier (Moon et al., 2008). The accuracy of the mapping was limited by the co-registration of Landsat mosaics to the 2000 base image. This resulted in estimates of inaccuracies in mapping of ±60 m (2010), ±180 m (1990) and ±250 m (1974). These are sufficient for extracting the decadal trends we present in this study and we note that most changes lie well outside these uncertainties. To allow comparison to several recent studies reporting changes in mass balance (King et al., 2012; Sasgen et al., 2013; Mcmillan et al., 2014), we analyse terminus position change within each previously defined drainage basins (Zwalley et al., 2011).

3.2.2 EN4 subsurface ocean reanalysis

We use the EN4.0.2 subsurface ocean temperature objective analysis dataset (Good et al., 2013), available at the UK Meteorological Office Hadley Centre (http://www.metoffice.gov.uk/hadobs/en4/download-en4-0-2.html). The objective analysis

dataset covers the entire study period at a monthly basis and is available at a 1° x 1° spatial resolution, with data obtained from the WOD09, GTSPP, Argo and ASBO collections (Good et al., 2013). The mean temperature value of the 31 grid cells covering the continental shelf boundary in Wilkes Land (Fig. 3.4a) was calculated for each month during the study period (1974-2012) and at 26 different depths (5, 15, 25, 35, 45, 55, 66, 76, 87, 98, 109, 121, 135, 149, 165, 184, 207, 235, 270, 315, 372, 446, 540, 657, 799, 967). Uncertainty estimates for the EN4 dataset are included in Fig. 3.5 and are also available at the UK Meteorological Office Hadley Centre (http://www.metoffice.gov.uk/hadobs/en4/download-en4-0-2.html).

3.2.3 Sea ice

We use the Bootstrap sea ice concentrations derived from the Nimbus-7 satellite and DMSP satellites (Comiso, 2014) to calculate trends in the number of sea ice days per year around Antarctica (http://nsidc.org/data/nsidc-0079). The dataset offers near complete coverage of the Antarctic sea ice zone on a daily basis since July 1987 and every two days prior to this stretching back to October 1978 at a spatial resolution of 25x25 km. There are brief gaps in the dataset in August 1982 (4, 8 and 16 August) and 1984 (13 through 23 August). These have been interpolated where missing pixels were present (see http://nsidc.org/data/nsidc-0079).

In line with other studies (Massom et al., 2013) a sea ice day was classified as a grid cell with a sea ice concentration greater than 15%. The total number of sea ice days was calculated for each year during the sea ice season (April-October), with sea ice days doubled between April 1979 and July 1987 to account for the two day temporal resolution of the satellites during that period. The mean number of sea ice days per year for each epoch was calculated before calculation the difference in sea ice days between epochs e.g. Fig 3.6.

3.2.4 Climate data

Monthly mean surface air temperature records from Casey Station were extracted from the SCAR Met reader project (https://legacy.bas.ac.uk/met/READER/). In addition, mean

monthly 0.25º ERA Interim (Dee et al., 2011) 2 m air temperature and 10 m meridional and zonal wind (http://apps.ecmwf.int/datasets/data/interim-full-moda/levtype=sfc/) from 1979 – 2012 was extracted from the Wilkes Land coastline. For the purpose of this study, we define the Wilkes Land coastline as a shapefile consisting of the coastline of DB13 with a 25 km buffer.

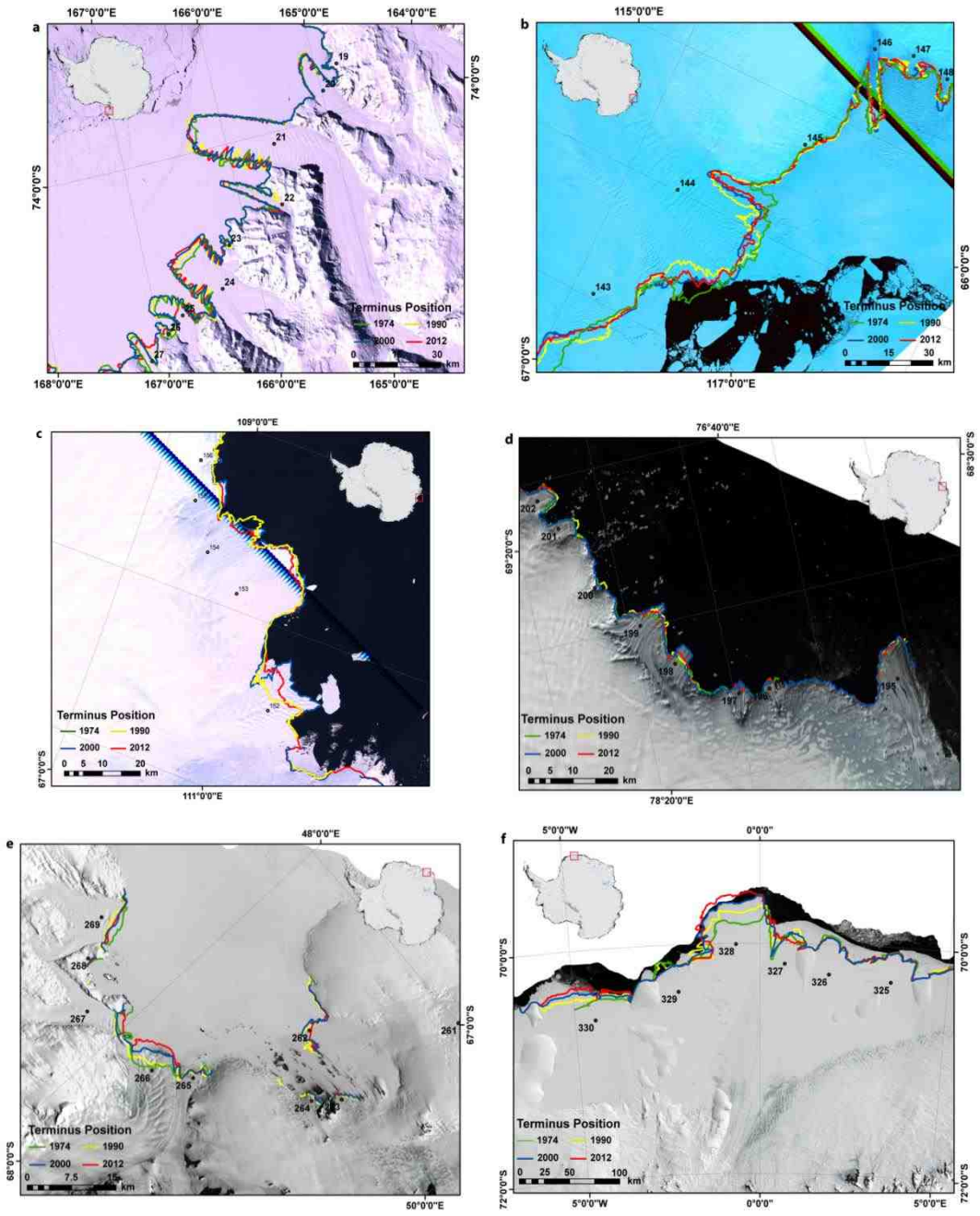

Figure 3.1: A series of mapping figures, with digitized terminus positions (green = 1974, yellow = 1990, blue = 2000 and red = 2012) and glacier ID numbers, overlain on the 2000 Landsat base image. **a)** Victoria Land (DB16) **b** and **c)** Wilkes Land (DB13) **d)** Queen Mary Land (DB12) **e)** Enderby Land (DB7) **f)** Dronning Maud Land (DB 5 and 6).

3.3 Results

Our results show clear decadal-scale patterns of terminus position around the entire EAIS marine margin (Table 3.1). During the 1974-1990 epoch, 65% of glaciers retreated at a median rate of 17.8 m yr^{-1}. From 1990-2000, however, there was a highly significant ($p<0.0005$) (Table 3.2) switch to 67% of glaciers advancing (median rate = 20.0 m yr^{-1}). This trend continued into the most recent epoch (2000-2012), when 65% of glaciers advanced at a median rate of 17.9 m yr^{-1}.

Table 3.1: Glacier terminus position change across each epoch. Red indicates retreat.

Epoch	n =	Advance (%)	Retreat (%)	median (m yr^{-1})
1974-2012	262	50	50	-0.4
1974-1990	254	35	65	-17.8
1990-2000	334	67	33	20.0
2000-2012	342	65	35	17.9

Table 3.2: Wilcoxon tests for significant differences between median Drainage Basin (DB) glacier terminus position change between each epoch. Red text indicates retreat, text highlighted yellow indicates that they are statistically significant.

Sample	Epoch	N=	Median	P=
All Glaciers	1974-1990	254	-17.8	
	1990-2000	334	20.0	**0.0000**
	1990-2000	334	20.0	
	2000-2012	342	17.9	0.1314
DB16	1974-1990	18	7.5	
	1990-2000	19	1.8	0.7382
	1990-2000	19	1.8	
	2000-2012	16	10.9	0.8167
DB15	1974-1990	69	-3.5	
	1990-2000	70	12.6	**0.0001**
	1990-2000	70	12.6	
	2000-2012	71	20.6	0.8787
DB14	1974-1990	24	-43.5	**0.0001**

	1990-2000	35	30.3	
	1990-2000	35	30.3	
	2000-2012	38	19.4	0.7999
DB13	1974-1990	15	-49.4	
	1990-2000	37	54.9	**0.0002**
	1990-2000	37	54.9	
	2000-2012	39	-63.6	**0.0000**
DB12	1974-1990	33	-3.4	
	1990-2000	40	8.9	0.2014
	1990-2000	40	8.9	
	2000-2012	41	15.9	0.8386
DB8/DB9/DB11	1974-1990	19	-1.4	
	1990-2000	34	14.2	**0.0438**
	1990-2000	34	14.2	
	2000-2012	35	13.8	0.4545
DB7	1974-1990	43	-38.0	
	1990-2000	60	24.5	**0.0000**
	1990-2000	60	24.5	
	2000-2012	62	29.1	0.7648
DB6/DB5	1974-1990	15	-66.1	
	1990-2000	18	158.7	0.1118
	1990-2000	18	158.7	
	2000-2012	20	72.4	0.0854
DB4	1974-1990	18	-23.6	
	1990-2000	21	54.5	**0.0139**
	1990-2000	21	54.5	
	2000-2012	21	49.9	0.3392

Regionally, trends in glacier retreat in the 1970s and 1980s (Fig. 3.2a) are most pronounced between Dronning Maud and Enderby Lands (Drainage Basin's (DB) 5 to DB7) and between Oates and Wilkes Lands (DB13-DB15), where 74% and 79% of glaciers retreated, respectively (median rates = -34.4 m yr^{-1} and -21.9 m yr^{-1}). Between Queen Mary and Kemp Lands (DB8-DB12) there was less obvious change, with 53% retreating (median rate of 1.4 m yr^{-1}). During the periods 1990-2000 and 2000-2012, however, outlet glaciers within every drainage basin showed a dominant signal of advance (Fig. 3.2b, c). The one exception is Wilkes Land (DB13), where 74% of glaciers retreated

at a median rate of -63.6 m yr^{-1} between 2000 and 2012 (Fig. 3.2c, and Table 3.3). This represents a highly significant ($p<0.0005$; Table 3.2) switch from the 1990s, when 75% of glaciers in Wilkes Land advanced. This is the first demonstration that glacier terminus changes in the region are linked to recently observed trends in mass loss (King et al., 2012; Sasgen et al., 2013; Mcmillan et al., 2014), i.e. Wilkes Land is the only area of significant mass loss in East Antarctica and the only area where outlet glaciers are retreating. We now turn our attention to analysing the potential causes of this anomalous retreat, focussing on atmospheric warming, changes in ocean conditions and alterations in sea ice patterns.

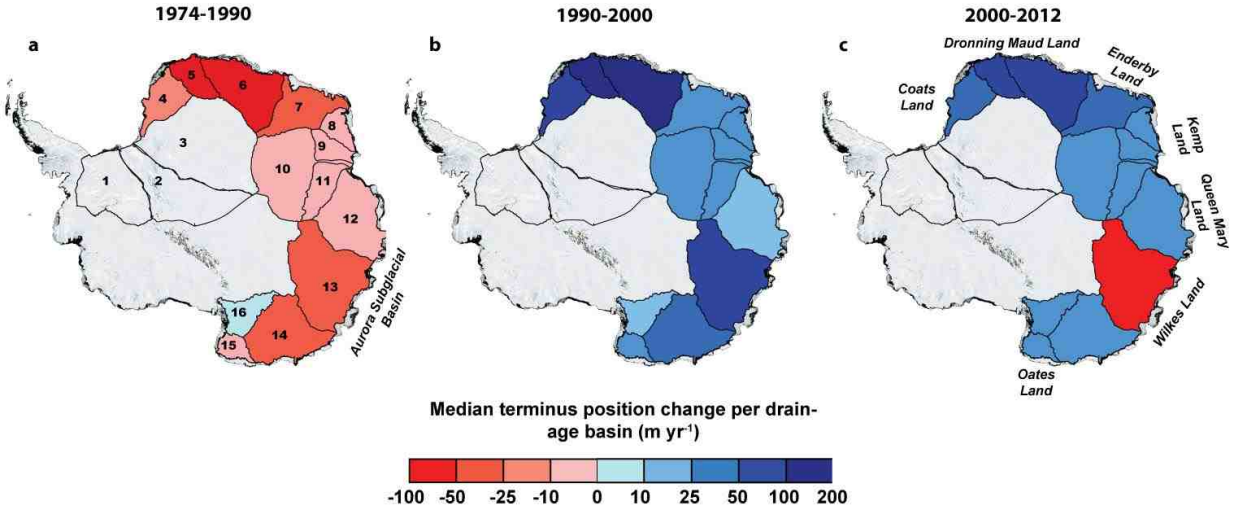

Figure 3.2 Median rate of East Antarctic outlet glacier terminus position in each drainage basin (red = retreat, Blue = advance) a) 1974-1990, b) 1990-2000 and c) 2000-2012. Note the anomalous retreat of outlet glaciers in Wilkes Land between 2000 and 2012.

Table 3.3: Glacier terminus position change across the entire EAIS at each epoch. Note: results from DB16-DB13 were obtained from Miles et al. (2013). Red indicates retreat.

Sample	1974-1990		1990-2000		2000-2010	
	n=	median (m yr^{-1})	n=	median (m yr^{-1})	n=	median (m yr^{-1})
All Glaciers	254	-17.8	334	20.0	342	17.9
DB16	18	7.5	19	1.8	16	10.9
DB15	69	-3.5	70	12.6	71	20.6
DB14	24	-43.5	35	30.3	37	19.4
DB13	15	-49.4	37	54.9	39	-63.6
DB12	33	-3.4	40	8.9	41	15.9
DB8/DB9/DB11	19	-1.4	34	14.2	35	13.8
DB7	43	-38.0	60	24.5	62	29.1
DB6/DB5	15	-66.1	18	158.7	20	72.4
DB4	18	-23.6	21	54.5	21	49.9

3.4. Discussion

In the Antarctic Peninsula, atmospheric warming has been linked to the ongoing retreat of glaciers (Cook et al., 2005) and the disintegration of ice shelves through excess surface meltwater driving hydro-fracturing (Scambos et al., 2009) and increased basal melt (Pritchard et al., 2012). Mean austral summer temperature (December- February) records in Wilkes Land show a period of relatively warm temperatures between 1974 and 1990, a cooling in the 1990s, and a slight increase in mean temperature between 2000 and 2012, although not to the same levels as in the 1970s and 1980s (Fig.3.3). These temperature patterns are broadly consistent with the observed trends in glacier terminus position in Wilkes Land, raising the possibility that the observed changes might be driven by air temperatures. Moreover, although the mean monthly air temperatures are relatively cold (< 0°C) surface temperature can still climb above freezing on a daily basis and are likely to produce some surface melt (Trusel et al., 2013). However, the amount surface melt

produced in Wilkes Land is considerably lower than that produced in other regions of Antarctica (Trusel et al., 2013) (e.g. the Antarctic Peninsula), where surface-melt induced hydro-fracture has been a proposed mechanism of glacier retreat (Scambos et al., 2014). Thus, we suggest that surface melt is unlikely to have driven the anomalous retreat of outlet glaciers in Wilkes Land. Rather, we suggest that changes in the ocean system (sea ice and ocean temperatures) might play a predominant role, but which are nevertheless likely to be linked to changes in air temperature trends.

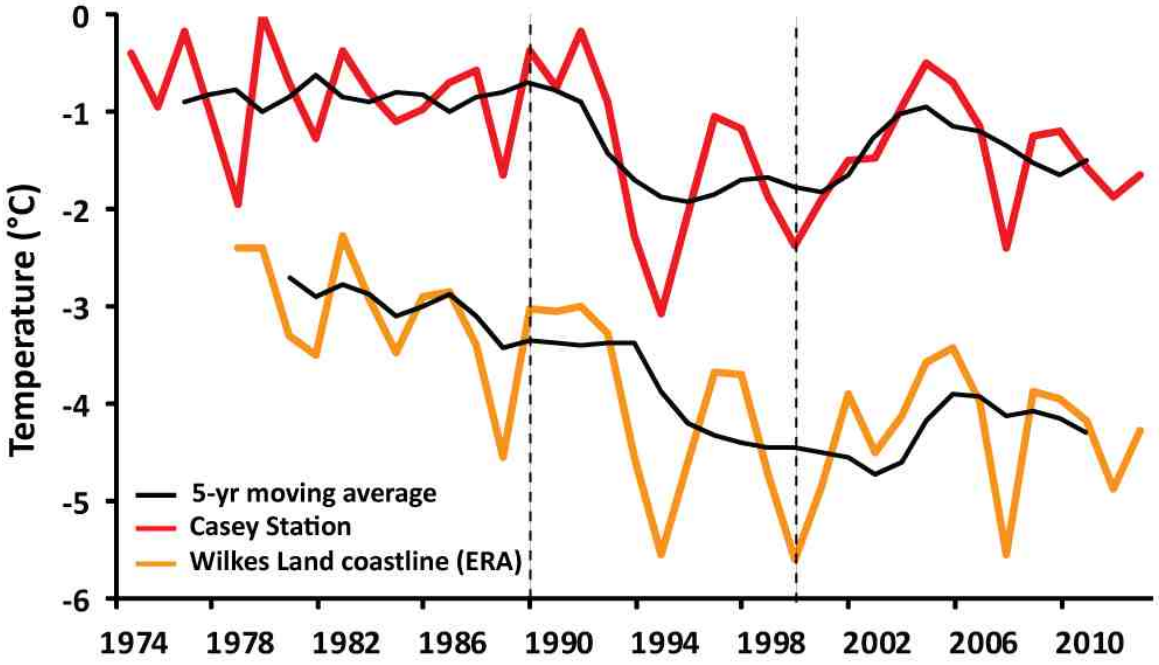

Figure 3.3: Mean austral summer (Dec – Feb) air temperature from Casey station (red) and entire Wilkes Land coastline (orange) (sourced from the ERA-Interim dataset).

Ocean-driven basal melt can enhance iceberg calving (Liu et al., 2015) and ultimately influence glacier terminus positions. For example, in the Amundsen Sea, West Antarctica, the retreat (MacGregor et al., 2012) and increased discharge from outlet glaciers has been linked to increased upwelling of warm Circumpolar Deep Water (CDW) across the continental shelf break (Thoma et al., 2008; Dutrieux et al., 2014). Rates of basal melting in Wilkes Land are comparable to some West Antarctic ice shelves (Depoorter et al., 2013; Rignot et al., 2013), but limited observational records mean it is unclear whether this is attributable to CDW, although it has been hypothesised (Rignot et al., 2013).

In the absence of long-term observational records of ocean temperatures for Wilkes Land, we use EN4 subsurface ocean temperature objective analysis data (Good et al., 2013) to gain a plausible insight into potential changes in the upwelling of CDW at the continental shelf boundary since 1974 (Figs. 3.4a & 4b). We acknowledge that the nature of these data creates very high uncertainty estimates (Fig. 3.5), meaning that trends cannot be considered statistically significant. However, these data provide the only indication of possible changes in ocean temperatures in the absence of direct observations and we include them to simply examine any possible trends that might be consistent with the glacier changes we observe. Estimates from EN4 indicate a cooling trend in the top 109 m of the water column (0.084 °C per decade, Fig.3. 5a), a warming trend at depths between 109 and 446 m (0.036 °C per decade , Fig. 3.5b) and no trend at depths between 446 and 967 m (Fig. 3.5c). Despite the large uncertainties with the EN4 data, we also note that the only observational records which exist in this region (Williams et al., 2011) suggest the presence of modified Circumpolar Deep Water (mCDW) at depths similar to the warming trend between 109 and 446 m on the continental shelf break in Wilkes Land. Moreover, the potential discovery of an inland trough connecting Totten glacier cavity to the ocean in this region (Greenbaun et al., 2015) increases the likelihood of mCDW crossing the continental shelf boundary and enhancing basal melt. However, whilst EN4 data might hint at a long term warming trend at intermediate depths, this is not entirely consistent with the longer-term trend in glacier terminus position, i.e. glacier advance in the 1990s deviates from the potential warming trend. Thus, we suggest that processes more local to the glacier termini may modulate whether the warm waters can access the glacier terminus and sea ice processes are known to modify ocean stratification.

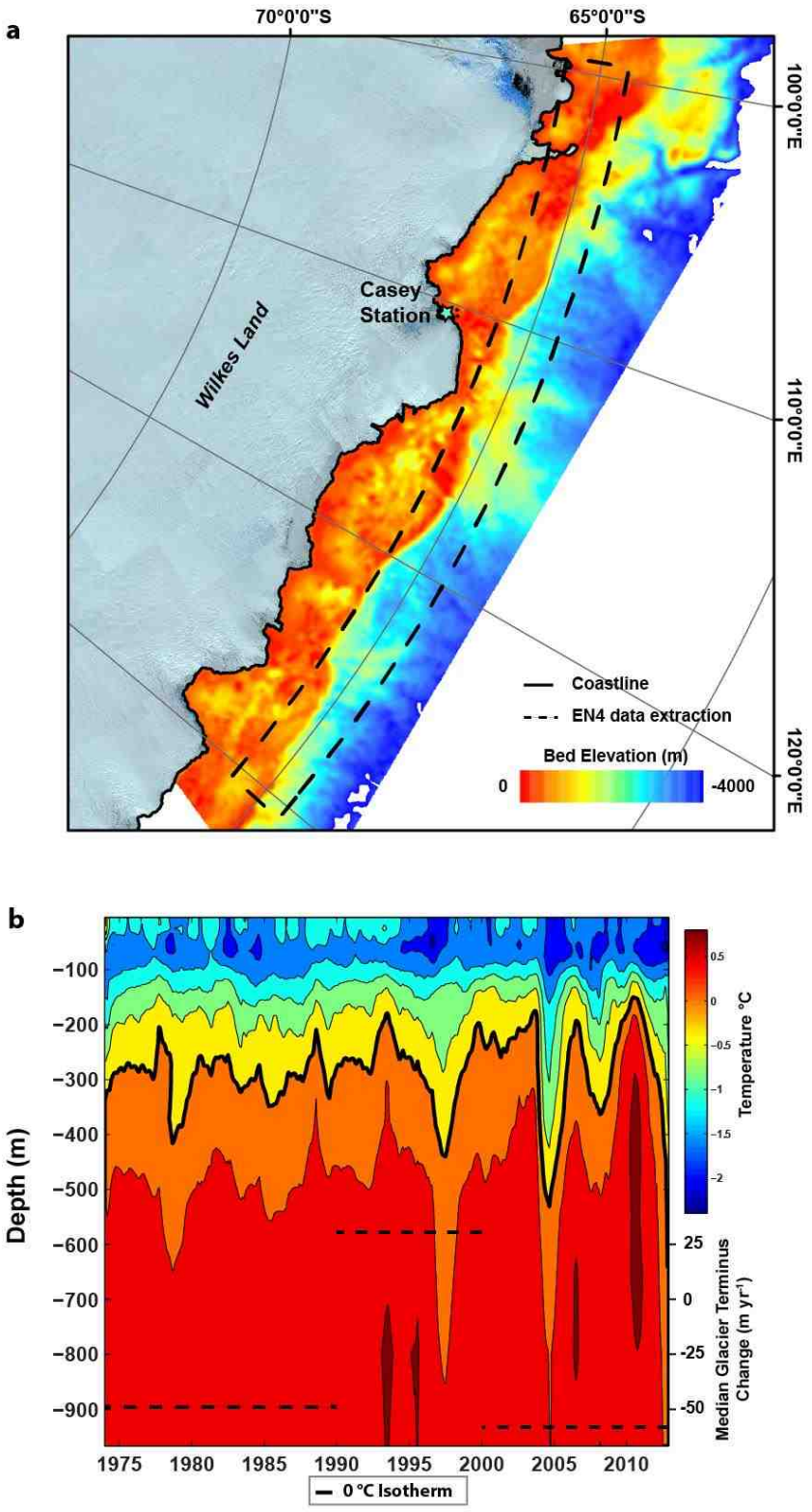

Figure 3.4: a) Bed topography of Wilkes Land (from Bedmap2; Fretwell et al., 2013), with the spatial location of the EN4 data extraction on the continental shelf boundary. **b)** EN4 subsurface objective analysis temperature depth profile 1974-2012. Data was extracted from 31 grid cells between 100 -130° E, 64° S (continental shelf boundary - Wilkes Land), with the black dashed line representing the median glacier terminus position change of outlet glaciers per epoch in Wilkes Land.

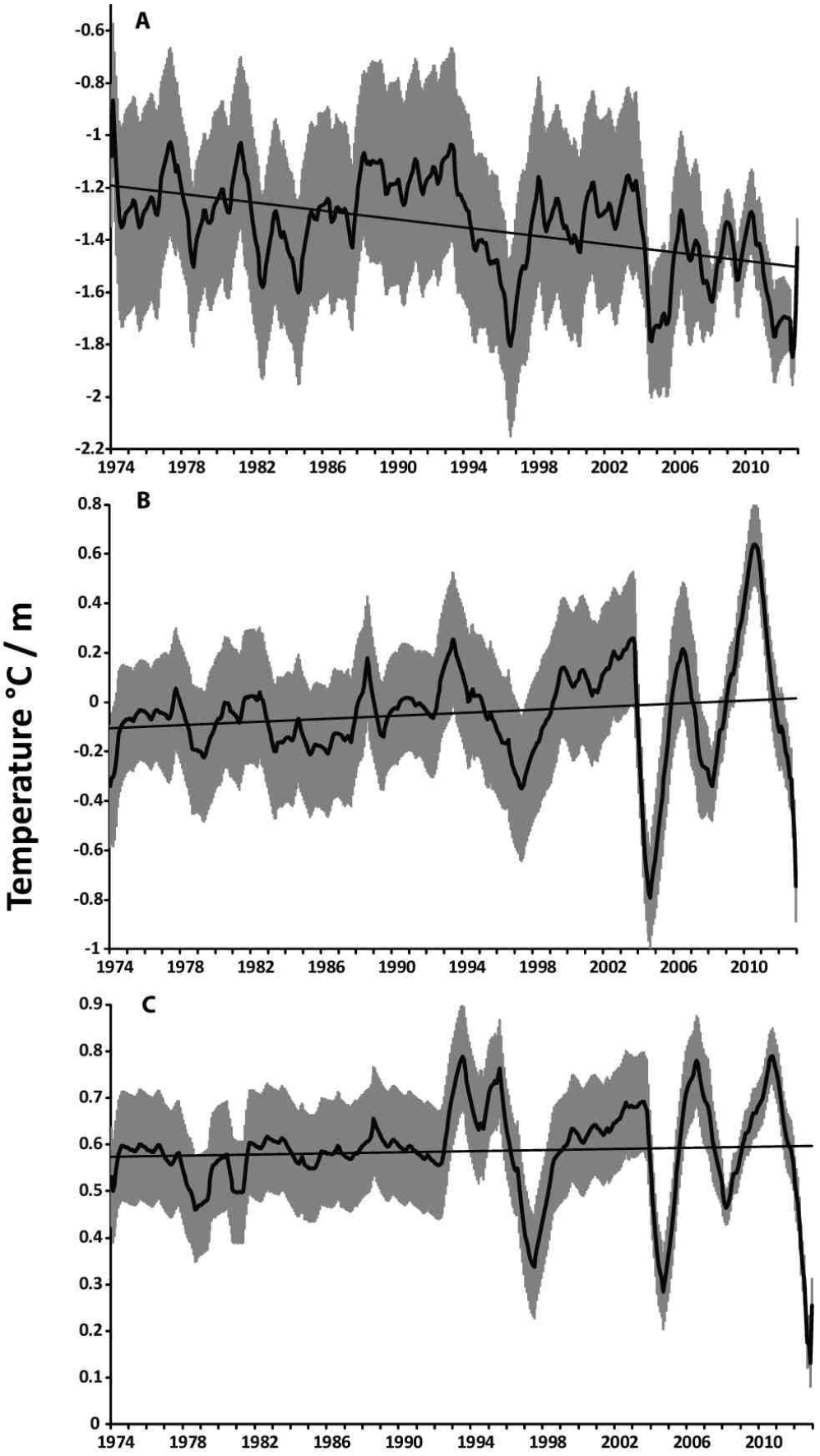

Figure 3.5: Subsurface ocean temperature change per m in DB13 with uncertainty estimates (e.g. Fig.3.4) **a)** 5-109 m **b)** 109-446 m **c)** 446-967 m

Differences in the number of sea ice days per year (April-October) between each epoch reveal clear spatial trends across Antarctica (Fig. 3.6). In East Antarctica, there were, on average, 2.5 fewer sea days per year in the period from 1979-1990 compared to the 1990s (Fig. 3.6). Negative anomalies were concentrated between Oates Land (DB15) and Queen Mary Land (DB12), and between Enderby Land (DB7) and Coats Land (DB4). In both of these regions there was a dominant signal of glacier retreat between 1974 and 1990 (Fig. 3.4a), with a mean reduction in sea ice of 11.9 and 7.0 days per year, respectively. However, between Princess Elizabeth Land (DB12) and Kemp Land (DB8) there were, on average, 1.4 more sea ice days per year in the period 1979-1990 than in the 1990s. Here, there was little change in glacier terminus position between 1974 and 1990 (Fig. 3.6a; Table 3.1).

More recently, there has been only a small change in the overall average number of sea ice days per year between 2000 and 2012, compared to the 1990s (Fig. 3.6b). However, there is considerable spatial variability, with an average increase of 5.3 days per year (maximum: 31 days per year) in the outer sea ice pack off the coast of Oates Land, eastern Dronning Maud Land and Kemp Land, where there was also a signal of glacier advance between 2000 and 2012 (Fig 3.6b). However, in Wilkes Land, where 74% of glaciers retreated between 2000 and 2012, there was an average decrease of 11.5 sea ice days per year (maximum: -27 days per year) (Fig. 3.6b). Thus, patterns in sea ice change correspond to changing patterns in glacier terminus position.

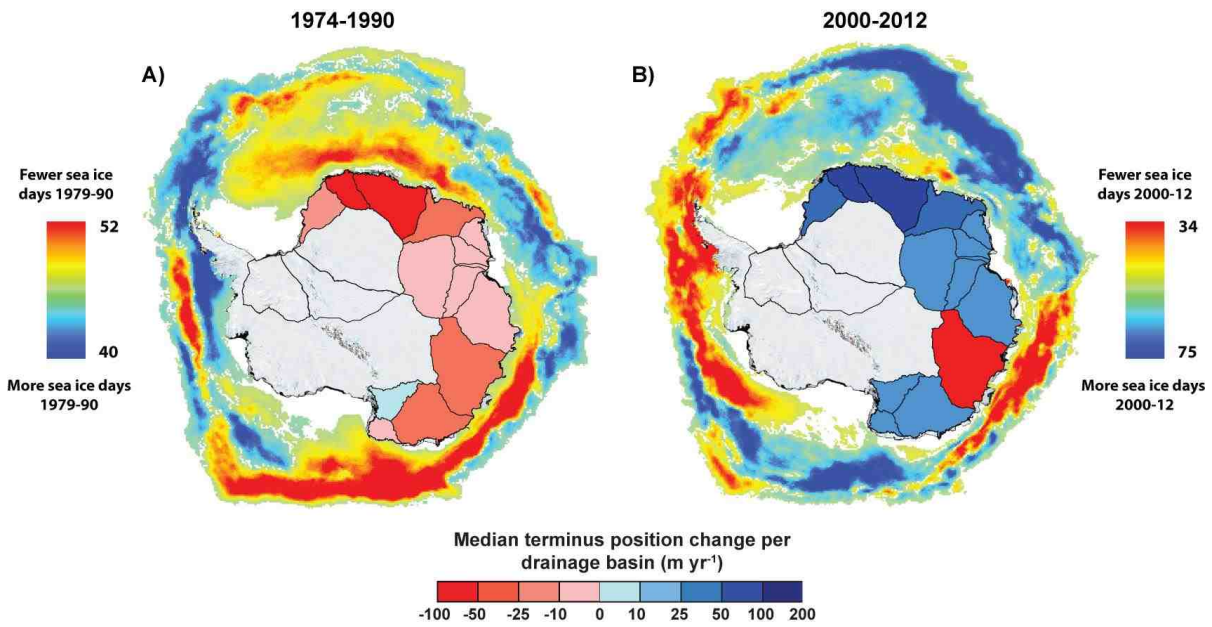

Figure 3.6: Difference in the number of sea ice days per year during the sea ice season (April-October) compared to 1990-2000, with shaded drainage basins representing glacier terminus position trends (red = retreat, blue = advance, as in Fig.1) **A)** 1974-1990 and **B)** 2000-2012. Note: Sea ice data only extends back to 1979 (see Methods).

Coastal polynyas are important in driving sea ice variability in Antarctica. They produce around 10% of total sea ice, despite representing only 1% of the maximum sea ice area (Tamura et al., 2008). These polynyas form through katabatic winds and are thought to be sensitive to small changes in climate (Maqueda et al., 2004). In Wilkes Land, there are major negative sea ice anomalies in both 1979-1990 and 2000-2012, relative to 1990-2000. Analysis of mean ERA-interim (Dee et al., 2011) meridional flow, zonal flow and air temperatures on the coastline of Wilkes Land during the sea ice production season (April – October), suggest a tendency for more Northerly winds and higher temperatures during periods of negative sea ice anomalies (1979-1990 and 2000-2012), with no clear change in zonal flow (Fig. 3.7). We suggest that this is likely to represent a suppression in katabatic winds that, in turn, decreases coastal polynya intensity and results in a decrease in sea ice production in Wilkes Land in both 1974-1990 and 2000-2012, relative to the 1990s.

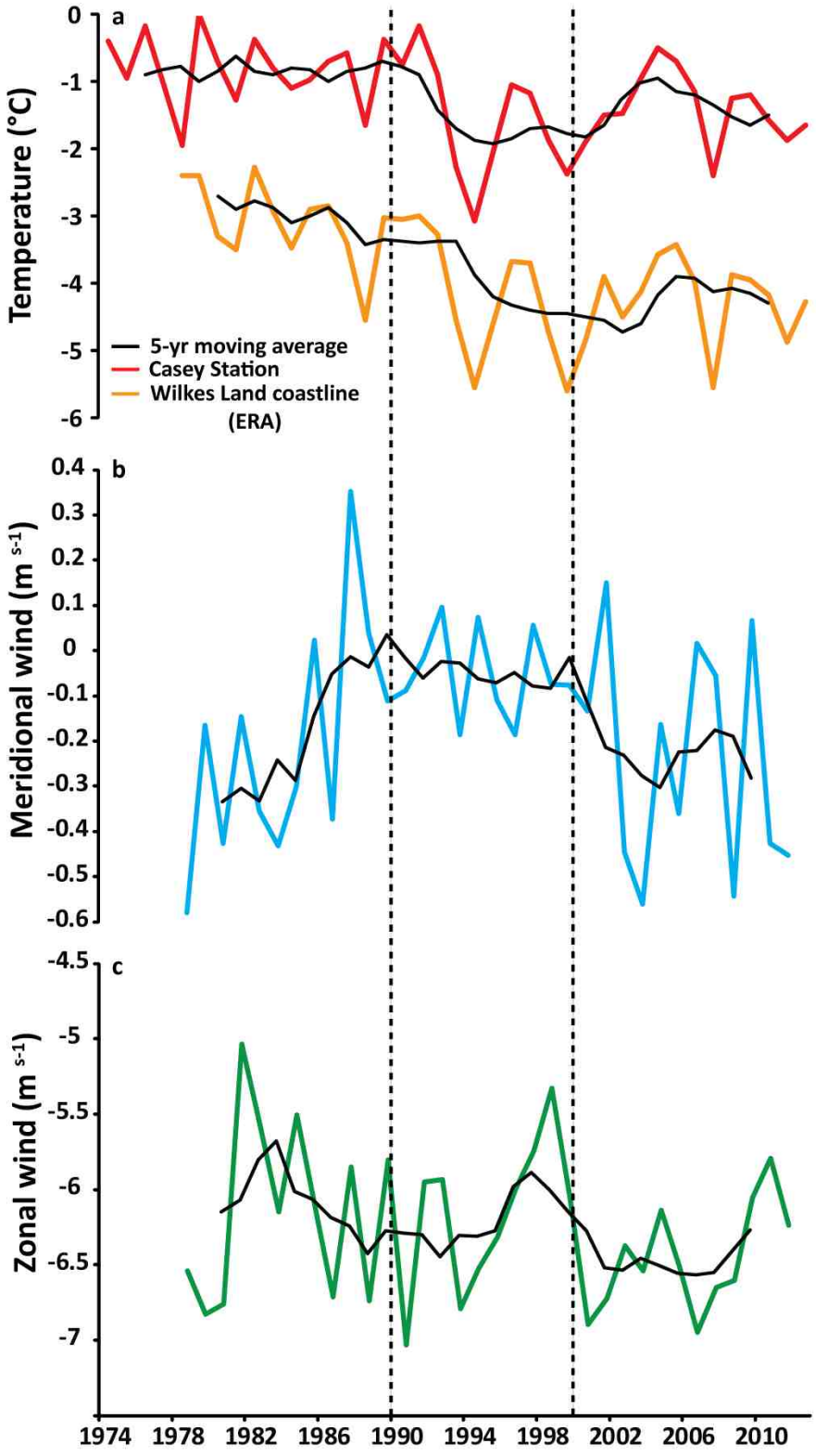

Figure 3.7: Time series of winter air temperature and wind flow. a) Mean winter (Apr-Oct) air temperature from Casey station (red) and the entire Wilkes Land coast from the ERA-interim dataset (orange). b) Mean monthly meridional flow on the Wilkes Land coast, positive values indicate southerly winds (south to north). c) Mean monthly zonal flow on the Wilkes Land coast, positive values indicate westerly winds (west to east).

Changes in the amount of sea ice production can alter the mixing of shelf waters, which can drive variability in the basal melt rate of glacier termini (Holland et al., 2010; Khazendar et al., 2013; Gwyther et al., 2014). Wilkes Land is a region of intense wind-driven coastal polynya activity, which (as a consequence) has high rates of sea ice production (Tamura et al., 2008). During sea ice production, brine rejection leads to the deepening of the cold surface mixed layer and to increased destratification of the water column (Petty et al., 2014). The depth of the mixed layer is intrinsically linked to the net salt flux, which is controlled by the amount of sea ice produced, with higher rates of sea ice production on the continental shelf resulting in a deeper mixed layer (Petty et al., 2014). In some medium to large polynyas in Wilkes Land, models have suggested that sufficient sea ice production can cause the complete destratification of the water column (i.e. the mixed layer extends to the sea bed), resulting in the formation of High Salinity Shelf Water (HSSW) (Kusahara et al., 2010), and direct observations have confirmed this in the Vincennes Bay polynya (Kitade et al., 2014). HSSW is important because it is the densest and coolest water mass on the continental shelf and its presence can prevent the less dense and warmer mCDW from directly accessing glacier cavities, thus suppressing basal melt. Therefore, any variation in sea ice production and the subsequent supply of HSSW has the potential to influence the basal melt rate of glaciers (Fig. 3.8). This is confirmed by recent reports that directly link inter-annual variations in the sea ice production of the Dalton polynya, to the basal melt rate of the nearby Totten glacier in Wilkes Land (Khazendar et al., 2013; Gwyther et al., 2014).

We therefore hypothesize that the recent reduction in sea ice days in Wilkes Land (2000-2012: Fig. 3.6) has led to decreased brine rejection and thus a decreased supply of HSSW. This, combined with a possible longer term underlying trend of increased entrainment of CDW at the continental shelf boundary (Fig. 3.4), has increased the likelihood of warm mCDW reaching glacier cavities, enhancing basal melt and driving glacier retreat. This is consistent with the reported high rates of basal melt (Depoorter et al., 2013; Rignot et al., 2013) and mass loss (King et al., 2012; Sasgen et al., 2013; Mcmillan et al., 2014) in Wilkes Land during the same time period. The relationship we identify between glacier trends and changes in the number of sea ice days in each year is consistent throughout the study period in Wilkes Land, with positive sea ice anomalies from 1990-2000 corresponding to glacier advance during the same time period, and negative sea ice anomalies from 1979-1990 corresponding to glacier retreat. Indeed, the close relationship

between glacier terminus position and sea ice conditions around the entire EAIS (Fig. 3.6) raises the possibility that this process may be driving glacier terminus position trends in other areas of high sea ice production in the EAIS.

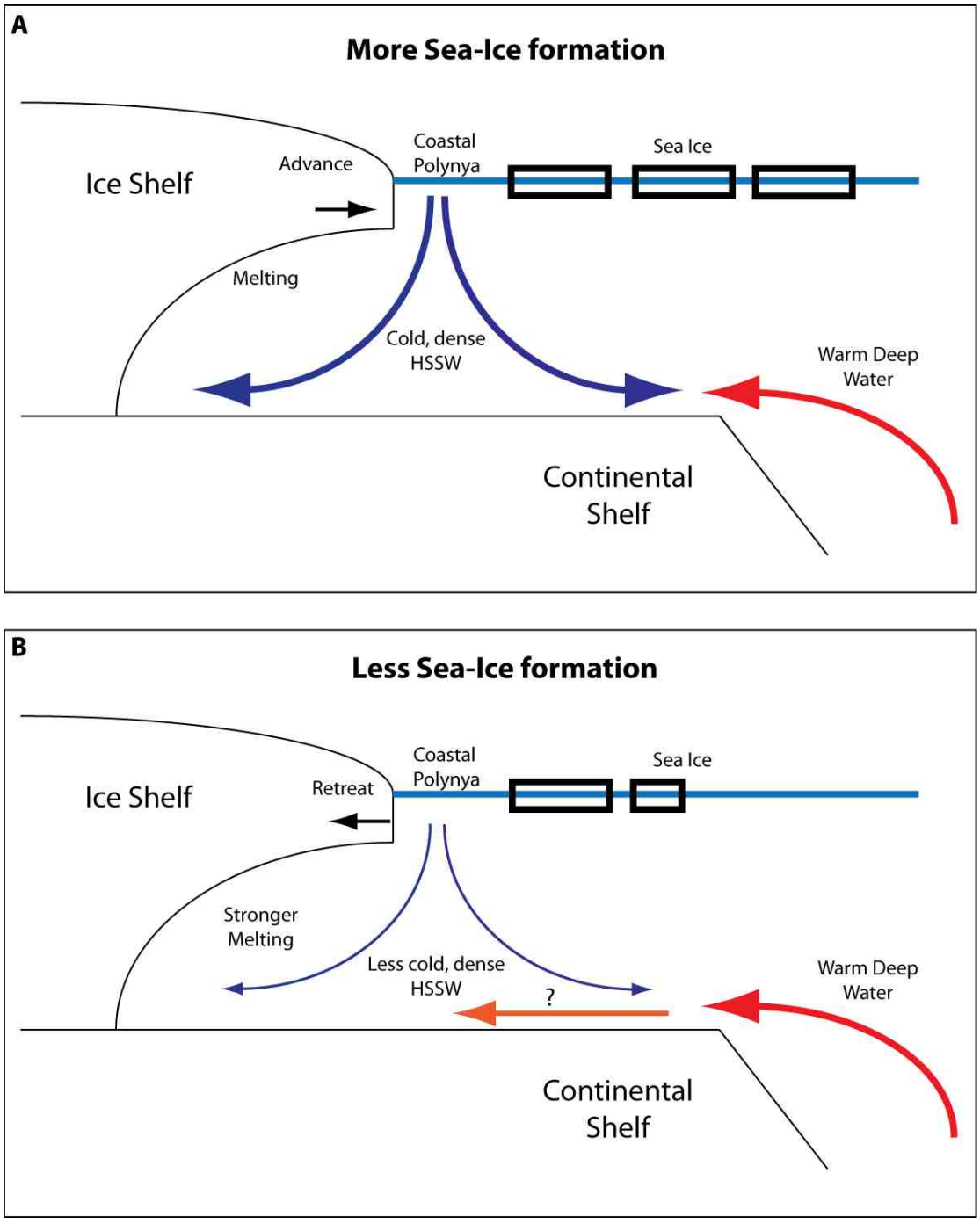

Figure 3.8: Schematic diagram of shelf water dynamics in Wilkes Land **A)** More sea ice formation (1990s): increase sea ice production results in a greater supply of HSSW, resulting in less basal melt and glacier advance. **B)** Less sea ice formation (1974-1990; 2000-2012): Less sea ice formation results in less HSSW, stronger basal melt and glacier retreat

3.5 Conclusion

We note that the only regions of Antarctica with similarly large reductions in sea ice days per year to those observed offshore of Wilkes Land is the Amundsen Sea Sector of West Antarctica and the west coast of the Antarctic Peninsula (Fig. 3.6). The Amundsen Sea Sector has long been recognised as West Antarctica's 'weak underbelly'(Hughes, 1981) where glacier retreat (MacGregor et al., 2012) and mass loss (King et al., 2012; Sasgen et al., 2013; Mcmillan et al., 2014) has been linked to CDW driving marine ice sheet instability. Our results suggest a similar scenario is emerging in Wilkes Land, which our data show is the only region of East Antarctica where outlet glaciers are both losing mass (King et al., 2012; Sasgen et al., 2013; Mcmillan et al., 2014) and retreating during the last decade. However, whilst the retreat and mass loss of glaciers in the Amundsen Sea Sector has been linked to wind-driven upwelling of CDW across the continental shelf (Thoma et al., 2008; Dutrieux et al., 2014), we hypothesize that the retreat of glaciers in Wilkes Land is linked to a reduction in sea ice production, which is consistent with meridional wind patterns. Given the potential sea level contribution of outlet glaciers in Wilkes Land, there is an urgent need for further integration of glaciological and oceanographic data to inform numerical modelling and constrain future predictions of this potentially 'weak underbelly' of East Antarctica.

Chapter 4: Simultaneous disintegration of outlet glaciers in Porpoise Bay (Wilkes Land), East Antarctica, driven by sea ice break-up.

Miles, B.W.J., Stokes, C.R. & Jamieson, S.S.R. 2017. Simultaneous disintegration of outlet glaciers in Porpoise Bay (Wilkes Land), East Antarctica, driven by sea ice break-up. Cryosphere, 10.5194/tc-11-427- 2017.

Abstract: The floating ice shelves and glacier tongues which fringe the Antarctic continent are important because they help buttress ice flow from the ice sheet interior. Dynamic feedbacks associated with glacier calving have the potential to reduce buttressing and subsequently increase ice flow into the ocean. However, there are few high temporal resolution studies on glacier calving, especially in East Antarctica. Here we use ENVISAT ASAR wide swath mode imagery to investigate monthly glacier terminus change across six marine-terminating outlet glaciers in Porpoise Bay (-76°S, 128°E), Wilkes Land (East Antarctica), between November 2002 and March 2012. This reveals a large near-simultaneous calving event in January 2007, resulting in a total of ~2,900 km^2 of ice being removed from glacier tongues. We also observe the start of a similar large near-simultaneous calving event in March 2016. Our observations suggest that both of these large calving events are driven by the break-up of the multi-year sea ice which usually occupies Porpoise Bay. However, these break-up events appear to have been driven by contrasting mechanisms. We link the 2007 sea ice break-up to atmospheric circulation anomalies in December 2005 weakening the multi-year sea ice through a combination of surface melt and a change in wind direction prior to its eventual break-up in January 2007. In contrast, the 2016 break-up event is linked to the terminus of Holmes (West) Glacier pushing the multi-year sea ice further into the open ocean, making the sea ice more vulnerable to break-up. In the context of predicted future warming and the sensitivity of sea ice to changes in climate, our results highlight the importance of interactions between landfast sea ice and glacier tongue stability in East Antarctica.

4.1 Introduction

Iceberg calving is an important process that accounts for around 50% of total mass loss to the ocean in Antarctica (Depoorter et al., 2013; Rignot et al., 2013). Moreover, dynamic feedbacks associated with retreat and/or thinning of buttressing ice shelves or floating glacier tongues can result in an increased discharge of ice into the ocean (Rott et al., 2002;

Rignot et al., 2004; Wuite et al., 2015; Fürst et al., 2016). At present, calving dynamics are only partially understood (Benn et al., 2007; Chapuis and Tetzlaff, 2014) and models struggle to replicate observed calving rates (van der Veen, 2002; Astrom et al., 2014). Therefore, improving our understanding of the mechanisms driving glacier calving and how glacier calving cycles have responded to recent changes in the ocean-climate system is important in the context of future ice-sheet mass balance and sea level.

Calving is a two-stage process that requires both the initial ice fracture and the subsequent transport of the detached iceberg away from the calving front (Bassis and Jacobs, 2013). In Antarctica, major calving events can be broadly classified into two categories: the discrete detachment of large tabular icebergs (e.g. Mertz glacier tongue: Massom et al., 2015) or the spatially extensive disintegration of floating glacier tongues or ice shelves into numerous smaller icebergs (e.g. Larsen A & B ice shelves Rott et al., 1996; Scambos et al., 2009). Observations of decadal-scale changes in glacier terminus position in both the Antarctic Peninsula and East Antarctica have suggested that despite some degree of stochasticity, iceberg calving and glacier advance/retreat is likely driven by external climatic forcing (Cook et al., 2005; Miles et al., 2013). However, despite some well-documented ice-shelf collapses (Scambos et al., 2003; Banwell et al., 2013) and major individual calving events (Masson et al., 2015) there is a paucity of data on the nature and timing of calving from glaciers in Antarctica (e.g. compared to Greenland: Moon and Joughin, 2008; Carr et al., 2013), and particularly in East Antarctica.

Following recent work that highlighted the potential vulnerability of the East Antarctic Ice Sheet in Wilkes Land to ocean-climate forcing and marine ice-sheet instability (Greenbaum et al., 2015; Aitken et al., 2016; Miles et al., 2013; 2016), we analyse the recent calving activity of six outlet glaciers in the Porpoise Bay region using monthly satellite imagery between November 2002 and March 2012. In addition, we also observe the start of a large calving event in 2016. We then turn our attention to investigating the drivers behind the observed calving dynamics.

4.2 Study area

Porpoise Bay (76°S, 128°E) is situated in Wilkes Land, East Antarctica, approximately 300 km east of Moscow University Ice Shelf and 550 km east of Totten glacier (Fig. 4.1). This area was selected for study because it occupies a central position in Wilkes Land, which is thought to have experienced mass loss over the past decade (King et al., 2012; Sasgen et

al., 2013; McMillan et al., 2014), and which is the only region of East Antarctica where the majority of marine-terminating outlet glaciers have experienced recent (2000-2012) retreat (Miles et al., 2016). This is particularly concerning because Wilkes Land overlies the Aurora Subglacial Basin and, due to its reverse bed slope and deep troughs (Young et al., 2011), it may have been susceptible to unstable grounding line retreat in the past (Cook et al., 2014), and could make significant contributions to global sea level in the future (DeConto and Pollard, 2016). However, despite some analysis of glacier terminus positions on decadal timescales (Frezzotti and Polizzi, 2002; Miles et al., 2013; 2016), there has yet to be any investigation of inter-annual and sub-annual changes in terminus position and calving activity in the region.

Porpoise Bay is 150 km wide and is typically filled with landfast multi-year sea ice (Fraser et al., 2012). In total, six glaciers were analysed, with glacier velocities (from Rignot et al., 2011b) ranging from ~440 m yr^{-1} (Sandford Glacier) to ~2000 m yr^{-1} (Frost Glacier). Recent studies have suggested that the largest (by width) glacier feeding into the bay - Holmes Glacier - has been thinning over the past decade (Pritchard et al., 2009; McMillan et al., 2014).

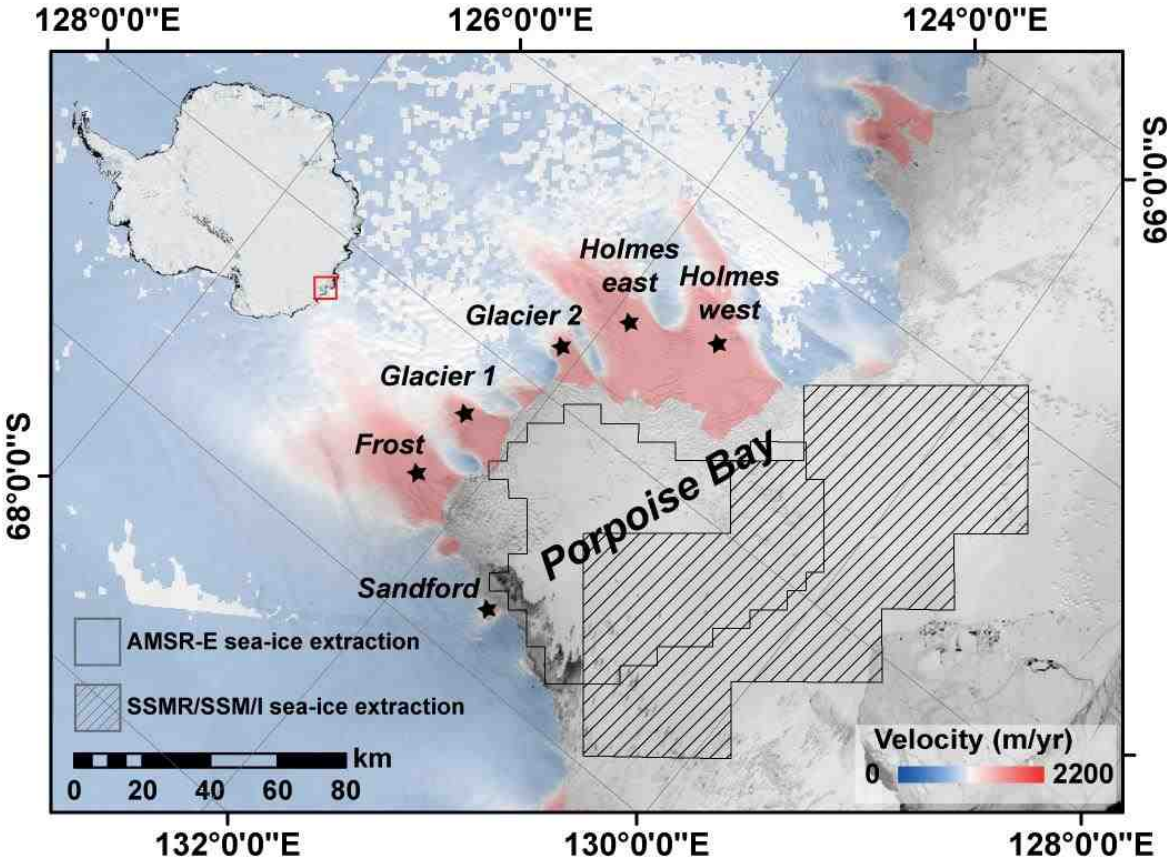

Figure 4.1: MODIS image of Porpoise Bay, with glacier velocities overlain (Rignot et al., 2011b). The hatched polygon represents the region where long-term 25 km resolution SMMR/SSM/I sea ice concentrations were extracted. The non-hatched polygon represents the region where the higher resolution (6.25 km) AMSR-E sea ice concentrations were extracted.

4.3 Methods

4.3.1 Satellite imagery and terminus position change

Glacier terminus positions were mapped at approximately monthly intervals between November 2002 and March 2012, using Envisat Advanced Synthetic Aperture Radar (ASAR) Wide Swath Mode (WSM) imagery across six glaciers, which were identified from the Rignot et al. (2011b) ice-velocity dataset (Fig. 4.1). Additional sub-monthly imagery between December 2006 and April 2007 were used to gain a higher temporal resolution following the identification of a major calving event around that time. During the preparation for this manuscript we also observed the start of another large calving event with Sentinel-1 imagery (Table 4.1).

Table 4.1: Satellite imagery used in the study

Satellite	Date of Imagery
ARGON	October 1963 (Kim et al., 2007)
Envisat ASAR WSM	August 2002, November 2002 to March 2012 (monthly)
Landsat	January 1973; February 1991
MODIS	January 2001; December/January 2005/6; March 2016
RADARSAT	September 1997 (Liu and Jezek, 2004)
Sentinel-1	February-July, 2016

Approximately 65% of all glacier frontal measurements were made using an automated mapping method. This was achieved by automatically classifying glacier tongues and sea ice into polygons based on their pixel values, with the boundary between the two taken as the terminus position. The threshold between glacial ice and sea ice was calculated automatically based on the image pixel statistics, whereby sea ice appears much darker than the glacial ice. In images where the automated method was unsuccessful, terminus position was mapped manually. The majority of these manual measurements were undertaken in the austral summer (December – February) when automated classification was especially problematic due to the high variability in backscatter on glacier tongues as a result of surface melt. Following the mapping of the glacier termini, length changes were calculated using the box method (Moon and Joughin, 2008). This method calculates the glacier area change between each time step divided by the width of the glacier, to give an estimation of glacier length change. The width of glacier was obtained by a reference box which approximately delineates the sides of the glacier.

Given the nature of the heavily fractured glacier fronts and the moderate resolution of Envisat ASAR WSM imagery (80 m) it was sometimes difficult to establish whether individual or blocks of icebergs were attached to the glacier tongue. As a result, there are errors in precisely determining terminus change on a monthly time-scale (~± 500 m). However, because our focus is on major calving events, absolute terminus position is less important than the identification of major episodes of calving activity. Indeed, because estimations of terminus position were made at approximately monthly intervals, calving events were easily distinguished because the following month's estimation of terminus position would clearly show the glacier terminus in a retreated position. In addition, each image was also checked visually to make sure no small calving events were missed (i.e. as indicated by the presence of icebergs proximal to the glacier tongue).

4.3.2 Sea ice

Sea ice concentrations in Porpoise Bay were calculated using mean monthly Bootstrap sea ice concentrations derived from the Nimbus-7 satellite and the Defence Meteorological Satellite Program (DMSP) satellites, which offers near complete coverage between October 1978 and December 2014 (Comiso, 2014; http://dx.doi.org/10.5067/J6JQLS9EJ5HU). To extend the sea ice record, we also use mean monthly Nimbus-5 Electrically Scanning Microwave Radiometer (ESMR) derived sea ice concentrations (Parkinson et al., 2004; https://nsidc.org/data/docs/daac/nsidc0009_esmr_seaice.gd.html), which offer coverage between December 1972 and March 1977. However, from March to May 1973, August 1973, April 1974 and June to August 1975, mean monthly sea ice concentrations were not available. Sea ice concentrations were extracted from 18 grid cells, covering 11,250 km^2 across Porpoise Bay, but not into the extended area beyond the limits of the bay (Fig. 4.1). Grid cells which were considered likely to be filled with glacial ice were excluded. Pack-ice concentrations were also extracted from a 250 x 150 km polygon adjacent to Porpoise Bay. The dataset has a spatial resolution of 25 km and monthly sea ice concentration anomalies were calculated from the 1972-2016 monthly mean.

Daily sea ice concentrations derived from the Artist Sea ice (ASI) algorithm from Advanced Microwave Scanning Radiometer - EOS (AMSR-E) data (Spreen et al., 2008) were used to calculate daily sea ice concentration anomalies during the January 2007 sea ice break-up (http://icdc.zmaw.de/1/daten/cryosphere/seaiceconcentration-asi-amsre.html). This dataset was used because it provides a higher spatial resolution (6.25 km) compared to those available using Bootstrap derived concentrations (25 km). This is important because it provides a more accurate representation of when sea ice break-up was initiated and, due to its much higher spatial resolution, it provides data from much closer to the glacier termini (see Fig. 4.1).

4.3.3 RACMO

We used the Regional Atmospheric Climate Model (RACMO) V2.3 (van Wessem et al., 2014) to simulate daily surface melt fluxes in the study area between 1979 and 2015 at a 27 km spatial resolution. The melt values were extracted from floating glacier tongues in Porpoise Bay because the model masks out sea ice, equating to seven grid points. The

absolute surface melt values are likely to be different on glacial ice, compared to the sea ice, but the relative magnitude of melt is likely to be similar temporally.

4.3.4 ERA-Interim

In the absence of weather stations in the vicinity of Porpoise Bay we use the 0.25° ERA-Interim reanalysis dataset (http://apps.ecmwf.int/datasets/data/interim-full-moda/levtype=sfc/) to calculate mean monthly wind-field and sea-surface temperature (SST) anomalies, with respect to the 1979-2015 monthly mean. Wind-field anomalies were calculated by using the mean monthly 10 m zonal (U) and meridional (V) wind components. We also used the daily 10 m zonal (U) and meridional (V) components to simulate wind-field vectors in Porpoise Bay on January 11th 2007 and March 19th 2016 which are the estimated dates of sea ice break-up.

4.4 Results

4.4.1 Terminus position change

Analysis of glacier terminus position change of six glaciers in Porpoise Bay between November 2002 and March 2012 reveals three broad patterns of glacier change (Fig. 4.2). The first pattern is shown by Holmes (West) Glacier, which advances a total of ~13 km throughout the observation period, with no evidence of any major iceberg calving that resulted in substantial retreat of the terminus beyond the measurement error (+/- 500 m). The second is shown by Sandford Glacier tongue, which advanced ~1.5 km into the ocean between November 2002 and April 2006, before its floating tongue broke away in May 2006. A further smaller calving event was observed in January 2009. Overall, by the end of the study period, its terminus had retreated around 1 km from its position in November 2002. The third pattern is shown by Frost Glacier, Glacier 1, Glacier 2 and Holmes (East) Glaciers, which all advanced between November 2002 and January 2007, albeit with a small calving event in Frost Glacier in May 2006. However, between January and April 2007, Frost Glacier, Glacier 1, Glacier 2 and Holmes (East) Glaciers all underwent a large near-simultaneous calving event. This led to 1,300 km^2 of ice being removed from glaciers in Porpoise Bay, although we also note the disintegration of a major tongue from an unnamed glacier further west, which contributed a further 1,600 km^2. Thus, in a little over three months, a total of 2,900 km^2 of ice was removed from glacier tongues in the study

area (Fig. 4.3). Following this calving event, the fronts of these glaciers stabilised and began advancing at a steady rate until the end of the study period (March, 2012) (Fig. 4.2), with the exception of Frost Glacier which underwent a small calving event in April 2010.

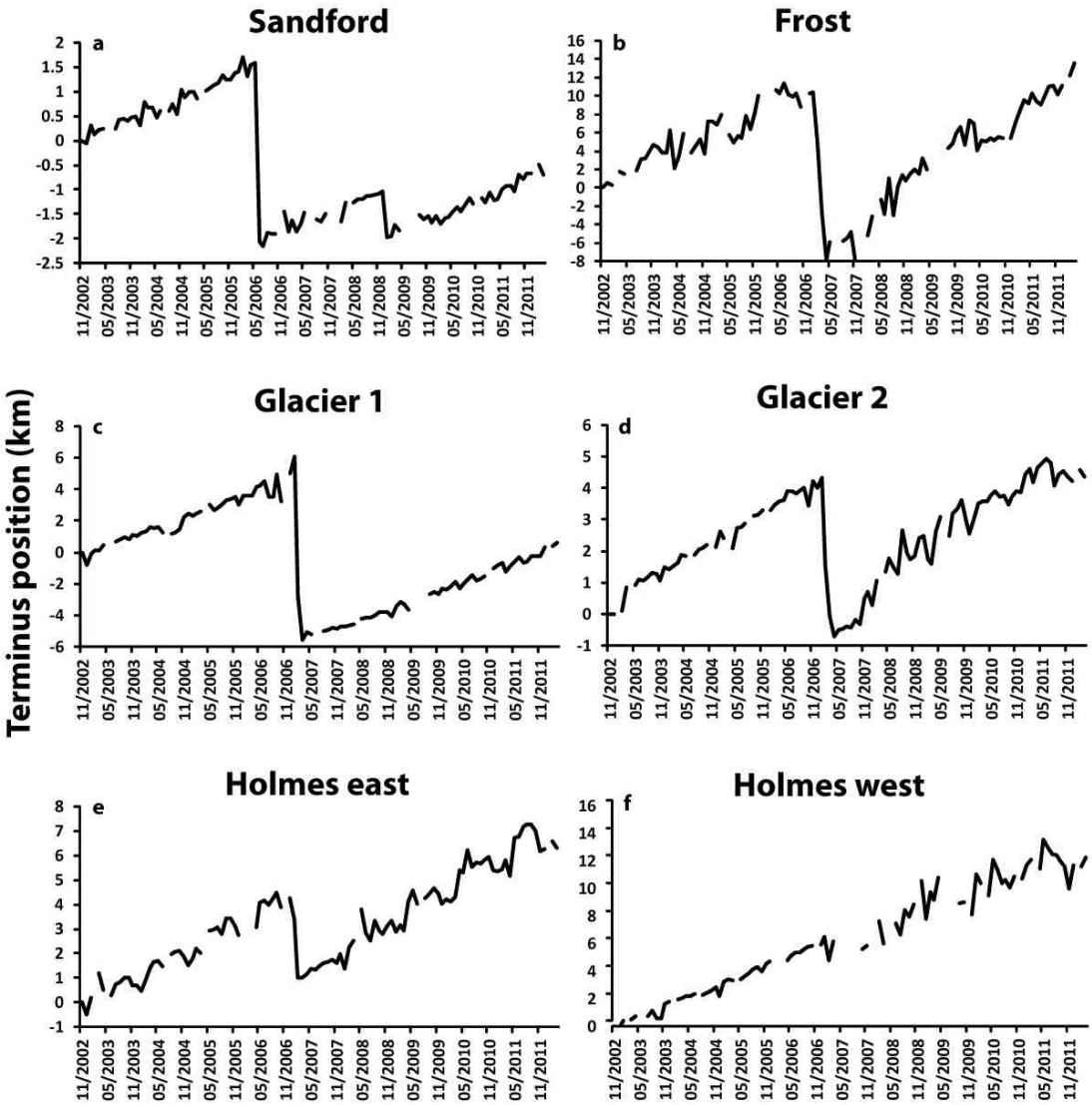

Figure 4.2: Terminus position change of six glaciers in Porpoise Bay between November 2002 and March 2012. Note the major calving event in January 2007 for 5 of the glaciers. Terminus position measurements are subject to +/- 500 m. Note the different scales on y-axis.

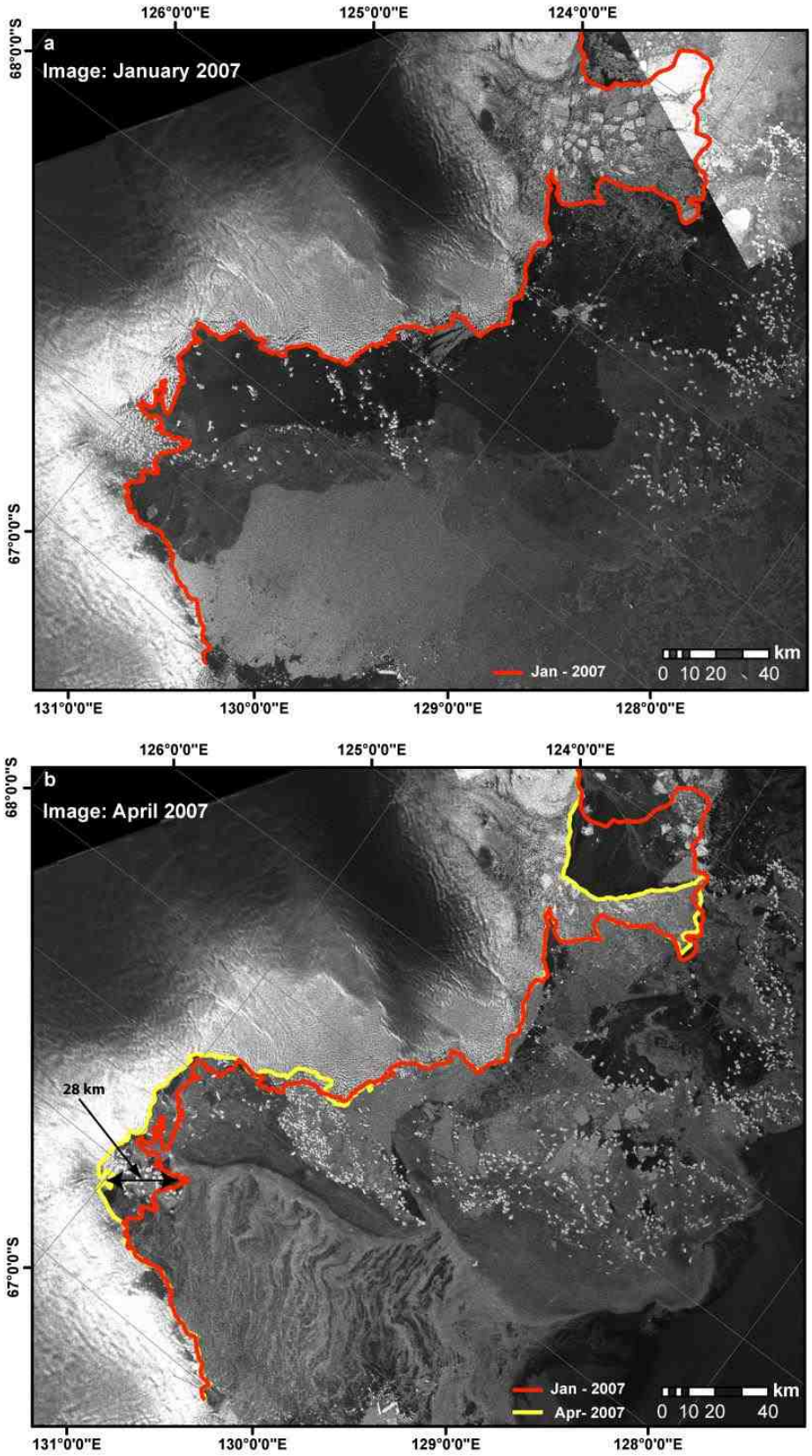

Figure 4.3: Envisat ASAR WSM imagery in January 2007 **a)** and April 2007 **b)**, which are immediately prior to and after a near-simultaneous calving event in Porpoise Bay. Red line shows terminus positions in January 2007 and yellow line shows the positions in April 2007.

4.4.2 Evolution of the 2007 calving event

A series of eight sub-monthly images between December 11th 2006 and April 8th 2007 shows the evolution of the 2007 calving event (Fig. 4.4). Between December 11th 2006 and January 2nd 2007, the landfast sea ice edge retreats past Sandford Glacier to the edge of Frost Glacier and there is some evidence of sea ice fracturing in front of the terminus of Glacier 2 (Fig. 4.4b). From January 2nd to January 9th a small section (~40 km^2) of calved ice broke away from Frost Glacier, approximately in line with the retreat edge of landfast sea ice (Fig. 4.4c). By January 25th, significant fracturing in the landfast sea ice had developed, and detached icebergs from Frost, Glaciers 1, Glacier 2 and Holmes (East) Glaciers begin to breakaway (Fig. 4.4d). This process of rapid sea ice breakup in the east section of the bay and the disintegration of sections of Frost glacier, Glacier 1, Glacier 2 and Holmes (East) Glaciers continues up to March 10th 2007 (Fig. 4.4g). In contrast, the west section of Porpoise Bay remains covered in sea ice in front of Holmes (West) Glacier, which does not calve throughout this event. By April 8th, the calving event had ended with a large number of calved icebergs now occupying the bay (Fig. 4.4h).

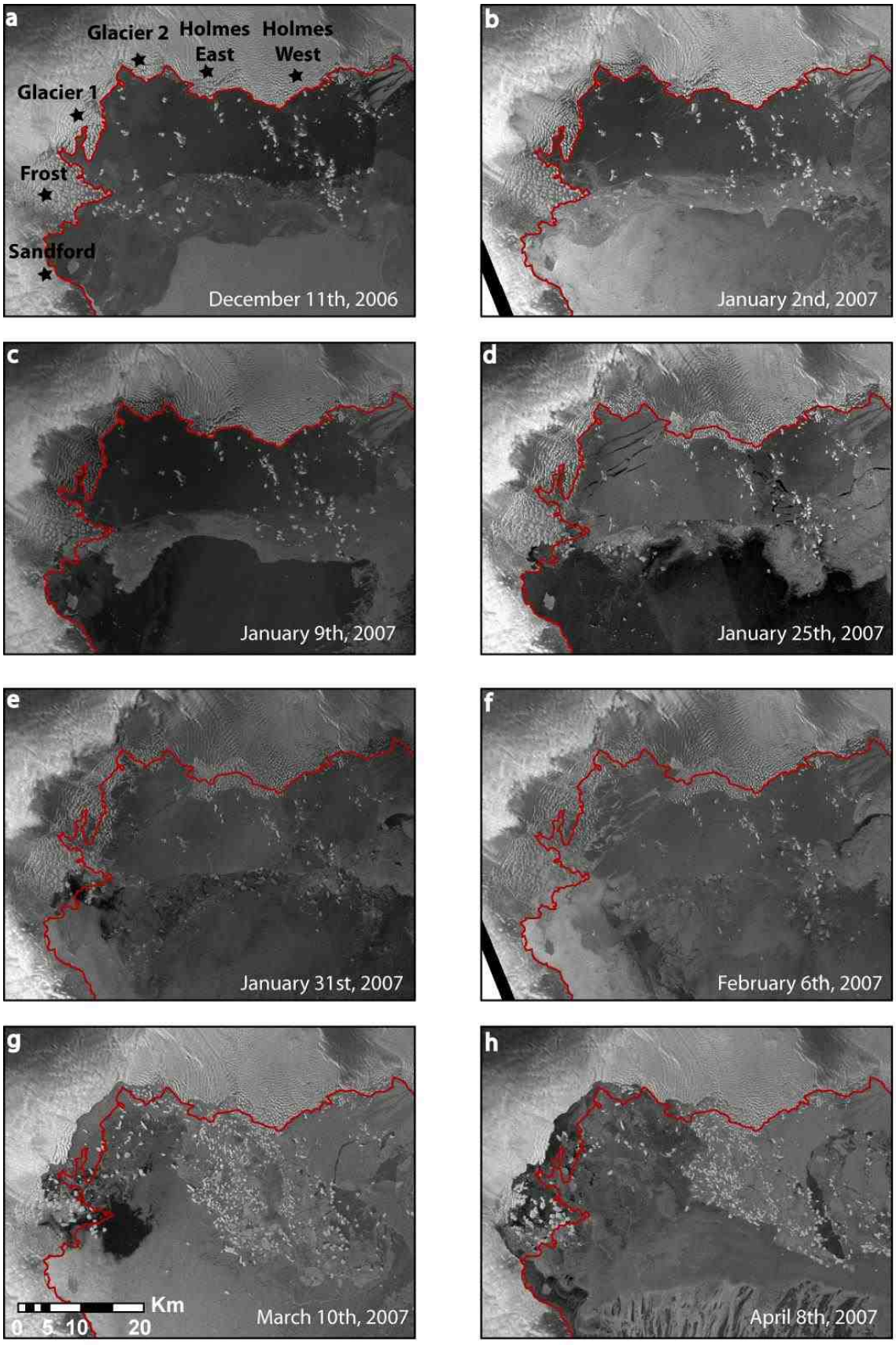

Figure 4.4: Envisat ASAR WSM imagery showing the evolution of the 2007 calving event. Red line shows the terminus positions from December 11th 2006 on all panels.

4.4.3 2016 calving event

During the preparation of this manuscript (submitted for open discussion on 10 June 2016) satellite observations of Porpoise Bay revealed that another large near-simultaneous disintegration of glacier tongues in Porpoise Bay was underway. This event was initiated on March 19th where the edge of the multi-year sea ice retreated to the Holmes (West) Glacier terminus, removing multi-year sea ice which was at least 14 years old. By March 24th this had led to the rapid disintegration of an 800 km^2 section of the Holmes (West) Glacier tongue (Fig. 4.5). This was the first observed calving of Holmes (West) glacier at any stage between November 2002 and March 2016. Throughout March and April the break-up of sea ice continued and by May 13th it had propagated to the terminus of Frost Glacier, resulting in the disintegration of large section of its tongue (Fig. 4.6). By 24th July sea ice had been removed from all glacier termini in Porpoise Bay at some point during the event, resulting in a total of ~2,200 km^2 ice being removed from glacier tongues (Fig. 4.6).

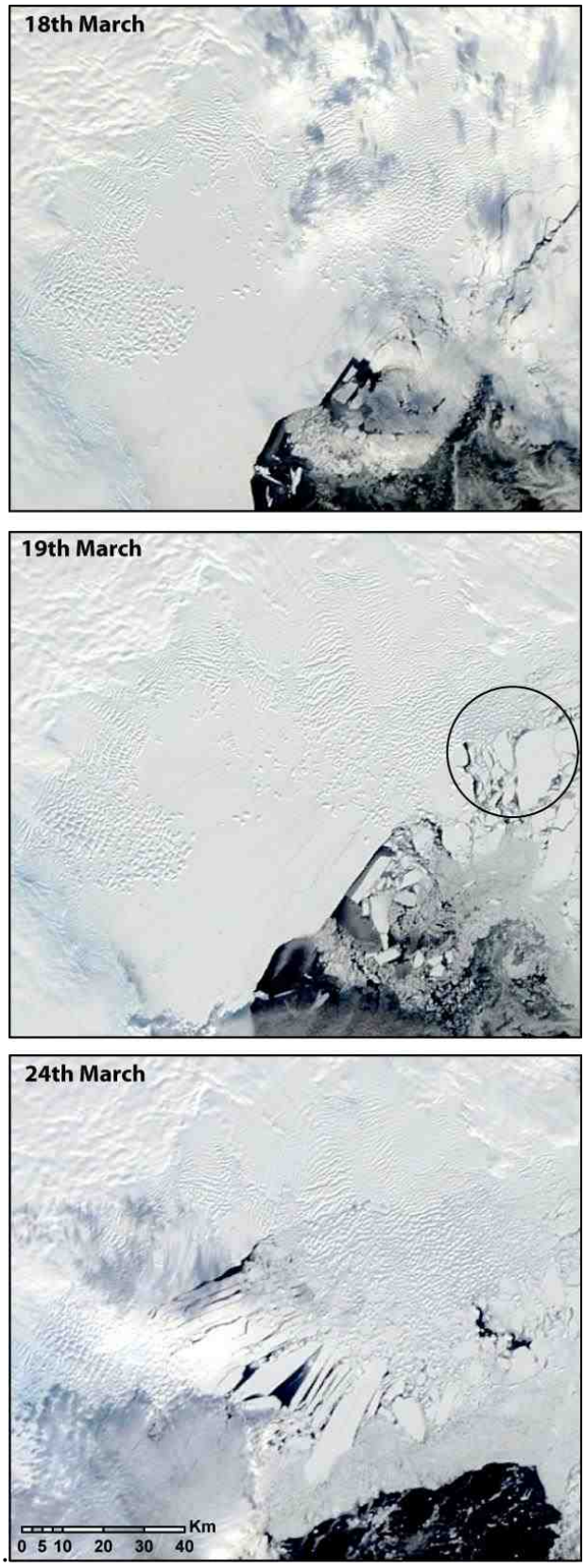

Figure 4.5: MODIS imagery showing the initial stages of disintegration of Holmes (West) Glacier in March 2016. On March 19th a large section of sea ice breaks away from the terminus (circled), initiating the rapid disintegration process. By the 24th March an 800 km^2 section of Holmes (West) Glacier tongue had disintegrated.

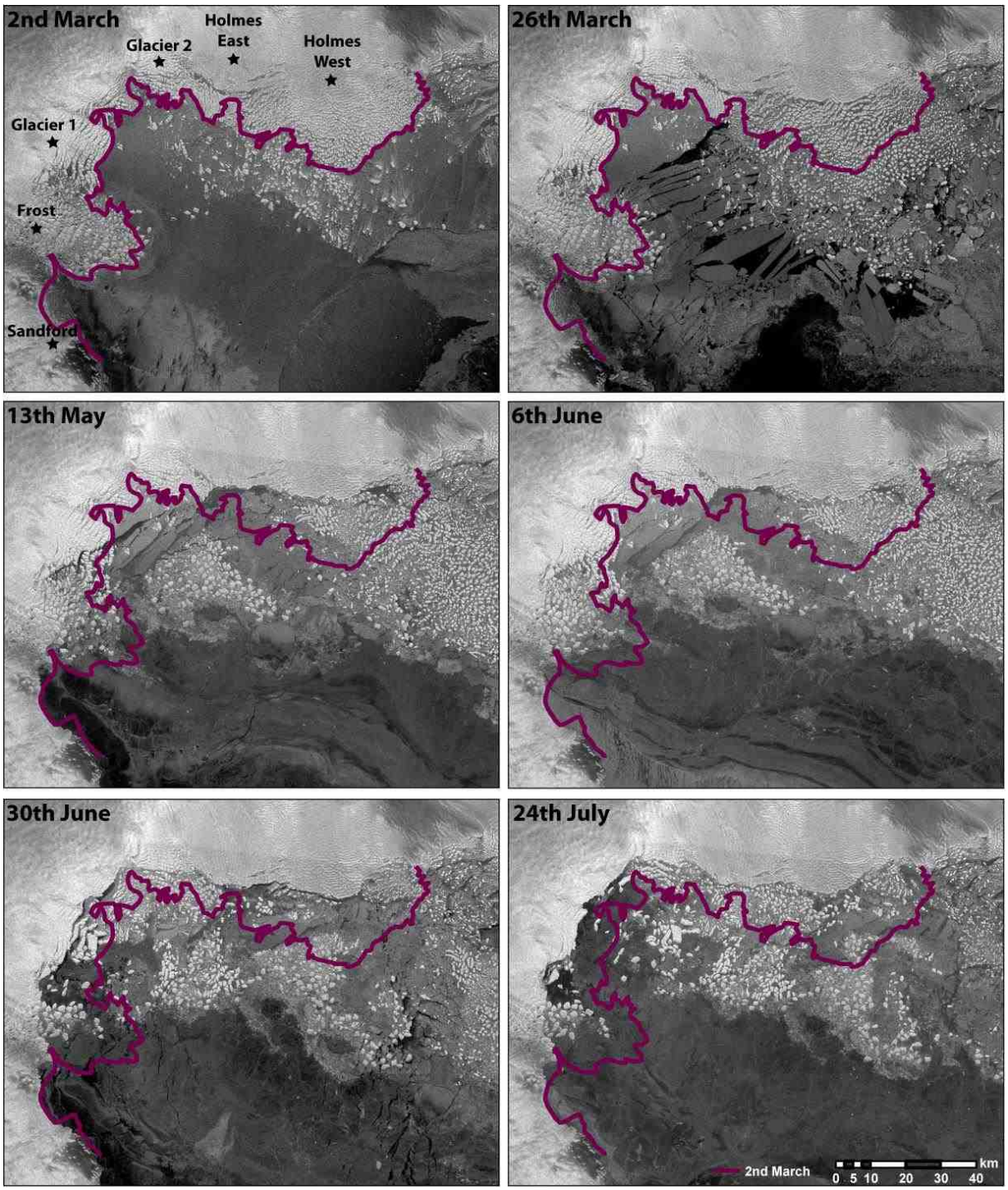

Figure 4.6: Sentinel-1 imagery showing the evolution of the 2016 calving event. Purple line shows the terminus position from 2nd March on all panels.

4.4.4 The link between sea ice and calving in Porpoise Bay

Analysis of mean monthly sea ice concentration anomalies in Porpoise Bay between November 2002 and June 2016 (Fig. 4.7) reveals a major negative sea ice anomaly occurred between January and June 2007, where monthly sea ice concentrations were between 35% and 40% below average. This is the only noticeable (>20%) negative ice anomaly in Porpoise Bay and it coincides with the major January 2007 calving event (see

Fig. 4.4). However, despite satellite imagery showing the break-up of sea ice prior to the 2016 calving event (Fig. 4.5 and 4.6), in a similar manner to that in 2007 (e.g. Fig. 4.4), no large negative anomaly is present in the sea ice concentration data. This is likely to reflect the production of a large armada of icebergs following the disintegration of Holmes (West) Glacier (e.g. Fig. 4.6), helping to promote a rapid sea ice reformation in the vicinity of Porpoise Bay. Furthermore, we note that the smaller calving events of Sandford and Frost Glaciers all take place after sea ice had retreated away from the glacier terminus (Fig. 4.8). Indeed, throughout the study period, there is no evidence of any calving events taking place with sea ice proximal to glacier termini. This suggests that glaciers in Porpoise Bay are very unlikely to calve with sea ice present at their termini.

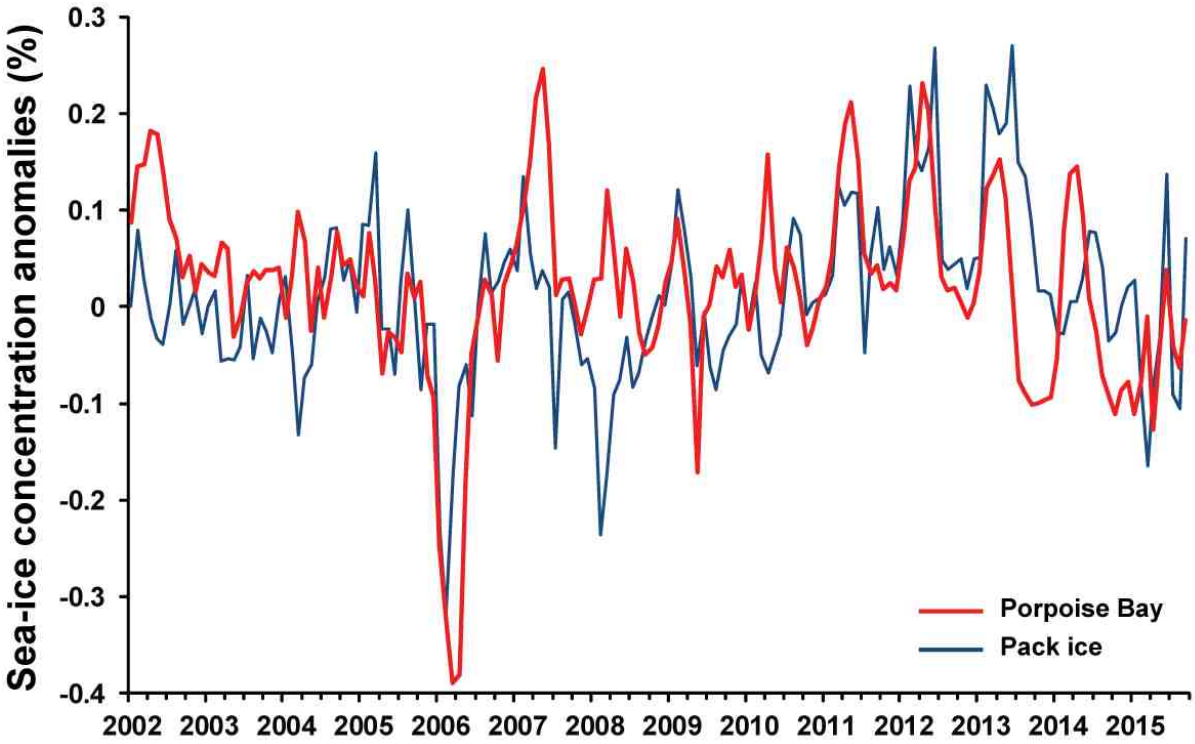

Figure 4.7: Mean monthly sea ice concentration anomalies from November 2002 to June 2016. The red line indicates sea ice concentration anomalies in Porpoise Bay and the blue line indicates pack-ice-concentration anomalies.

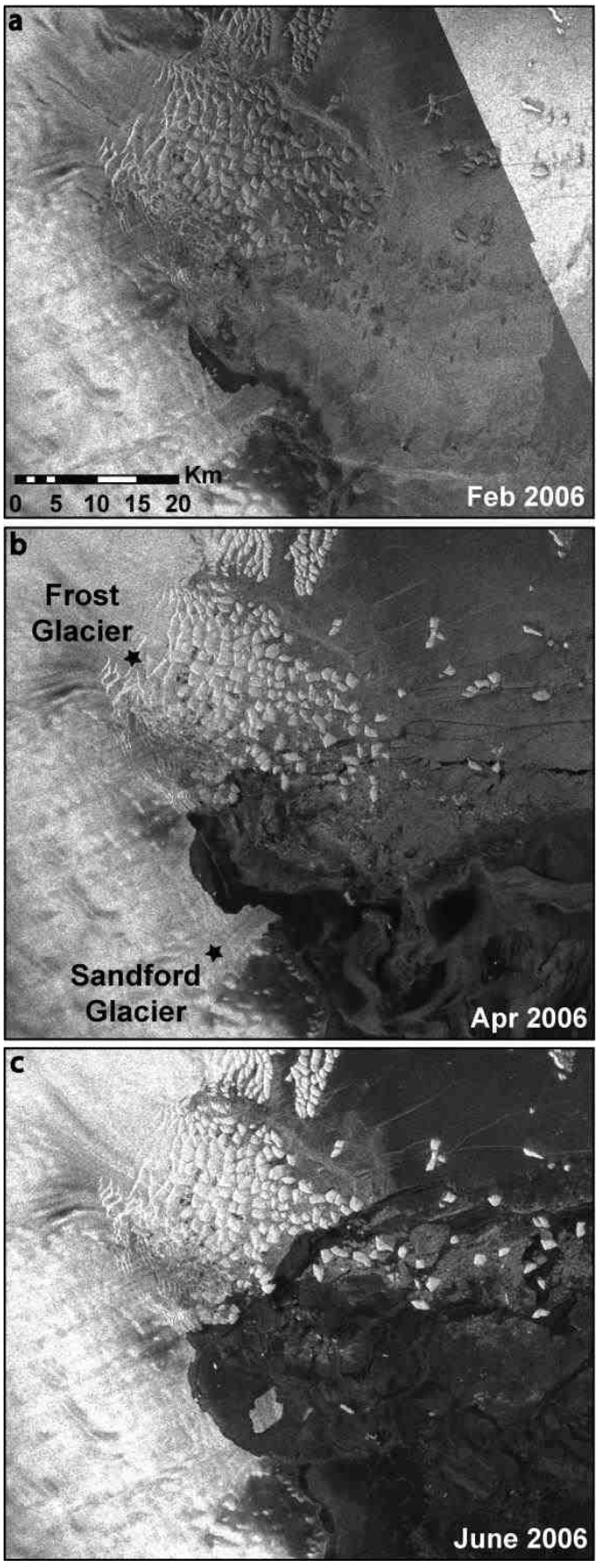

Figure 4.8: Time series of Frost and Sandford Glaciers calving showing that sea ice clears prior to calving and dispersal of icebergs.

4.4.5. Atmospheric circulation anomalies

Atmospheric circulation anomalies in the months preceding the January 2007 and March 2016 sea ice break-ups reveal contrasting conditions. In the austral summer which preceded the January 2007 break-up there were strong positive SST anomalies and atmospheric-circulation anomalies throughout December 2005 (Fig. 4.9a). The circulation anomaly was reflected in a strong easterly airflow offshore from Porpoise Bay. This is associated with a band of cooler SSTs close to the coastline and the northward shift of the Antarctic Coastal Current in response to the weakened westerlies (e.g. Langlais et al., 2015). A weakened zonal flow combined with high SST in the South Pacific would allow the advection of warmer maritime air into Porpoise Bay. Consistent with warmer air, are estimates of exceptionally high melt values in Porpoise Bay during December 2005 derived from the RACMO2.3, which contrasts with the longer-term trend of cooling (Fig. 4.10). However, the December 2005 anomaly was short-lived and, by January 2006, the wind-field conditions were close to average, although SST remained slightly higher than average (Fig. 4.9b).

In December 2006 and January 2007, which are the months immediately before and during the break-up of sea ice, atmospheric conditions were close to average, with very little deviation from mean conditions in the wind field and a small negative SST anomaly (Fig. 4.9c). However, on January 11th 2007, which is the estimated date of sea ice break-up from AMSR-E data, we note that there were very high winds close to Porpoise Bay (Fig. 4.11a).

In contrast to the months preceding the January 2007 event, we find little deviation from average conditions prior to the March 2016 break-up event. In the austral summer which preceded the 2016 break-up (2014/15), there was little deviation from the average wind field and only a small increase from average SSTs (Fig 4.9d). In December and January 2015/16, there was evidence for a small increase in the strength of westerly winds, and cooler SSTs in the South Pacific (Fig. 4.9e). However, in February and March 2016 there was no change from the average wind field and slightly cooler SSTs (Fig. 4.9f).We note, however, that there was a low pressure system passing across Porpoise Bay on March 19th 2016, the estimated date of break-up initiation (Fig. 4.11b).

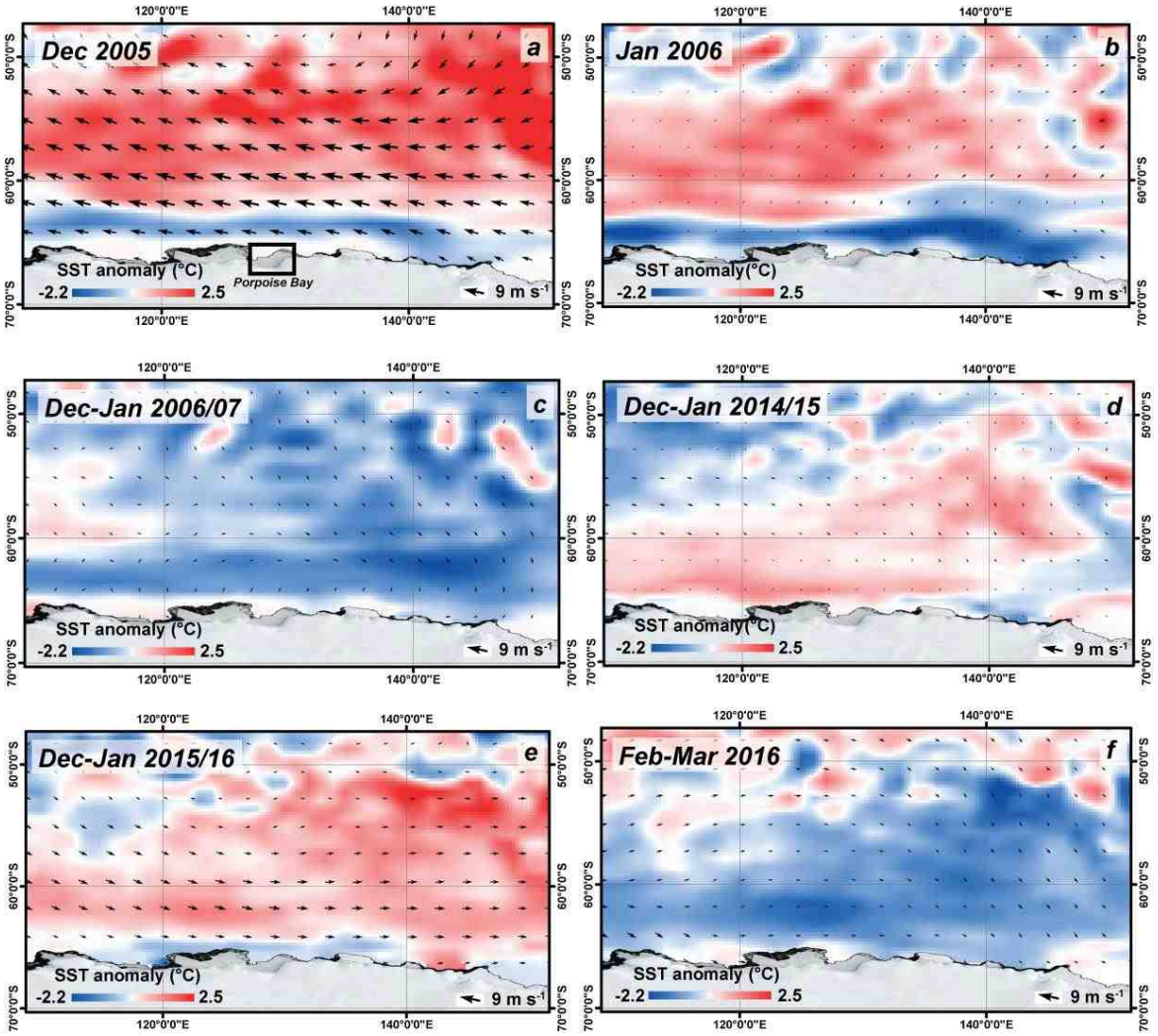

Figure 4.9: Mean monthly ERA-Interim derived wind-field and sea-surface-temperature anomalies in the months preceding the 2007 and 2016 sea ice break-ups. **a)** December 2005 **b)** January 2006 **c)** Mean December and January 2006/07 **d)** Mean December and January 2014/15 **e)** Mean December and January 2015/16 **f)** Mean February and March 2016.

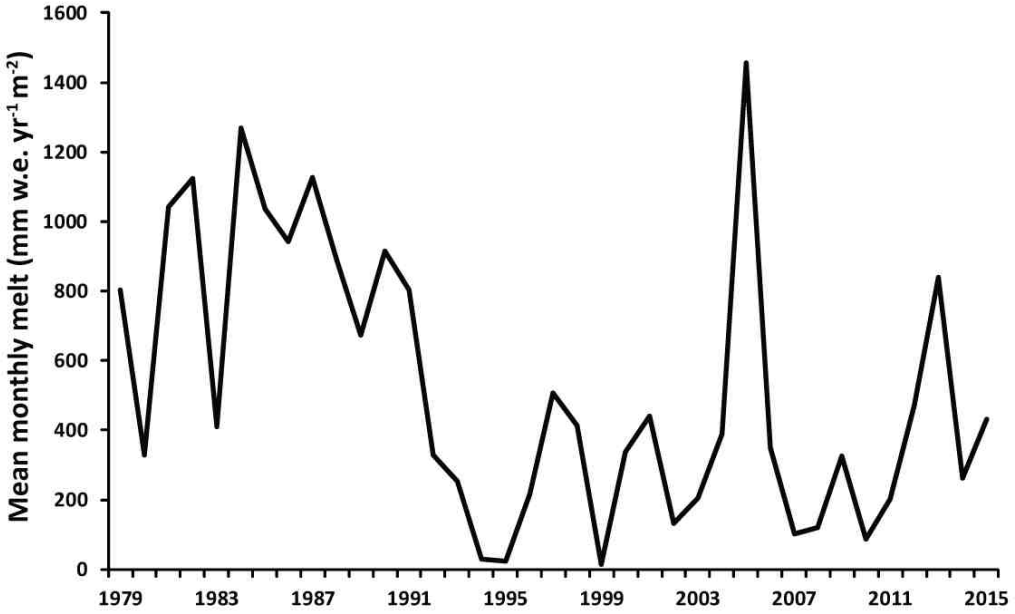

Figure 10: Mean RACMO2.3-derived December melt 1979-2015 in Porpoise Bay.

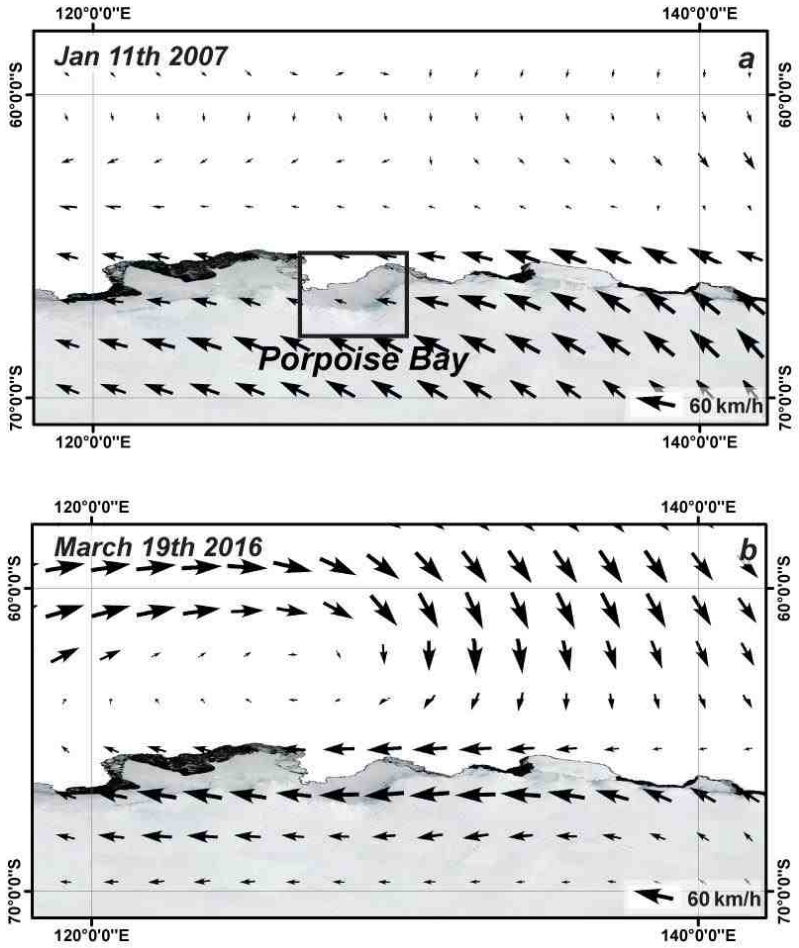

Figure 4.11: ERA-Interim derived wind fields for the estimated dates of sea ice break-up. **a)** January 11th 2007 and **b)** March 19th 2016

4.4.6 Holmes (West) Glacier calving cycle

Through mapping the terminus position in all available satellite imagery (Table 4.1) dating back to 1963, we are able to reconstruct large calving events on the largest glacier in Porpoise bay, Holmes (West) (Fig. 4.12). On the basis that a large calving event is likely during the largest sea ice break-up events, we estimate the date of calving based on sea ice concentrations in Porpoise Bay when satellite imagery is not available. Our estimates suggest that Holmes (West) Glacier calves at approximately the same position in each calving cycle, including the most recent calving event in March 2016.

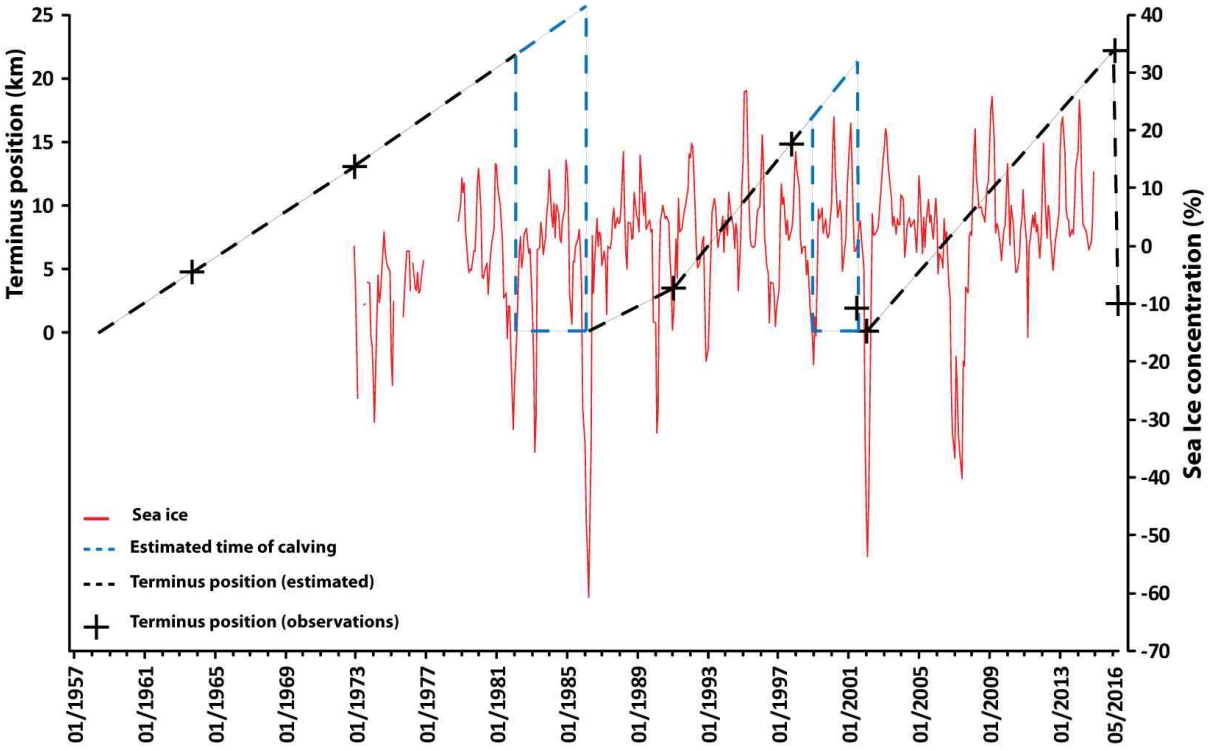

Figure 4.12: Reconstruction of the calving cycle of Holmes (West) Glacier. All observations are represented by black crosses. The estimated terminus position is then extrapolated linearly between each observation. In periods without observations the date of calving is estimated by negative sea ice concentration anomalies.

4.5 Discussion

4.5.1 Sea ice break-up and the disintegration of glacier tongues in Porpoise Bay

We report a major, near-synchronous calving event in January 2007 and a similar event that was initiated in 2016. This resulted in ~2,900 km^2 and 2,200 km^2 of ice, respectively, being removed from glacier tongues in the Porpoise Bay region of East Antarctica. These calving events are comparable to some of the largest disintegration events ever observed in Antarctica (e.g. Larsen A in 1995, 4,200 km^2 and Larsen B in 2002, 3,250 km^2); and is the

largest event to have been observed in East Antarctica. However, they differ from those observed on the ice shelves of the Antarctic Peninsula, in that they may be more closely linked to a cycle of glacier advance and retreat, as opposed to a catastrophic collapse that may be unprecedented.

Given the correspondence between the sea ice and glacier-terminus changes, we suggest that these disintegration events were driven by the break-up of the multi-year landfast sea ice which usually occupies Porpoise Bay and the subsequent loss of buttressing of the glacier termini. A somewhat similar mechanism has been widely documented in Greenland, where the dynamics of sea ice melange in proglacial fjords have been linked to inter-annual variations in glacier terminus position (Amundson et al., 2010; Carr et al., 2013; Todd and Christoffersen, 2014; Cassotto et al., 2015). Additionally, the mechanical coupling between thick multi-year landfast sea ice and glacier tongues may have acted to stabilise and delay the calving of the Mertz Glacier tongue (Massom et al., 2010) and Brunt/Stancomb-Wills Ice Shelf system (Khazendar et al., 2009). However, this is the first observational evidence directly linking multi-year landfast sea ice break-up to the large-scale and rapid disintegration of glacier tongues. This is important because landfast sea ice is highly sensitive to climate (Heil, 2006; Mahoney et al., 2007) and, if future changes in climate were to result in a change to the persistence and/or stability of the landfast ice in Porpoise Bay, it may result in detrimental effects on glacier tongue stability. An important question, therefore, is: what process(es) cause sea ice break-up?

4.5.2 What caused the January 2007 and March 2016 sea ice break-ups?

The majority of sea ice in Porpoise Bay is multi-year sea ice (Fraser et al., 2012), and it is likely that various climatic processes operating over different timescales contributed to the January 2007 sea ice break-up event. Although there are no long-term observations of multi-year sea ice thickness in Porpoise Bay, observations and models of the annual cycle of multi-year sea ice in other regions of East Antarctica suggest that multi-year sea ice thickens seasonally and thins each year (Lei et al., 2010; Sugimoto et al., 2016; Yang et al., 2016). Therefore, the relative strength, stability and thickness of multi-year sea ice over a given period are driven not only by synoptic conditions in the short term (days/weeks), but also by climatic conditions in the preceding years.

In the austral summer (2005/06) which preceded the break-up event in January 2007, there was a strong easterly airflow anomaly throughout December 2005 directly adjacent to

Porpoise Bay (Fig. 4.9a). This anomaly represents the weakening of the band of westerly winds which encircle Antarctica, and is reflected in an exceptionally negative Southern Annular Mode (SAM) index in December 2005 (Marshall, 2003). This contrasts with the long-term trend for a positive SAM index (Marshall, 2007; Miles et al., 2013). A weaker band of westerly winds combined with anomalously high SST in the Southern Pacific (Fig. 4.9a) would allow a greater advection of warmer maritime air towards Porpoise Bay. Indeed, RACMO2.3-derived surface-melt estimates place December 2005 as the second highest mean melt month (1979-2015) on the modelled output in Porpoise Bay (Fig. 4.10). To place this month into perspective, we note that it would rank above the average melt values of all Decembers and Januarys since 2000 on the remnants of Larsen B Ice Shelf. Comparing MODIS satellite imagery from before and after December 2005 reveals the development of significant fracturing in the multi-year sea ice (Fig 4.13a, b). These same fractures remain visible prior to the break-out event in January 2007 and, when the multi-year sea ice begins to break-up, it ruptures along these pre-existing weaknesses (Fig. 4.13c). As such, this strongly suggests that the atmospheric-circulation anomalies of December 2005 played an important role in the January 2007 multi-year sea ice break-up and near-simultaneous calving event.

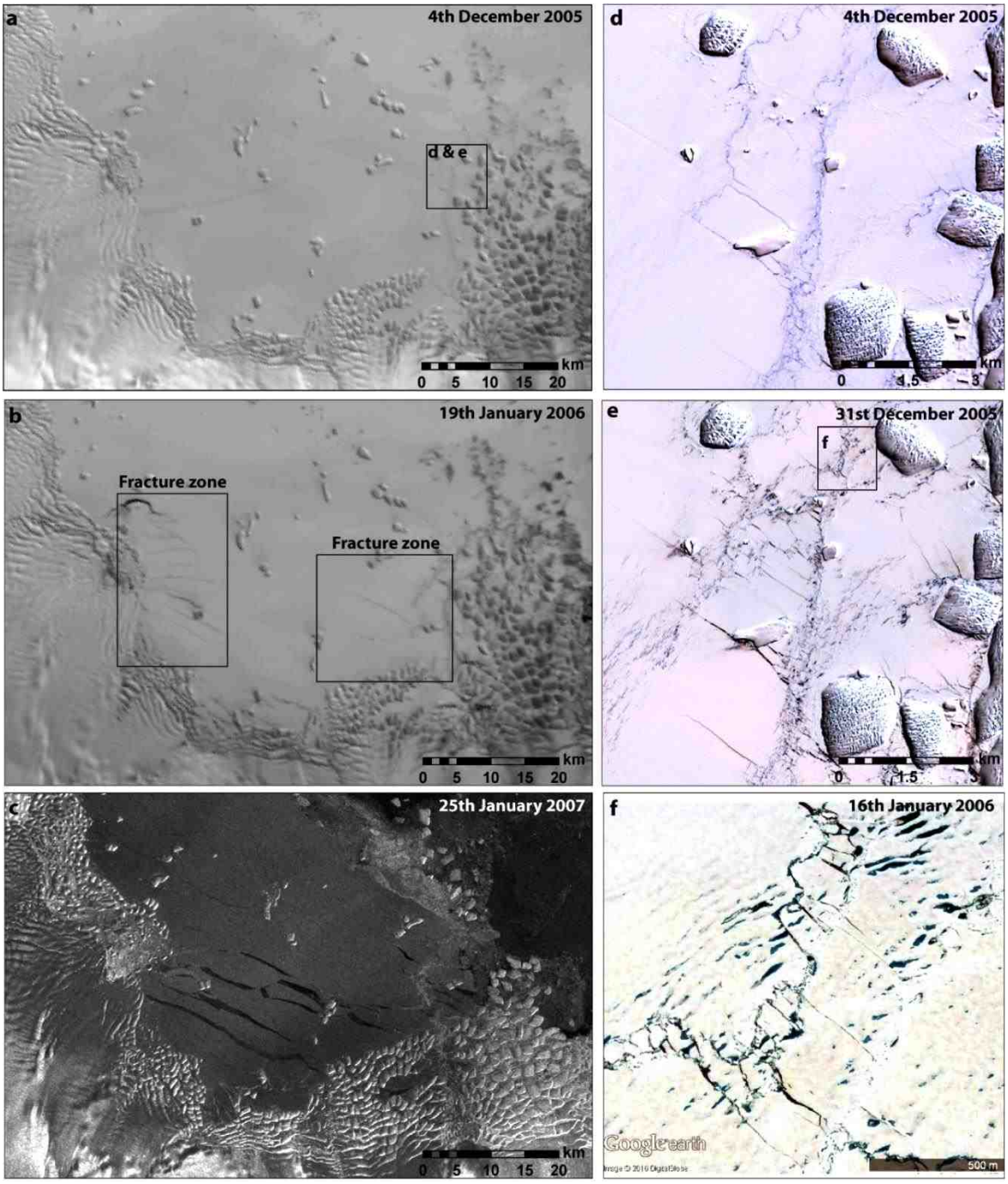

Figure 13: a and b) MODIS imagery showing the development of fractures in the landfast sea ice between 4th December 2005 and 19th January 2006 (http://dx.doi.org/10.7265/N5NC5Z4N.) **c)** The landfast sea ice ruptures along some of the same fractures which formed in December/January 2005/06, eventually leading to complete break-up in January 2007. **d and e)** ASTER imagery showing surface melt features and the development of smaller fracture between 4th and 31st December 2005. **f)** High resolution optical satellite imagery from 16th January 2006 showing sea ice fracturing and surface melt ponding. This image was obtained from Google Earth.

The break-up of landfast sea ice has been linked to dynamic wind events and ocean swell (Heil, 2006; Ushio, 2006; Fraser et al., 2012). Thus, it is possible that the wind anomalies in December 2005 may have been important in initiating the fractures observed in the sea ice in Porpoise Bay, through changing the direction and/or intensity of oceanic swell. However, this mechanism is thought to be at its most potent during anomalously low pack-ice concentrations because pack ice can act as a buffer to any oceanic swell (Langhorne et al., 2001; Heil, 2006; Fraser, 2012). That said, we note that pack-ice concentrations offshore from Porpoise Bay were around average during December 2005 (Fig. 4.7). This may suggest that there are other mechanisms that were important in the weakening of the multi-year sea ice in Porpoise Bay in December 2005.

In the Arctic, sea ice melt-ponding along pre-existing weaknesses has been widely reported to precede sea ice break-up (Ehn et al., 2011; Petrich et al., 2012; Landy et al., 2014; Schroder et al., 2014; Arntsen et al., 2015). Despite its importance in the Arctic, it has yet to be considered as a possible factor in landfast sea ice break-up in coastal Antarctica. As a consequence of the high melt throughout December 2005, the growth of sea ice surface ponding would be expected, in addition to surface thinning of the sea ice. High-resolution cloud-free optical satellite coverage of Porpoise Bay throughout December 2005 is limited, but ASTER imagery in the vicinity of Frost Glacier on the 4th and 31st December 2005 shows surface melt features and the development of fractures throughout the month (Fig. 4.13d,e), similar to those observed elsewhere in East Antarctica (Kingslake et al., 2015; Langley et al., 2016). High-resolution imagery from 16th January 2006 (via GoogleEarth) shows the development of melt ponds on the sea ice surface (Fig. 4.13f). Therefore, it is possible that surface melt had some impact on the fracturing of landfast sea ice in Porpoise Bay. This may have caused hydro-fracturing of pre-existing depressions in the landfast ice or surface thinning may have made it more vulnerable to fracturing through ocean swell or internal stresses. Additionally, the subsequent refreezing of some melt ponds may temporally inhibit basal ice growth, potentially weakening the multi-year sea ice and predisposing it to future break-up (Flocco et al., 2015). It is important to note that the atmospheric circulation anomalies which favoured the development of fractures in the multi-year sea ice in December 2005 were short-lived. By January 2006, atmospheric conditions had returned close to average (Fig. 4.9b) and remained so until the austral winter, where sea ice break-up is less likely. This may explain the lag between the onset of sea ice fracturing in December 2005 and its eventual break-up in the following summer (January 2007).

Consistent with the notion that the multi-year sea ice was already in a weakened state prior to its break-up in 2007, is that the break-up occurred in January, several weeks before the likely annual minima in multi-year sea ice thickness (Yang et al., 2016; Lei et al., 2010) and landfast ice extent (Fraser et al., 2012). Additionally, atmospheric circulation anomalies indicate little deviation from average conditions in the immediate months preceding break-up (Fig. 4.9b, c), suggesting that atmospheric conditions were favourable for sea ice stability. Despite this, a synoptic event is still likely required to force the break-up in January 2007. Daily sea ice concentrations in Porpoise Bay in January 2007 show a sharp decrease in sea ice concentrations after 12th January, representing the onset of sea ice break-out (Fig 4.14). This is preceded by a strong melt event recorded by the RACMO2.3 model, centred on January 11th, which may represent a low-pressure system. Indeed, ERA-Interim estimates of the wind field suggest strong south-easterly winds in the vicinity of Porpoise Bay (Fig 4.11 a). Unlike in December 2005, pack-ice concentrations offshore of Porpoise Bay were anomalously low (Fig. 4.7). Therefore, with less pack-ice buttressing, it is possible that the melt event, high winds and associated ocean swell may have initiated the break-up of the already weakened multi-year sea ice in Porpoise Bay.

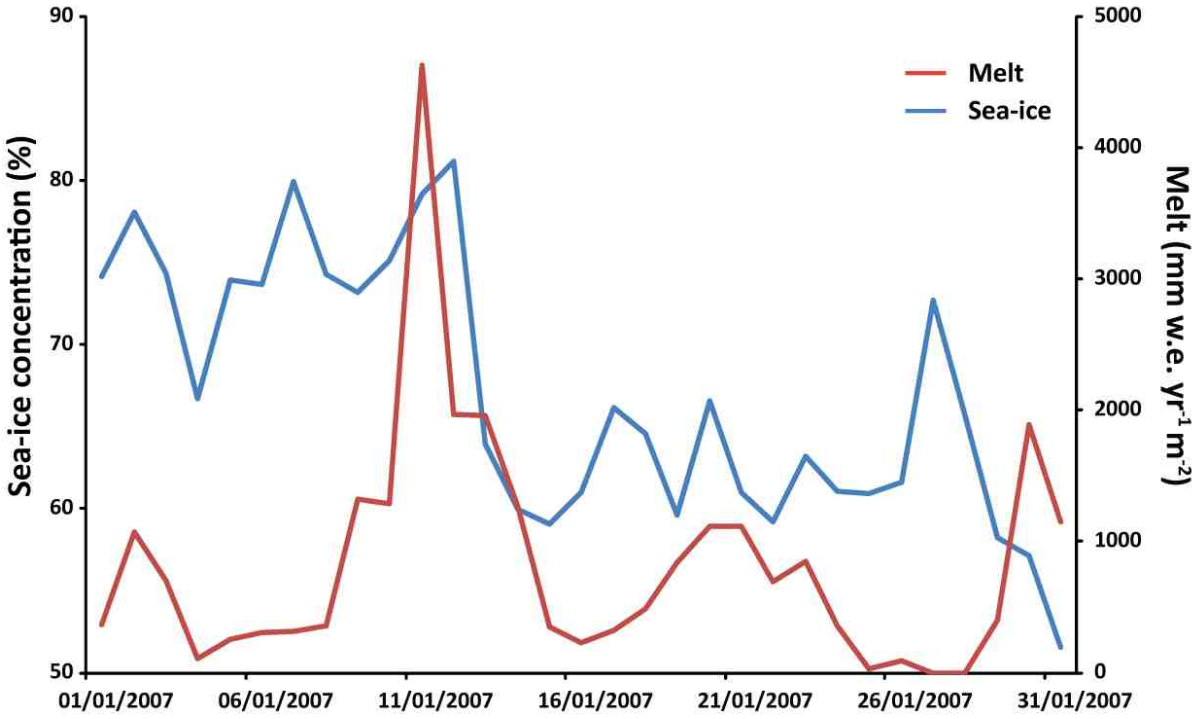

Figure 4.14: Daily sea ice concentrations and RACMO2.3 derived melt during January 2007 in Porpoise Bay. Sea ice concentrations start to decrease after the melt peak on January 11th.

In contrast to January 2007, we find no link between atmospheric-circulation anomalies and the March 2016 sea ice break-up. In the preceding months to the March 2016 break-up, wind and SST anomalies indicate conditions close to average conditions favouring sea ice stability (Fig. 4.9 d, e, f). This suggests another process was important in driving the March 2016 sea ice break-up. A key difference between the 2007 and 2016 event is that the largest glacier in the bay, Holmes (West) Glacier, only calved in the 2016 event. Analysis of its calving cycle (Fig. 4.12) indicates that it calves at roughly the same position in each cycle and that its relative position in early 2016 suggests that calving was 'overdue' (Fig. 4.12). This indicates that the calving cycle of Holmes (West) Glacier has not necessarily been driven by atmospheric circulation anomalies. Instead, we suggest that as Holmes (West) Glacier advances, it slowly pushes the multi-year sea ice attached to its terminus further towards the open ocean to the point where the sea ice attached to the glacier tongue becomes more unstable. This could be influenced by local bathymetry and oceanic circulation, but no observations are available. However, once the multi-year sea ice reaches an unstable state, break-up is still likely to be forced by a synoptic event. This is consistent with our observations, where ERA-Interim derived wind fields show the presence of a low-pressure system close to Porpoise Bay on the estimated date of sea ice break-up in March 2016 (Fig. 4.11b). Whilst we suggest that the March 2016 sea ice break-up and subsequent calving of Holmes (West) are currently part of a predictable cycle, we note that this could be vulnerable to change if any future changes in climate alter the persistence and/or strength of the multi-year sea ice, which is usually attached to the glacier terminus.

4.6 Conclusion

We identify two large near-simultaneous calving events in January 2007 and March 2016 which were driven by the break-up of the multi-year landfast sea ice which usually occupies the bay. This provides a previously unreported mechanism for the rapid disintegration of floating glacier tongues in East Antarctica, adding to the growing body of research linking glacier tongue stability to the mechanical coupling of landfast ice (e.g. Khazander et al., 2009; Massom et al., 2010). Our results suggest that multi-year sea ice break-ups in 2007 and 2016 in Porpoise Bay were driven by different mechanisms. We link the 2007 event to atmospheric-circulation anomalies in December 2005 weakening multi-year sea ice through a combination of surface melt and a change in wind direction, prior to its eventual break-up in 2007. This is in contrast to the March 2016 event, which

we suggest is part of a longer-term cycle based on the terminus position of Holmes (West) Glacier that was able to advance and push sea ice out of the bay. The link between sea ice break-up and major calving of glacier tongues is especially important because it suggests that, with predictions of future warming (DeConto and Pollard, 2016), multi-year landfast ice may become less persistent. Therefore, the glacier tongues which depend on landfast ice for stability may become less stable in the future. In a wider context, our results also highlight the complex nature of the mechanisms which drive glacier calving position in Antarctica. Whilst regional trends in terminus position can be driven by ocean-climate-sea ice interaction (e.g. Miles et al., 2013; 2016), individual glaciers and individual calving events have the potential to respond differently to similar climatic forcing.

Chapter 5: Dynamic instabilities at the Cook Glacier in the recent past

Miles, B.W.J., Stokes, C.R. & Jamieson, S.S.R. 2017. Dynamic instabilities at the Cook Glacier in the recent past. *To be submitted.*

Abstract: Cook Glacier is a major outlet that drains a large proportion of the Wilkes Subglacial Basin, which is thought to be vulnerable to marine ice sheet instability and is likely to have made substantial sea level contributions during past warm periods. Despite this, Cook Glacier is currently considered to be relatively stable because of the absence of dynamic thinning in the past decade. However, through analysing glacier velocity from 1973-2017, rates of ice shelf thickness changes from 1994-2012, and ice-front position from 1947-2017, we show that there have been dynamic instabilities in the recent past. Specifically, we show that Cook West Ice Shelf retreated ~13 km to at or near its current grounding line between 1974 and 1989, which lead to a doubling in the velocity of the inland ice which the former ice shelf buttressed. However, its ice-front has since been stabilised by landfast sea ice, which now semi-permanently occupies the embayment formed by the initial ice shelf retreat. The remaining, and larger, Cook East ice shelf rapidly thinned by 7.5 m yr^{-1} between 1998 and 2002, which we link to a stepped increase in its velocity of ~10% during the same time period. We link this to periodic intrusions of warm water, which have the potential to rapidly thin the Cook East Ice Shelf because of its low steady-state basal melt rate. Given the vulnerable topographic configuration of the Wilkes Subglacial Basin and the observed sensitivity of Cook Glacier to changes in its ice shelves in the recent past, we suggest that it is a prime candidate to make contributions to future sea level if intrusions of warm water persist in the future.

5.1 Introduction

Ice which is grounded well below sea level in marine basins is potentially vulnerable to marine ice sheet instability. This is because an initial grounding line retreat into deeper water creates an unstable and self-sustaining feedback leading to increased ice discharge and inland thinning (Weertman, 1974; Mercer et al., 1978; Hughes, 1981). Recent geological evidence (Young et al., 2011; Cook et al., 2013; Greenbaum et al., 2015; Aitken et al., 2016) and improvements in numerical modelling (DeConto and Pollard, 2016) have both suggested that there were major retreats of the marine basins of East Antarctica during the warm periods of the Pliocene, which may have made substantial contributions to sea

level (e.g. several metres). This is important because the warm periods of the Pliocene may represent the best analogue for near future climate conditions.

The Wilkes Subglacial Basin (WSB) in East Antarctica contains enough ice grounded deep below sea level to raise sea level by 3-4 m (Mengel and Levermann, 2014). Cook Glacier drains a large proportion of the WSB and discharges around 40 km^3 of ice per year, which is one of the highest rates of all outlet glaciers in both Antarctica and Greenland (Stokes et al, 2016). Dynamical ice-sheet modelling of the present day ice-sheet margin of the WSB shows that the stability of the basin is controlled by a relatively small band of coastal ice in the vicinity of Cook Glacier (Mengel and Levermann, 2104). As such, Cook Glacier has drawn parallels with Pine Island, Thwaites and Totten Glaciers in that they are all major outlet glaciers that drain marine basins and have the potential to rapidly increase their discharge into the ocean through marine ice sheet instability (Shepherd and Wingham, 2008). Unlike Pine Island, Thwaites and Totten glaciers, there have been very few process-based studies analysing recent changes in glacier behaviour and its vulnerability to future warming over the coming decades and centuries is uncertain (IPCC, 2013). The majority of numerical models now predict a sea level contribution from the WSB in the coming decades to centuries (e.g. Ritz et al., 2015; Golledge et al., 2015; DeConto and Pollard, 2016), although they disagree on the timing and magnitude of these contributions. In order to constrain estimates of future sea level contributions of the WSB, it is imperative to increase our understanding of glacier dynamics in the recent past, which also serves as useful calibration data for numerical modelling (Ritz et al., 2015).

Crucial to the stability of Cook Glacier is its large floating ice shelf which helps to buttress glacier flow from the ice sheet interior into the ocean (Furst et al., 2016). Glaciological theory dictates that the rate of ice discharge into the ocean is sensitive to changes in the thickness and extent of these ice shelves (Gagliardini et al., 2010). This is evident from the recent dramatic increase in velocity of glaciers in the Antarctic Peninsula and Amundsen Sea following the collapse and rapid thinning of floating ice shelves (Shepherd et al.; 2004; Payne et al., 2004; Joughin et al., 2012). This has widely been attributed to the wind-driven delivery of warm circumpolar deep water (CDW) to ice shelf cavities increasing basal melt rates (e.g. Dutrieux et al., 2014). In contrast to the Amundsen Sea sector, satellite based estimates in the mid-2000s indicate a much lower basal melt rate under Cook Ice Shelf (Rignot et al., 2013; Depoorter et al., 2013), owing to a relatively weak ocean heat source, which could be interpreted as a sign of stability. However, a large section of the Cook Ice Shelf has undergone significant retreat since 1947 (Frezzotti et al., 1996; Miles et al.,

2013) and examinations of changes in the thickness of the ice shelf indicate a marked thinning between 1994 and 2012 (Paolo et al., 2015). This, combined with indicators of inland thinning in the late 1990s and early the 2000s, raises the prospect of dynamically-induced change (Davis et al., 2005; Shepherd et al., 2007), but any inland thinning appears to have reduced in the past decade (McMillan et al., 2014). However, unlike in other regions of East Antarctica that are potentially vulnerable (e.g. Totten Glacier; Li et al., 2016) there has yet to be a comprehensive study analysing temporal changes in the velocity of Cook Glacier in relation to changes in its ice shelf geometry. In this study we investigate the dynamics of Cook Glacier trough compiling a velocity record from 1973 to 2017.

5.2 Cook Glacier

Cook Glacier (68° S, 152° E) is located in George V Land, East Antarctica, ~225 km east of Ninnis Glacier (Fig. 2.1 & 5.1). Its present-day coastal configuration consists of two distinct tributaries: Cook East and Cook West. Cook East flows into a large 80 km long ice shelf and its terminus has been advancing following a major calving event in the early 1970s (Frezzotti et al., 1996; Miles et al., 2013; Lovell et al., 2017). In contrast, Cook West terminates close to, or at, its grounding line (Rignot et al., 2006b). The absence of an ice shelf near the western outlet is unusual given the close proximity to the stabilising ice rise to the west and Cook East ice shelf to the east (Fig. 5.1). Indeed, estimates of past terminus position indicate that a large ice shelf was present in front of Cook West as recently as 1947 (Fig. 5.1), merging with the Cook East ice shelf (Frezzotti et al., 1996). Its retreat was initiated between 1947 and 1963 and, by the late 1970s, the western ice shelf was completely removed (Fig. 5.1). It is notable that in the ~35 years since the removal of the Cook West ice shelf there has been no signs of a sustained re-advance (Miles et al., 2013; Lovell et al., 2017), suggesting this retreat is semi-permanent. This is highly unusual in the context East Antarctic outlet glaciers in the past 50 years, where broad trends in their ice-front position can be linked to climate at decadal timescales, but no other ice shelves have retreated to their grounding lines and then not advanced (Miles et al., 2013; 2016). Instead, the semi-permanent nature of the retreat is more akin to the recent behaviour of ice shelves in the Antarctic Peninsula (Rott et al., 1996; Cook et al., 2005).

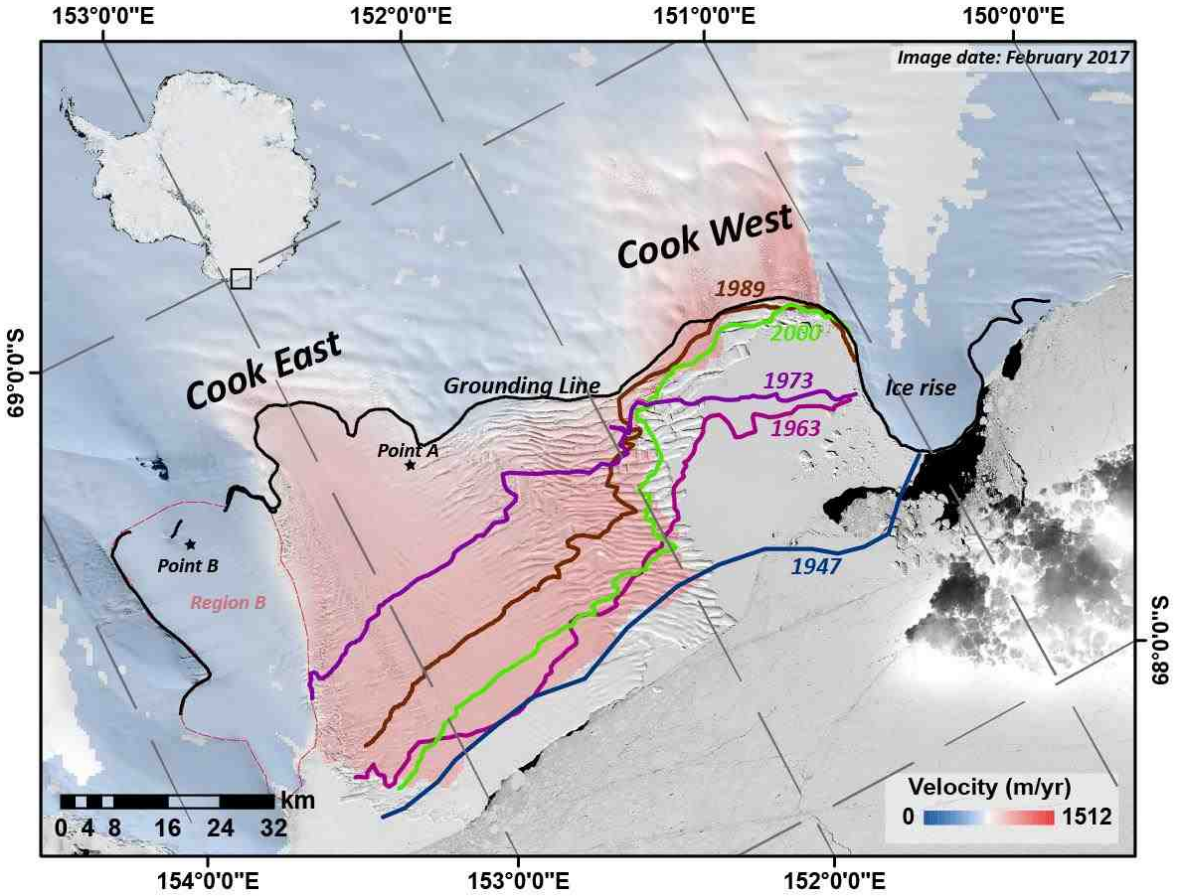

Figure 5.1: Location of Cook West and Cook East Glaciers in February 2017. Velocity (Rignot et al., 2011b), grounding line (Rignot et al., 2011c) and terminus positions from 1947 (Operation Highjump aerial photography), 1963 (ARGON), 1973 (Landsat 1), 1989 (Landsat 4) and 2000 (Landsat 7). Note the complete removal of Cook West Ice Shelf between 1947 and 1989, along with the major calving event of Cook East Ice Shelf between 1963 and 1973. Point A and B represent the cells used to calculate ice shelf thickness change in Paolo et al. (2015).

5.3. Methods and Data

5.3.1 Ice-front position

We collated and extended the ice-front position records of Frezzoti et al. (1998) and Miles et al. (2013) to create an ice-front time series from 1947-2017. Aerial photography from 'Operation Highjump' was used to estimate ice-front position in 1947, declassified ARGON photography was used in 1967, RADARSAT SAR imagery in 1997 and Landsat imagery was used between 1973 and 2017.

5.3.2 Glacier velocity from feature-tracking

We used a combination of Landsat 1, 4, 7 and 8, ASTER and WorldView-2 images to create a velocity time series for both Cook East and West Glaciers (Table 5.1 & 5.2). Velocity was extracted from regions near the grounding lines of Cook West and East Glaciers in areas where surface features were prevalent (Fig. 5.2). Estimates of glacier velocity were derived using COSI-Corr (Co-registration of Optically Sensed Images and Correlation) feature tracking software (e.g. Leprince et al., 2007; Scherler et al., 2008). This software tracks spectral signatures which relate to features on the glacier surface that can be identified in multiple images through time, and it has been shown to be one of the most robust methods of glacier velocity mapping (Heid and Kaab, 2012). This requires pairs of optical images which are free from cloud cover and ideally spaced around 1 year apart so a mean annual velocity can be estimated. In this study, the temporal resolution of image pairs was largely determined by the availability of appropriate satellite imagery, which is generally sparse due to a combination of poor coverage and persistent cloud cover. The temporal resolution was also limited by the structural stability of the features tracked on the glacier surface. Over time, surface features such as crevasses deform and become difficult to be identified in subsequent images. From manually analysing surface features on Cook Glacier, we estimate that most surface features persist for a maximum of two years. We obtained suitable images pairs in 1989, 2000-2001, 2001-02 and annually from 2006-2016 for Cook East Glacier, with the majority of image pairs having a temporal gap of 365 ± 100 days (Table 5.1). Image pairs for Cook West Glacier were available in 1973-74, 1989, 2001-02 and annually from 2006-2017 (Table 5.2). The only exceptions to this are in 1989, for both Cook East and Cook West, where the only available image pair was between March and November (Table 5.1 & 5.2); and in 1973/4 for Cook West, where the image pair was between 1st November 1973 and 5th March 1974.

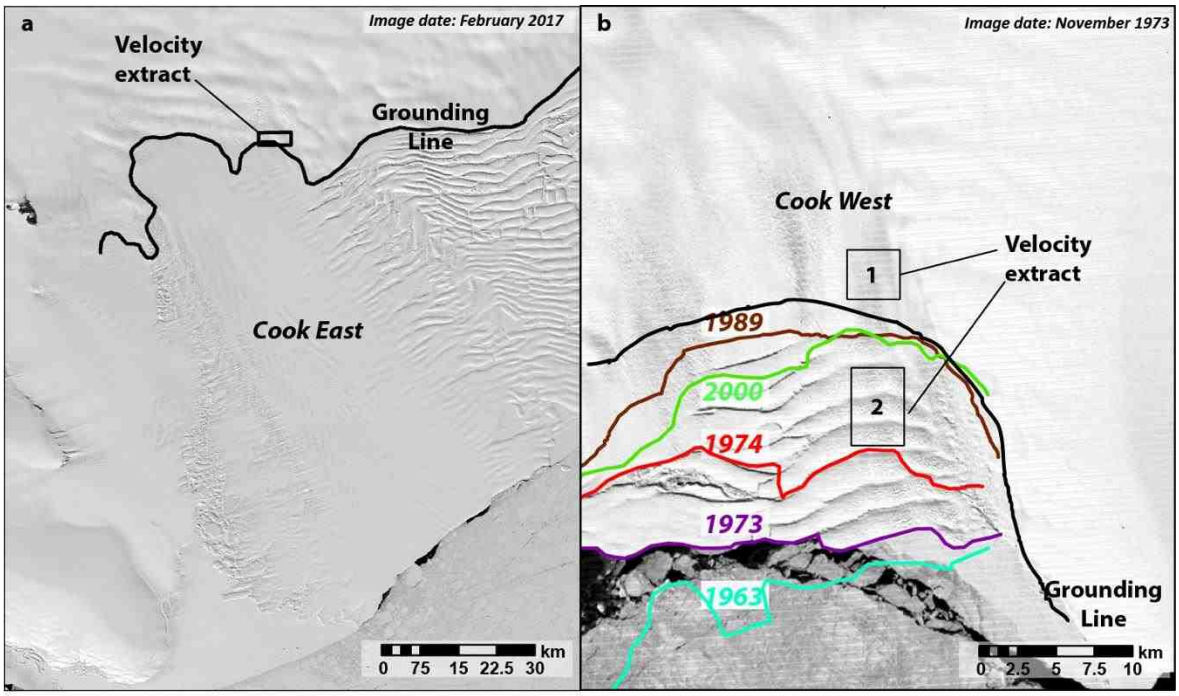

Figure 5.2: Locations of glacier velocity extraction. **a)** Location on Cook East. This region was chosen because it is on the grounding line and the most image pairs cover this section of the glacier. **b)** Location of the extraction of velocity on Cook West Glacier. All velocity estimates with the exception of 1973/4 were extracted in Box 1. Velocity estimates for 1973/4 were extracted from Box 2 because no surface features were visible in Box 1 because of the lower resolution of the Landsat 1 satellite.

Table 5.1: Image pairs and associated error for feature tracking on Cook East Glacier.

Date	Satellite	Resolution (m)	Co-registration error (m)	Displacement error (m)	Total Error per year (m)
05/03/1989	Landsat 4 - Band 4	30	30	15	51
16/11/1989	Landsat 4 - Band 4	30			
23/02/2000	Landsat 7 - Band 8	15	15	7.5	19
17/11/2001	Landsat 7 -Band 8	15			
17/11/2001	Landsat 7 - Band 8	15	15	7.5	22
24/12/2002	ASTER - Band 3	15			
12/12/2005	ASTER - Band 3	15	15	7.5	23
01/12/2006	Landsat 7 - Band 8	15			
01/12/2006	Landsat 7 - Band 8	15	15	7.5	22
04/12/2007	Landsat 7 -Band 8	15			
04/12/2007	Landsat 7 - Band 8	15	15	7.5	22
07/12/2008	Landsat 7 -Band 8	15			
07/12/2008	Landsat 7 - Band 8	15	15	7.5	23
07/11/2009	Landsat 7 -Band 8	15			

07/11/2009	Landsat 7 - Band 8	15	15	7.5	22
10/11/2010	Landsat 7 -Band 8	15			
10/11/2010	Landsat 7 - Band 8	15	15	7.5	22
23/12/2011	WorldView-2	15 (0.5*)			
23/12/2011	WorldView-2	15 (0.5*)	15	7.5	22
28/12/2012	WorldView-2	15 (0.5*)			
28/12/2012	WorldView-2	15 (0.5*)	15	7.5	24
10/11/2013	Landsat 8 - Band 8	15			
10/11/2013	Landsat 8 - Band 8	15	15	7.5	24
10/09/2014	Landsat 8 - Band 8	15			
10/09/2014	Landsat 8 - Band 8	15	15	7.5	21
16/11/2015	Landsat 8 - Band 8	15			
16/11/2015	Landsat 8 - Band 8	15	15	7.5	22
05/12/2016	Landsat 8 - Band 8	15			

Table 5.2: Image pairs and associated error for feature tracking on Cook West Glacier.

Date	Satellite	Resolution (m)	Co-registration error (m)	Displacement error (m)	Total Error per year (m)
04/11/1973	Landsat 1 - Band 4	60	60	30*	210
16/01/1974	Landsat 1 - Band 4	60			
05/03/1989	Landsat 4 - Band 4	30	30	15	51
16/11/1989	Landsat 4 - Band 4	30			
17/12/2001	Landsat 7 - Band 8	15	15	7.5	24
10/10/2002	ASTER - Band 3	15			
14/10/2006	ASTER - Band 3	15	15	7.5	22
09/11/2007	Landsat 7 - Band 8	15			
09/11/2007	Landsat 7 - Band 8	15	15	7.5	22
12/11/2008	Landsat 7 -Band 8	15			
12/11/2008	Landsat 7 - Band 8	15	15	7.5	22
14/11/2009	Landsat 7 -Band 8	15			
17/01/2010	Landsat 7 - Band 8	15	15	7.5	22
20/01/2011	Landsat 7 -Band 8	15			
20/01/2011	Landsat 7 - Band 8	15	15	7.5	22
08/02/2012	Landsat 7 -Band 8	15			
08/02/2012	Landsat 7 - Band 8	15	15	7.5	23
11/01/2013	ASTER - Band 3	15			
11/01/2013	ASTER - Band 3	15	15	7.5	22
20/01/2014	Landsat 8 - Band 8	15			
20/01/2014	Landsat 8 - Band 8	15	15	7.5	22

15/02/2015	Landsat 8 - Band 8	15			
15/02/2015	Landsat 8 - Band 8	15	15	7.5	24
01/01/2016	Landsat 8 - Band 8	15			
01/01/2016	Landsat 8 - Band 8	15	15	7.5	22
13/02/2017	Landsat 8 - Band 8	15			

The COSI-Corr procedure first requires the accurate co-registration of image pairs. For image pairs where the spatial resolution was not consistent (i.e. between Landsat7 and WorldView-2), the higher resolution image was resampled to match the coarser resolution image (Table 5.1). Co-registration was achieved by manually co-registering image pairs using a combination of nunataks and the boundaries of ice rises, which are known to be stable features over time. Because these features were relatively prevalent in the vicinity of Cook Glacier, images pairs were able to be co-registered to an estimated accuracy of 1 pixel. We used a window size of 256 x 256 pixels and a grid size of 20 x 20 pixels to detect surface displacement. Error in surface displacement was estimated at 0.5 pixels, which is consistent with other studies using this method (e.g. Scherler et al., 2008; Heid and Kaab, 2012). Total error ranged from ±51 m yr^{-1} in 1989 to between ±19 and ±24 m yr^{-1} from 2000-2017 (Table 5.1 and 5.2).

The velocity of Cook West Glacier in 1973-74 was estimated by manually tracking surface features on the glacier surface. This was because the coarse resolution of Landsat 1 (60 m) and the smaller temporal gap between the pair of images that were available (73 days) made it difficult to automatically track surface features through COSI-Corr. Surface features were only visible on the floating tongue ~10 km upstream of the other measurements (Fig. 52b). Because its floating tongue retreated at some point between 1974 and 1989, it means we could not sample this point on the glacier again, meaning the velocity estimate in 1973-74 is further upstream in comparison to other measurements. As the velocity of glaciers tends to decrease upstream, it suggests that the 1973/4 estimate of glacier velocity is likely to be an overestimate in comparison to velocity estimated from 1989-2017. The coarse resolution and small temporal gap between the image pair results in an error estimated at ± 210 m yr^{-1} for 1973-74 (Table 5.2).

5.3.3 Rate of ice-front advance

Inspection of the imagery clearly indicates that there have been no major calving events on Cook East Glacier since 1973 because the shape of the ice margin is largely unchanged.

Thus, we were also able to provide estimates of glacier velocity from 1973 to 2016 by simply calculating the rate of advance of its ice-front. Whilst feature-tracking is the preferred method because it can be estimated at the grounding line and provide a direct measurement of the flow of ice, the rate of ice-front advance is beneficial because it enables additional independent estimates further back in time (i.e. between 1973 and 1989) and allows more estimates in the 1990s (Table 5.3), which can be used to supplement the feature tracking method. This is because image pairs can be mixed between optical and SAR images because mapping the ice-front is not dependent on the spectral signature of surface features on the glaciers surface, enabling a greater number of image pairs. Moreover, because it is not dependent on temporary features on the glacier's surface, the time gap between image pairs can be much larger in comparison to feature-tracking. Any patterns in ice acceleration or deceleration at the grounding line would be expected to be reflected in the rate of advance over the same time periods if no major calving events took place. However, since the ice-front flows faster than ice at the grounding line because it has less resistance the absolute changes would be different, but the relative magnitudes of changes would be similar between the two methods.

Table 5.3: Image pairs and associated error for terminus advance rate on Cook East Glacier.

Date	Satellite	Resolution (m)	Co-registration error (m)	Mapping error (m)	Total Error (m)	Advance (m)	Minor Calving Correction (m)	Advance (m yr^{-1})
11/1973	Landsat 1	60	60	30	6	10780	115.1	709.7
03/1989	Landsat 4	30						
03/1989	Landsat 4	30	30	30	86	451	5.3	649.8
11/1989	Landsat 4	30						
11/1989	Landsat 4	30	30	30	8	5547	59.1	711.5
10/1997	RADARSAT	25						
10/1997	RADARSAT	25	25	25	21	1727	18.0	727.9
02/2000	Landsat 7	15						
02/2000	Landsat 7	15	15	15	17	1262	13.0	735.2
11/2001	Landsat 7	15						
11/2001	Landsat 7	15	15	15	27	811	8.3	743.4
12/2002	Landsat 7	15						
12/2002	Landsat 7	15	15	15	8	2958	29.5	758.2
12/2006	Landsat 7	15						
12/2006	Landsat 7	15	15	15	30	808	7.6	808.4
12/2007	Landsat 7	15						

12/2007	Landsat 7	15	15	15	30	755	7.6	754.3
12/2008	Landsat 7	15						
12/2008	Landsat 7	15	15	15	33	710	6.9	780.5
11/2009	Landsat 7	15						
11/2009	Landsat 7	15	15	15	30	768	7.6	768.7
11/2010	Landsat 7	15						
11/2010	Landsat 7	15	15	8	21	870	8.4	785.4
12/2011	WorldView-2	0.5						
12/2011	WorldView-2	0.5	0.5	0.5	1	782	7.6	776.4
12/2012	WorldView-2	0.5						
12/2012	WorldView-2	0.5	15	8	26	646	6.5	750.7
11/2013	Landsat 8	15						
11/2013	Landsat 8	15	15	15	36	629	6.2	762.7
09/2014	Landsat 8	15						
09/2014	Landsat 8	15	15	15	25	911	8.9	776.8
11/2015	Landsat 8	15						
11/2015	Landsat 8	15	15	15	28	800	7.9	765.9
12/2016	Landsat 8	15						

Whilst there have been no major calving events on the Cook East Glacier, the cumulative effect of small icebergs being calving away from the ice-front could influence ice-front advance rate estimates. This is particularly problematic because some image pairs have a temporal spacing of up to 16 years (Table 5.3), potentially allowing a large amount of ice to calved from the terminus via low magnitude, high frequency calving events. We used a pair of very high resolution (0.5 m) WorldView-2 images to attempt to quantify the amount of ice lost between January 2011 and December 2012, to quantify an approximate value of the low-magnitude, high frequency calving. To account for the advance of Cook East Glacier between the two dates, we co-registered the image pair using surface features near the terminus. This aligned the two termini and the mean retreat of the most recent images (December 2012) represents the amount of calving, which was estimated to cause retreat of 7.5 m yr^{-1} (Fig. 5.3). This suggests that low magnitude, high frequency calving events have a limited influence on ice-front position. Consistent with this notion is that throughout the observational period (1973-2017), the shape of the ice-front has remained consistent. As such, the rate of ice-front advance was subsequently corrected based on the temporal spacing between image pairs (Table 5.3).

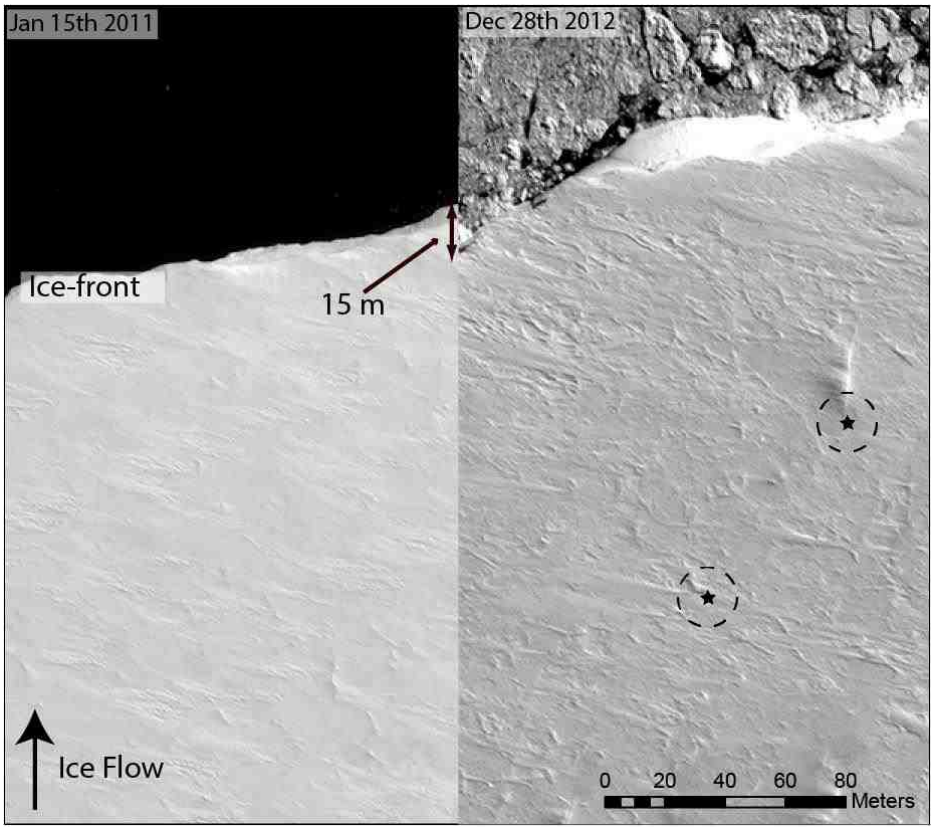

Figure 5.3: Example of the estimates of ice-front minor calving. The right image shows a high resolution WorldView-2 image from 28th December 2012, co-registered to an earlier image on 15th January 2011 using surface features near the ice-front (circled). The difference between the two termini (~15m) is taken as an estimate of ice-front minor calving.

Ice-front position change was calculated by taking an average of four measurements in the centre of Cook East Glacier. The centre was chosen because some images did not provide coverage for the entire ice-front. Co-registration was performed using the same method described in the feature tracking section, resulting in estimated an error of 1 pixel. Mapping error was estimated at 0.5 pixels per image. This results in a total error ranging from ±1 to ±86 m yr^{-1} (Table 5.3), with the range in error accounting for the varying temporal and spatial resolutions.

3.4 Ice shelf thickness

We use the satellite altimeter dataset from Paolo et al (2015) to examine changes in the thickness of Cook East ice shelf from 1994 to 2012. We note that Paolo et al (2015) calculate cumulative ice shelf thickness change for Cook East using an average of two

points (Point A and Point B; Fig. 5.1). We only analyse data from Point A because Point B is located on locally-sourced, thinner and slow-moving (> 100 m yr^{-1}) ice which is not part of the main ice shelf and which would therefore result in an incorrect measurement of thinning.

5.3.5 Sea ice concentration

Sea ice concentrations were calculated using mean monthly Bootstrap sea ice concentrations derived from the Nimbus-7 satellite and the Defence Meteorological Satellite Program (DMSP) satellites between November 1978 and July 2016. Concentrations were extracted from a single 25x25 km grid cell in the embayment which was formed following the retreat of Cook West Ice Shelf.

5.4. Results

5.4.1 Cook West

The velocity of Cook West Glacier has approximately doubled from 600 ±210 m yr^{-1} in 1973-1974 to 1340 ±51 m yr^{-1} in 1989, following the retreat of its buttressing floating ice shelf 13 km to near its present-day grounding line at some point between 1974 and 1989 (Fig. 5.1 & 5.4). The Cook West ice-front reached its most retreated position on record in 2000, where it was ~13.75 km behind its 1973 position. This coincided with the highest estimate of glacier velocity, where Cook West was flowing at 1489 ±24 m yr^{-1} between 2001 and 2002. Throughout the period 2001-2017, the velocity of Cook West decreased by 15% to 1269 ±22 m yr^{-1} in 2016-17, although there were interannual fluctuations in glacier flow during this time period (Fig. 5.5). These fluctuations and the overall decrease in velocity between 2001 and 2017 are consistent with relatively small changes in the terminus position of Cook West Glacier (R^2 = 0.85, Fig. 5.4 and 5.5). As the glacier advances, its flow speed decreases; whereas when the glacier retreats, its velocity increases.

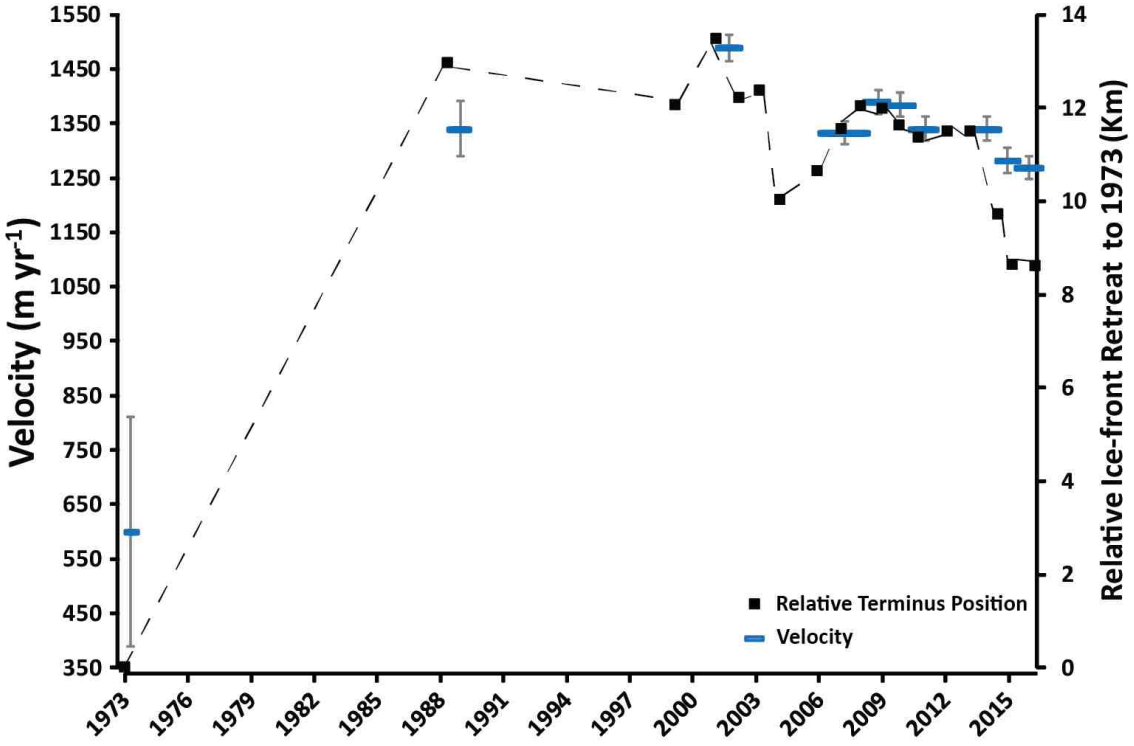

Figure 5.4: Velocity estimates and ice-front retreat of Cook West Glacier between 1973 and 2017 based on feature-tracking. The blue bars represent velocity and extend over the period of measurement, grey bars represent error and the dashed line represents the relative ice-front retreat to 1973. Note the increase in velocity between 1973-74 and 1989 coincides with the retreat of the Cook West Ice Shelf.

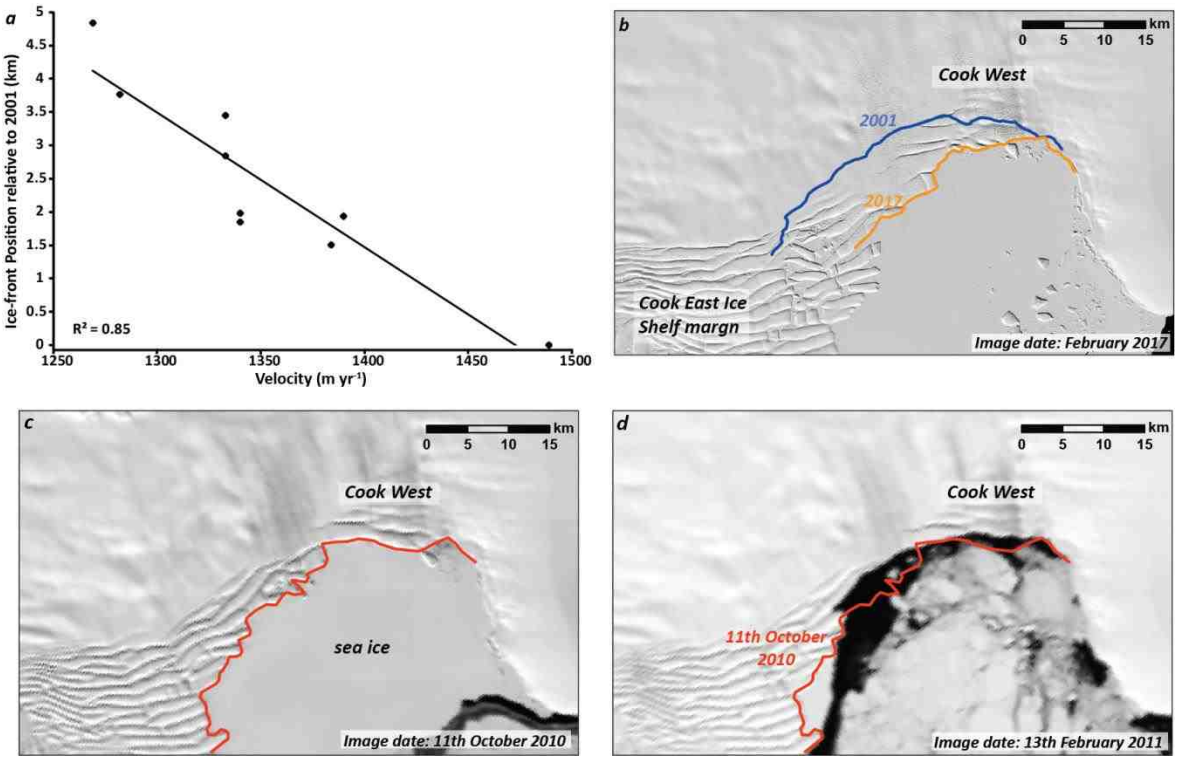

Figure 5.5a: Relationship between ice-front position change and glacier velocity between 2001 and 2017. As the ice-front advances/retreats, velocity decreases/increases accordingly in response to the change in buttressing,. **b)** Difference between glacier terminus position in 2001 (blue) and 2017 (orange).. **c & d)** MODIS imagery (Scambos et al., 1996) showing an example of the calving and retreat of Cook West glacier following a sea ice break-out event.

5.4.2 Cook East

Estimates of glacier velocity derived from feature-tracking near the grounding line of Cook East Glacier show an approximately 20% increase in mean velocity from 327 ±51 m yr^{-1} in 1989 to a mean flow speed of 392 ±19 m yr^{-1} in 2000-01 (Fig. 5.6). Since 2001, glacier speed has remained constant, with small annual fluctuations of about 5%. The only exception to this was between 2006 and 2007 where there was a short-term increase in glacier velocity, where glacier flow speed was 19% (456 ±22 m yr^{-1}) faster than the 2001-2016 average (Fig. 5.6).

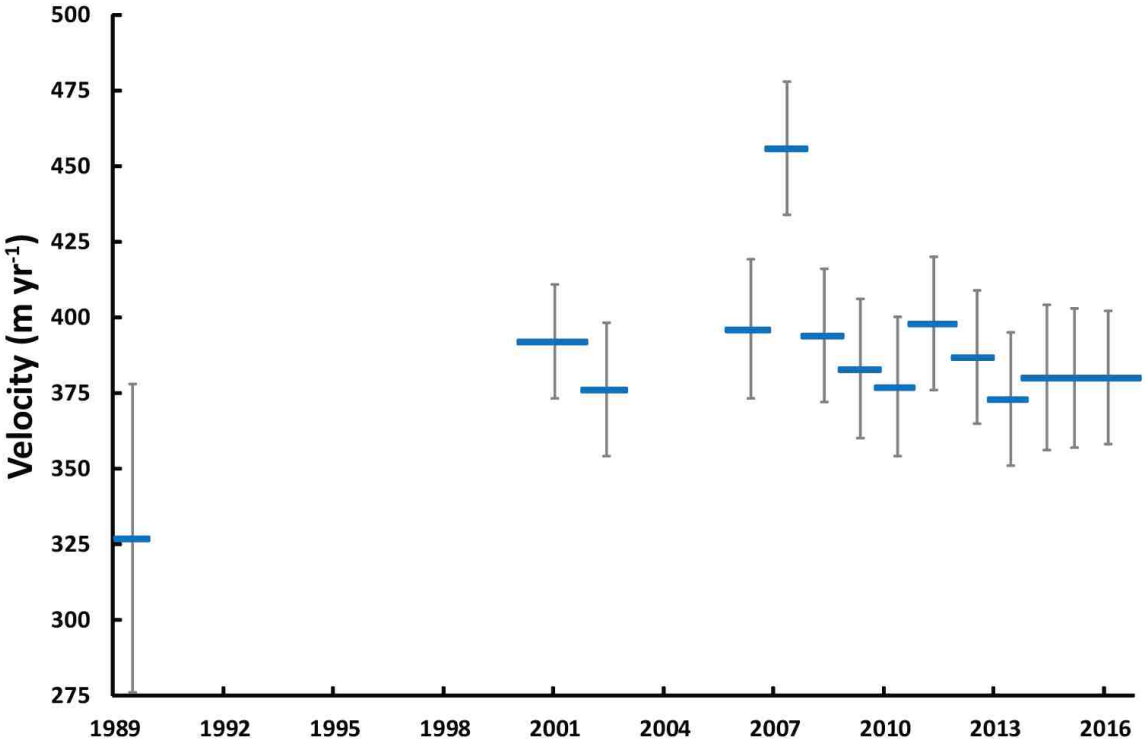

Figure 5.6: Velocity estimates from Cook East Glacier using feature tracking. Note the increase in velocity between 1989 and 2000-01, along with the anomalously high velocity between 2006 and 2007.

The temporal patterns of glacier velocity derived from feature-tracking at the grounding line are consistent with independent velocity estimates derived from the advance rate of the Cook East ice-front, during the periods where the two methods overlap (Fig 5.6 & 5.7). This validates our approach to supplement the velocity record of Cook East (described above) with ice-front advance rate estimates, to provide a clearer picture of glacier velocity particularly during time periods where feature-tracking is not available from 1973-1989, 1989-1997 and 1997-2000.

The rate of ice-front advance estimated between 2000 and 2001 was 13% faster than in 1989. In 1989 the ice-front was advancing at 650 ±86 m yr^{-1}. Either side of this estimate, from 1973-1989 and 1989-1997, the ice-front was likely advancing at a faster rate of 710 ±6 m yr^{-1} and 712 ±8 m yr^{-1}, respectively (Fig. 5.7). Because the mean rate of ice-front advance was likely higher either side of the estimates in 1989, it suggests the advance rate estimated in 1989 was anomalously slow. We note that the image pair used to derive estimates of velocity in 1989 only covered the austral winter (March-November) and may explain why velocity was slower compared to multi-year estimates either side of this date. However, from 1997-2000 (728 ±21 m yr^{-1}), 2000-2001 (735 ±17 m yr^{-1}), 2001-2002 (743

±27 m yr-1) and 2002-2006 (758 ±8 m yr^{-1}), the ice-front advance rate accelerated, equating to a 7% increase between 1989-1997 and 2002-2006 (Fig. 5.7). These additional estimates suggest that the ice-front advance rate between 1989 and 2001 was anomalously slow and there then followed an increase in mean annual velocity in the late 1990s and early 2000s. Whilst the temporal patterns in velocity estimates derived from feature tracking and the rate of ice-front advance are consistent, the relative percentage magnitudes of change between epochs are not. For example between 1989 and 2000-2001, there was an increase of 13% in the rate of ice-front advance, whereas feature-tracking near the grounding line showed a 19% increase. Based on this ratio (i.e. 19/13), we estimate that the 7% increase in ice-front advance rate between 1989-1997 and 2002-2006 translates to a ~10% increase in velocity at the grounding line.

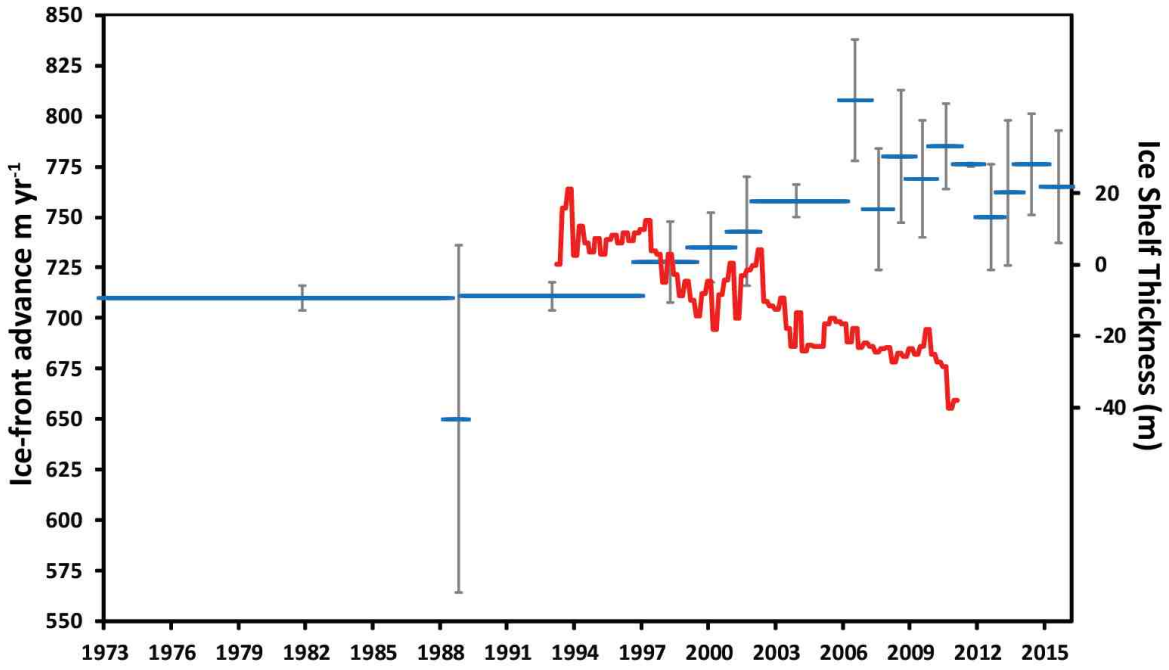

Figure 5.7: Ice-front advance rate estimates for Cook East glacier (blue) and ice shelf thinning (red; from Paolo et al., 2015). Note the period of rapid ice shelf thinning (1998-2005) coincides with the step increase in glacier velocity.

5.4.3 Ice shelf thickness change

There has been little change in the thickness of Cook East Ice Shelf between 1994 and mid-1998, where the ice shelf thickened at 0.75 m yr^{-1}. However between 1998 and 2005

Cook East Ice Shelf thinned rapidly at an average of 4.7 m yr^{-1}. That said, there is considerable variability in the rate of thinning during this period, with the rate of ice shelf thinning peaking between 1998 and 2002 at 7.5 m yr^{-1}, followed by a short lived period of ice shelf thickening in 2002. Between 2005 and 2011 there was little change in ice shelf thickness, with the ice shelf thinning on average at 0.75 m yr^{-1} (Fig. 5.7).

5.5. Discussion

5.5.1 Increased velocity of Cook West following the removal of its ice shelf

Satellite imagery and aerial photography reveal the retreat of Cook West Ice Shelf was initiated at some point between 1947 and 1963, when an estimated 650 km^2 of floating ice was removed. Between 1973/4 and 1989 the remaining section of the Cook West's Ice Shelf collapsed, resulting in the further loss of an estimated 350 km^2 of floating ice, leading to its ice front retreating close to or onto its present-day grounding line position (Fig. 5.1). Our results show that the near-complete loss of its remaining buttressing ice shelf between 1973/4 and 1989 was coincident with the speed up of Cook West Glacier by 220% (Fig. 5.4). This has subsequently increased the amount of ice Cook West discharges into the ocean and, assuming surface mass balance has remained constant, this will have placed the glacier out of balance, perhaps explaining the pattern of inland thinning detected upstream of Cook West Glacier (Davis et al., 2005; Shepherd et al., 2007; Pritchard et al., 2009). This is surprising given that there has been no evidence of warming in this region of Antarctica and Cook Glacier is presently is thought to have a relatively weak oceanic heat source (Depoorter et al., 2013; Rignot et al., 2013).

The loss of buttressing floating ice shelves and subsequent increase in ice discharge is predicted to happen in the coming decades and centuries in Antarctica, and is a key mechanism driving mass loss in numerical models (e.g. Golledge et al., 2015; DeConto and Pollard, 2016), but there have been few modern day observations of this process. In some respects, the loss of Cook West Glacier's floating tongue is analogous to the impact upon glaciers (e.g. Crane Glacier) in the Antarctic Peninsula following the collapse of buttressing ice shelves (e.g. Larsen A and B), driven by well documented atmospheric (Scambos et al., 2003) and oceanic warming (Pritchard et al., 2012). There, thinning and increase in velocity was observed in glaciers which previously flowed into the former ice shelves (De Angelis and Skvarca, 2003; Scambos et al., 2004; Rignot et al., 2004). However, the ice shelves which have collapsed in the Antarctic Peninsula drain relatively

small areas, whereas Cook West drains the much larger WSB which is vulnerable to marine ice sheet instability (Mengel and Levermann, 2014), and could have much greater sea level implications over the long term. Furthermore, the retreat of the Cook West Ice Shelf has also resulted in an increase in the thickness of its ice-front. Using Bedmap2 we estimate its current thickness to be ~750 m thick (Fretwell et al., 2013). This is close to the estimated thickness of ice required to initiate ice cliff failure, which could drive further instabilities and is predicted to be an important mechanism driving future rapid mass loss from Antarctica marine basins (DeConto and Pollard, 2016). Therefore, given its sea level potential, it is important to establish the processes driving glacier behaviour in the ~30-40 years following the retreat of Cook West Ice Shelf, to feed back into to numerical models and help constrain future sea level predictions.

Following the removal of the Cook West Ice Shelf between 1974 and 1989, satellite imagery from 2000 onwards shows that there have been small interannual variations in the ice-front position of Cook West Glacier (Fig. 5.4). These relatively small variations in ice-front position (of the order of 100s m) appear to be directly related to interannual variations in glacier velocity (Fig. 5.4 & 5.5). The sensitivity of glacier flow speed to small changes at the terminus is unusual for Antarctica and is more common in fjord terminating glaciers Greenland (Nick et al., 2009; Moon et al., 2014; Todd and Christoffersen, 2014). This relationship between ice-front position and velocity is driven by increased buttressing imposed upstream as the ice-front advances resulting in an deceleration in glacier flow; whereas retreat of the ice-front through calving events decrease buttressing and results in an increase in glacier velocity.

The initial retreat of Cook West Ice Shelf between 1974 and 1989 resulted in the formation of an embayment between the Cook East Ice Shelf and the ice rise to the west (Fig. 5.8). This embayment has created preferential conditions for multi-year landfast sea ice because it acts as an anchor for sea ice and negates the impact of oceanic swell (Ushio et al., 2006; Mahoney et al., 2007). This has resulted in a semi-permanent band of landfast sea ice forming in the region which the former ice shelf used to occupy. Analysis of satellite imagery shows that calving events at Cook West correlate with sea ice break-out events (Fig. 5.8). This suggests that the presence of multi-year landfast sea ice at the ice-front exerts enough back-pressure to inhibit calving from it's the potentially unstable ice-front and is acting as a mechanism of stability (e.g. Miles et al., 2017: Chapter 4). Since the initial formation of the embayment, it has continued to become more confined as the neighbouring Cook East Ice Shelf continues to advance (Fig. 5.8). It is plausible that a

more confined embayment may make the landfast sea ice more persistent and less likely to break-out, which is reflected in increases in mean monthly sea ice concentrations (Fig. 5.8). This is because it further limits oceanic swell and a greater proportion of the sea ice is anchored to land (Fig. 5.8). This may explain why Cook West has recently advanced to its most forward position between 2011 and 2017, because the more persistent sea ice is further inhibiting calving and promoting advance.

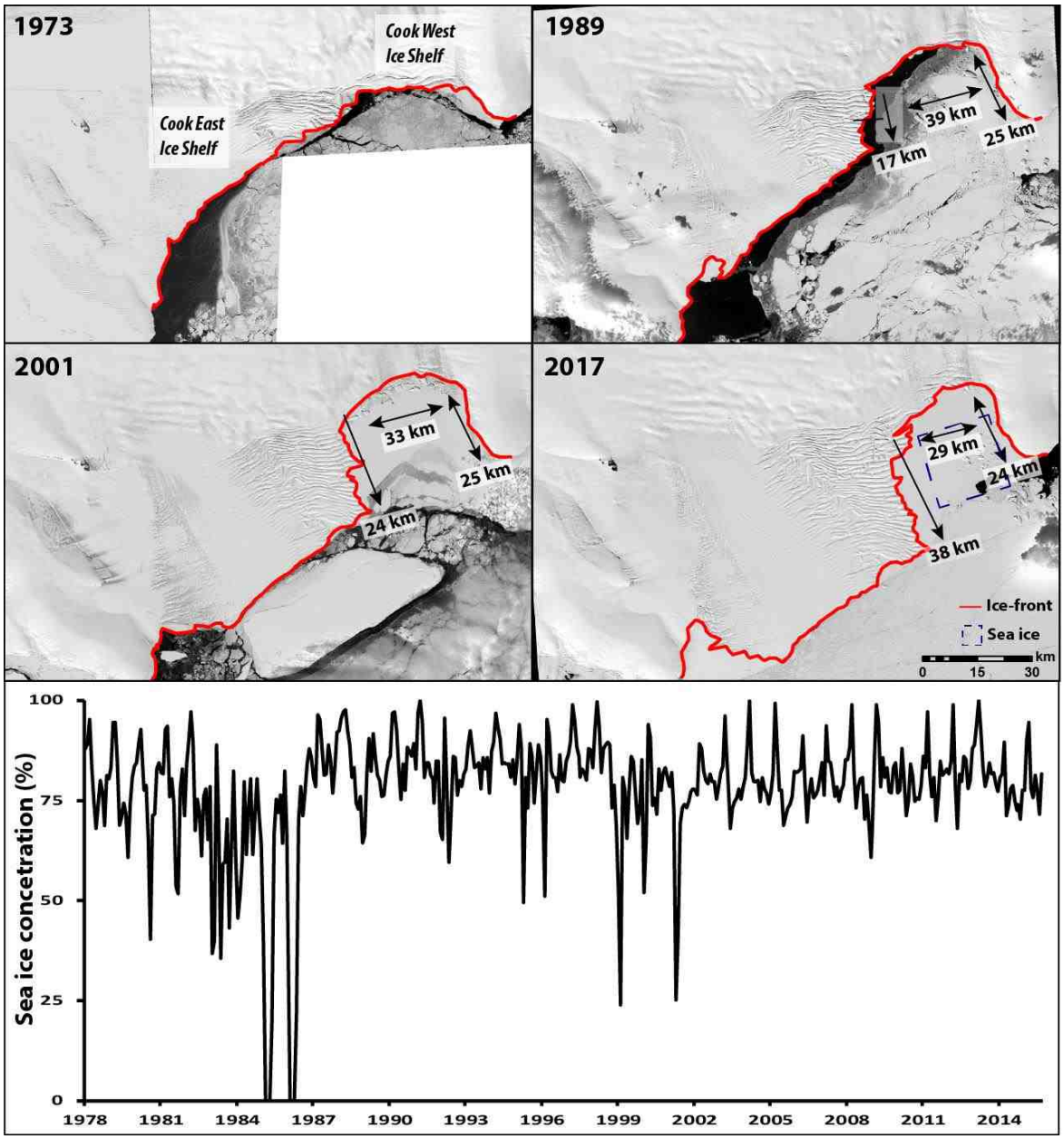

Figure 5.8: Evolution of the Cook West embayment. The embayment is formed following the retreat of Cook West Ice Shelf between 1973 and 1989. Since then the embayment has become progressively longer and more confined due the advance of the Cook East Ice Shelf. Sea ice concentrations, extracted from the blue dashed box suggest the continuing development of the embayment has increased the persistency of the landfast sea ice.

Our results suggest that the loss of buttressing following the retreat of Cook West's floating ice shelf has manifested in positive feedback mechanisms leading to a doubling of its velocity and an increase in the thickness of its ice-front to potentially unstable heights. However, we show that this ice-shelf retreat has also driven a previously unrecognised negative feedback mechanism. The embayment created by the removal of Cook West's Ice Shelf has created preferential landfast sea ice conditions which have stabilised the ice-front and inhibited calving. Whilst this does not counteract the instabilities created by the loss of buttressing following ice-shelf retreat, it may have prevented further ice discharge and has possibly driven ice-front advance and deceleration between 2011 and 2017. In some respects this is similar to the well-established relationship between seasonal sea ice melange choking glacial fjords and calving (Amundsen et al., 2010; Robel et al., 2017) in Greenland, which in turn has been linked to seasonal velocity fluctuations (Moon et al., 2014). However, in Antarctica, this mechanism has the potential to play a more permanent role because landfast sea ice can persist for years/decades before breaking-out and reforming (e.g. Massom et al., 2010, Miles et al., 2017: Chapter 4), as opposed to the seasonal cycles observed in Greenland. As most glaciers in Antarctica do not terminate in constraining fjords, this mechanism is dependent on changes to the local ice-scape to form similar embayments to our observations from Cook West. Therefore, this mechanism is likely to become more prominent in the future, if predicted ice shelf retreat results in the formation of similar embayment's and could be an important additional mechanism to include in numerical models.

5.5.2 Cook East velocity and ice shelf thinning

Our velocity estimates for Cook East Glacier show a step increase in glacier speed of around 10% between October 1997 and 2002-2006. It is notable that this period of glacier acceleration corresponds to the only period of rapid thinning of the Cook East Ice Shelf (Fig. 5.7). Between 1998 and 2005, the ice shelf thinned at an average rate of 4.7 m yr^{-1}, with this rate peaking at 7.5 m yr^{-1} between 1998 and 2002, which is comparable to the rapidly thinning ice shelves in the Amundsen Sea Sector e.g. Pine Island and Thwaites (Paolo et al., 2015). We note that either side of this thinning episode, from 1994-1998 and 2006-2012, there was little change in mean glacier velocity, despite some interannual variability. This suggests that the recent patterns in the velocity of Cook East Glacier have been driven by changes in the thickness of its ice shelf, with the overall trend of

acceleration being driven by the intense thinning episode between 1998 and 2005. This acceleration and subsequent drawdown of ice might explain the detection of inland thinning of Cook East Glacier in some of the earlier satellite altimetry records over a similar time period (Davis et al., 2005; Shepherd et al., 2007). Since 2005, the thinning of Cook East Ice Shelf appears to have abated (Fig. 5.7) and glacier acceleration has ceased, explaining why later satellite records show little change in the thickness of inland ice (McMillan et al., 2014).

Throughout the 2000s, annual estimates of glacier velocity varied on the order of ±5%, in relation to the 2000-2016 average (Fig. 5.6 & 5.7). However, between December 2006 and December 2007 glacier flow was ~19% faster than the 2000-2016 average, which is a greater magnitude of change than expected by interannual variability and lies well outside the error terms. In Antarctica, short-lived accelerations in glacier flow have been linked to subglacial flood events perturbing basal conditions and leading to enhanced lubrication (e.g. Stearns et al., 2008; Scambos et al., 2011; Siegfried et al., 2016). Between November 2006 and March 2008, we note that a large subglacial lake drained ~450 km upstream of Cook East Glacier, resulting in the discharge of ~6 Gt of water (McMillan et al., 2013). The calculated flow path, assuming correct knowledge of the subglacial topography, suggests that this subglacial flood could have reached Cook East Glacier (Flament et al., 2014). Because the timing of these two events coincide, we suggest that the acceleration of Cook East Glacier was triggered by the drainage of the Cook subglacial lake. This is because are no other known mechanisms which could drive such a large and short-lived increase in velocity. Flament et al. (2014) suggest that water may have not reached the coast until mid-2008, although they do not rule out the possibility of rapid flow through well carved channels. Our results suggest the latter must have occurred because we only observe a velocity increase from 2006-2007 and there is no significant change in the decadal average from 2007-2008 and 2008-2009. If our assessment is correct, it will be one of the few observations linking changes in subglacial hydraulic conditions to glacier flow dynamics in Antarctica (e.g. Stearns et al., 2008; Scambos et al., 2011; Siegfried et al., 2016) This is particularly important because variability in subglacial hydrology in Antarctica has been suggested to have an influence on millennial-scale fluctuations in ice sheet dynamics (Alley et al., 1994; Vaughan et al., 2008) and therefore may be important in the context of predicted future warming.

5.5.3 What is driving ice shelf instability?

At present, there have been no observations of subsurface ocean temperatures in the vicinity of Cook Glacier. Satellite-based estimates of the basal melt rate required to keep Cook East Ice Shelf in balance between 2007 and 2008 (i.e. difference between grounding line flux and calving flux, whilst accounting for surface mass balance) is very low (~2.9 m yr^{-1}) in comparison to other vulnerable glaciers in Antarctica (e.g. Pine Island, ~10.9 m yr^{-1}; Totten, ~8.2 m yr^{-1}) (Rignot et al., 2013). To estimate the actual basal melt rate between 2007 and 2008, the non-steady rate in ice shelf thickness change needs to be subtracted from the steady state basal melt rates. Rignot et al. (2013) estimated the non-steady state change in ice shelf thickness between 2003 and 2008 from Prichard et al (2012). During this time period it was estimated that Cook East Ice Shelf slightly thickened at ~1.6 m yr^{-1}, resulting in an actual basal melt rate of 1.3 m yr^{-1}, which means it receives a relatively weak oceanic heat source and implies ice shelf stability. For comparison Pine Island and Totten Glaciers thinned at ~5.3 and ~2.3 m yr^{-1} (Pritchard et al., 2012), resulting in actual basal melt rates of ~16.2 and 10.5 m yr^{-1} respectively (Rignot et al., 2013), which has been attributed to warm modified Circumpolar Deep Water (mCDW) and potential instability (Jenkins et al., 2010; Rintoul et al., 2016). However, there has been little consideration for the potential variability in the basal melt rates of Antarctica outlet glaciers. For example, between 1998 and 2002 Cook East Ice Shelf was thinning rapidly at ~7.5 m yr^{-1}, which coincides with the observed period of glacier acceleration (Fig. 5.7). Assuming a similar steady state basal melt rate to that derived from between 2007 and 2008 (e.g. ~ 2.9 m yr^{-1}; Rignot et al., 2013), it implies that between 1998 and 2002 the melt rate underneath the Cook East Ice shelf was around 10 m yr^{-1}. Based on our current understanding, the only way to ascertain basal melt rates of this magnitude is through intrusions of warm mCDW (e.g. Jenkins et al., 2010; Rintoul et al., 2016). As such, this hints at significant variability on the rate of melt underneath Cook East Ice Shelf.

Given the close proximity of Cook East Ice Shelf to Cook West Glacier, we suggest it is possible that similar periodic intrusions of warm water could have driven the retreat of Cook West Ice Shelf between 1947 and 1989. Consistent with our hypothesis that Cook East and Cook West have the potential to produce high level of basal melt are subsurface ocean measurements downstream of Cook Glacier, in the D'Urville Trough. These reveal a freshening trend between 1994 and 2012, despite increases in sea ice production which would lead to a greater brine rejection and more saline conditions (Aoki et al., 2013). It is possible that this freshening trend could have been driven from meltwater from the upstream Cook East and West Glaciers (Tamura et al., 2012), which would require relatively high level of basal melt.

In a wider context the potential for warmer water to reach Cook East Ice Shelf and Cook West Glacier has implications for their future vulnerability. The low steady-state basal melt of Cook East Ice Shelf had previously been considered indicator of stability. However, because of the potential for warm water to enhance its basal melt rates, we suggest the low steady-state basal melt rate could contribute towards instability in the future. This is because warm water of a similar temperature will drive a greater rate of thinning at Cook East Ice Shelf than other vulnerable glaciers (e.g. Pine Island and Totten) with higher steady-state basal melt rates. In contrast, the delivery of warmer water to the grounding line of Cook West Glacier could lead to rapid destabilisation because of its potentially unstable ice cliff. It is therefore important to improve our understanding on what drives such variability.

6. Conclusion

Our study has revealed that there have been dynamic instabilities at Cook Glacier in the recent past, which has been driven by changes in the thickness and extent of its ice shelf. Results show that the velocity of Cook West Glacier more than doubled as a consequence of the loss of buttressing driven by the retreat of its ice shelf to its grounding line between 1974 and 1989. To our knowledge, this is the only documented case of the complete removal of an ice shelf connected to the EAIS and may represent a good analogue for future changes. The embayment formed as a consequence of the removal of the ice shelf and has driven a negative feedback in that it has created preferential conditions for the formation of landfast sea ice, which is suppressing calving and promoting glacier stability. This mechanism may become increasingly important if predicted future warming manifests in ice shelf retreat.

Cook East Glacier accelerated by ~10% between 1997 and 2002. Our results suggest that this was driven by the rapid thinning of its ice shelf over the same time period. The estimated basal melt rates required to drive the rate of thinning observed suggest that warm mCDW is capable of reaching Cook Glacier and because it has a low steady state basal melt, it has the potential to rapidly thin its ice shelf. However, the absence of rapid thinning throughout the observational period suggests there is high variability in oceanic conditions in the vicinity of Cook Glacier. In a wider context, an important consideration is how this variability is incorporated into numerical models, which are usually calibrated against present-day observations (e.g. Timmerman and Hellmer, 2013). Given the potential for marine ice sheet instability in the WSB and the observed sensitivity of Cook Glaciers

dynamics to instabilities in its ice shelf, we suggest that Cook Glacier will make future sea level contributions if intrusions of warm water become more persistent in the future and it is one of the most vulnerable glaciers in East Antarctica.

Chapter 6: Discussion

1.1 Widespread decadal variations in glacier behaviour in East Antarctica

The results from Chapter 3 (Miles et al., 2016) demonstrate clear pan-ice sheet trends in decadal-scale outlet glacier change in East Antarctica. All drainage basins, with the exception of Victoria Land (DB16) displayed a median retreat value from 1974-1990. The majority of outlet glaciers (65%) retreated between 1974 and 1990, before switching to advance (67%) in the 1990s. This trend of advance largely continued between 2000 and 2012 (65% advance) with the exception of Wilkes Land (DB13), where 74% of glaciers retreated. Trends in glacier terminus position are linked to trends in the number of sea ice days, which may have altered ocean stratification and driven the observed trends in glacier terminus position. For example, between 2000 and 2012, the only area in East Antarctica which retreated, coincided with the only region of negative sea ice day anomalies. These results are important because it suggests that basin wide trends in mass gain/loss are consistent with trends in terminus advance/retreat throughout the 2000s (e.g. King et al., 2012). Moreover, they extend the record of satellite based ice sheet wide observations of East Antarctica further back in time.

Prior to the present study, most of our observations on how East Antarctica is currently behaving are based on satellite altimetry and InSAR data, which until the recent launch of the Cryosat-2, Landsat-8 and the Sentinel satellites in the 2010s, have only been sporadically available since the mid-1990s. As such, there is an understandable bias in our interpretation of the recent behaviour of the EAIS to data from the past ~20 years (mid-1990s – mid-2010s). Most indicators suggest that this has largely been a period of stability in East Antarctica, with the ice sheet slightly gaining mass (Shepherd et al., 2012) and most outlet glaciers advancing (Chapter 3). The only exception to this is between 2000 and 2012, where the majority of outlet glaciers retreated and lost mass in Wilkes Land (Chapter 3). However, in the ~20 years preceding the availability of satellite altimetry (e.g. 1974 – mid-1990s) and InSAR data, the results from Chapter 3 hint that the EAIS may have behaved differently. In addition to the pan-ice sheet retreat of the majority of outlet glaciers between 1974 and 1990, other key indicators of the overall behaviour of the ice sheet imply that, on average, the 1970-80s were warmer than the 1990-2000s. There were also reduced sea ice extent, fewer sea ice days, and a lower surface mass balance (Van der Berg et al., 2005) in the 1970-80s compared to the 1990-2000s. Therefore, it is important to consider if this switch towards cooler conditions in the 1990s is part of a longer-term trend of cooling or part of a longer-term cycle of decadal variability.

The dominant mode of atmospheric variability in the Southern Hemisphere is the Southern Annular Mode (SAM) (Marshall et al., 2003; Thompson et al., 2011), which is a proxy for the strength of the westerly winds that encircle Antarctica. A more positive (negative) SAM index results in stronger (weaker) and more (less) persistent westerly winds, which result in less (more) meridional heat transport from warmer mid-latitudes both in the atmosphere and in the ocean (Fig. 6.1a & b). Reconstructions and observations of the SAM throughout the 20th and 21st century suggest that there has been significant decadal variability in the Antarctic climate (Fig. 6.1c; Marshall, 2003; Fogt et al., 2009). There was a prolonged negative phase from ~1905-1930, before a switch to a positive phase between ~1930 and 1940. There was a further negative phase between ~1940 and 1955 before a switch to a positive phase from ~1955 to 1970. There was followed by another intense negative phases from 1970 to the mid-1980s, which coincides with observed warm conditions in East Antarctica and widespread outlet glacier retreat. From the late 1980s through to the 2000s there was a rapid shift towards a positive SAM (Fig. 6.1b) which coincides with cooler conditions and outlet glacier advance in East Antarctica. Reconstructions of the SAM over the past 1000 years suggest that this switch to an intensive and prolonged positive phase of the SAM is unprecedented (Abram et al., 2014), and several studies have linked this switch to ozone depletion (Thompson and Solomon, 2002; Turner et al., 2009; Thompson et al., 2011). Although, internal climate forcing may be playing a secondary role in driving the observed trends (Fogt et al., 2009). Predicted future ozone recovery may lead to a return to more negative extremes of the SAM and warm airflow into Antarctica (Mayewski et al., 2015).

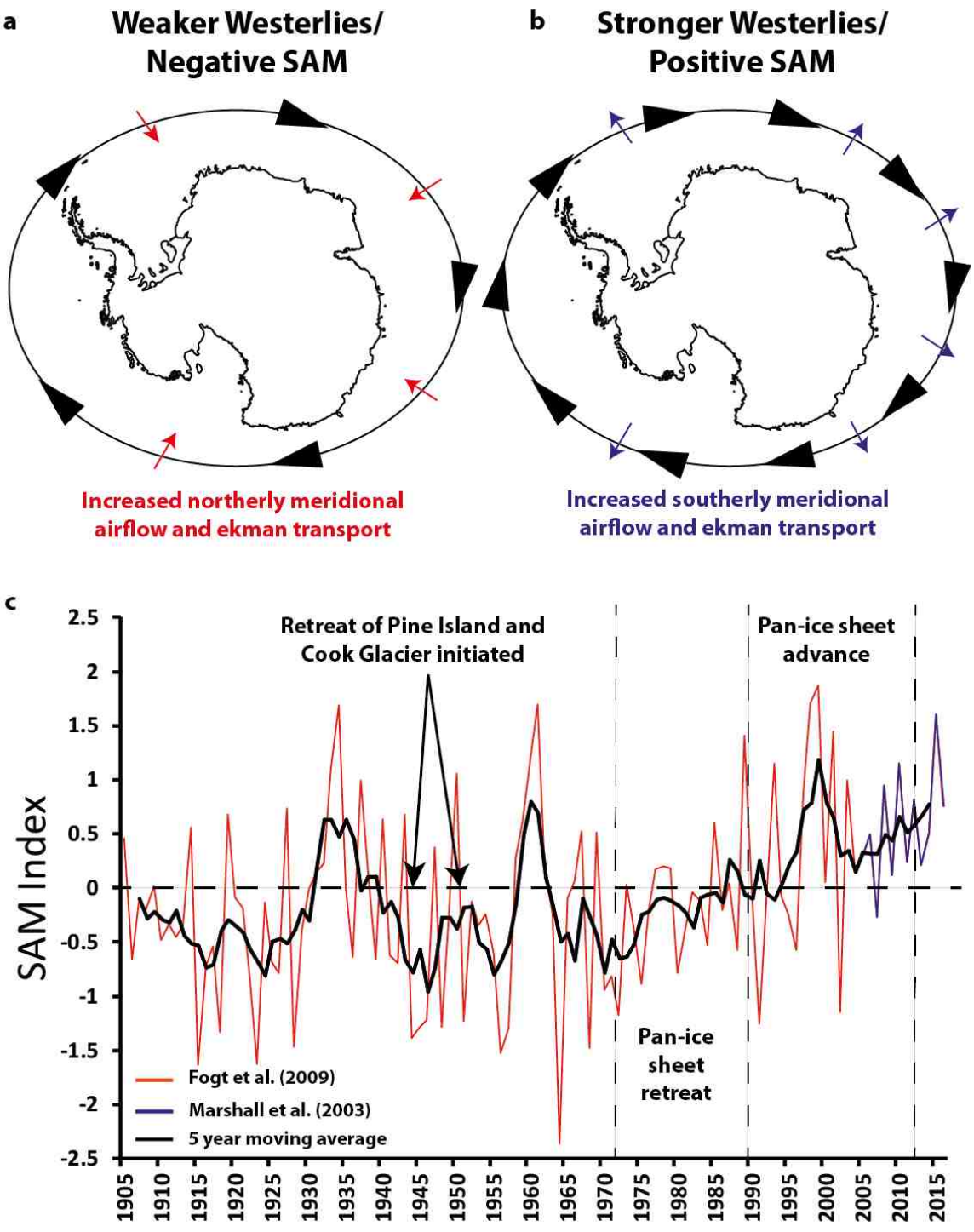

Figure 6.1: a and **b)** show schematic diagrams of the negative and positive phase of the SAM respectively. Negative phases promote poleward transport of airflow and Ekman transport leading to warmer conditions on average and *vice-versa* for the positive phase. **c)** The SAM index from 1905-2016, the majority of this index was created from the Fogt et al. (2009) index (orange; 1905-2004), but has been extended to present day using the Marshall et al. (2003) observational based index (blue; 2004-2016). Note the coincidence between the negative phases and glacier retreat and advance with the positive phases.

Whilst the SAM is a useful indicator of the overall state of the East Antarctic climate, conflicting regional trends in atmospheric circulation still occur. For example, meridional heat transport increased in Wilkes Land between 2000 and 2012 (Chapter 3, Fig. 3.7), despite there being a predominantly positive SAM during this period. This is likely to have been driven by strong zonal wave 3 circulation, which is major asymmetric part of meridional flow variability in the Southern Hemisphere associated meridional flow (Raphael, 2004). Indeed, the geographic positon makes Wilkes Land inherently susceptible to poleward meridional transport because it lies downstream of Australia (Fig. 6.2). It is important to note that other modes of atmospheric variability are important in East Antarctic climate e.g. ENSO (Turner et al., 2004) and the Pacific decadal oscillation (Meehl et al., 2016). However, and in general, regional climate proxies follow a similar decadal pattern to those displayed in the SAM index.

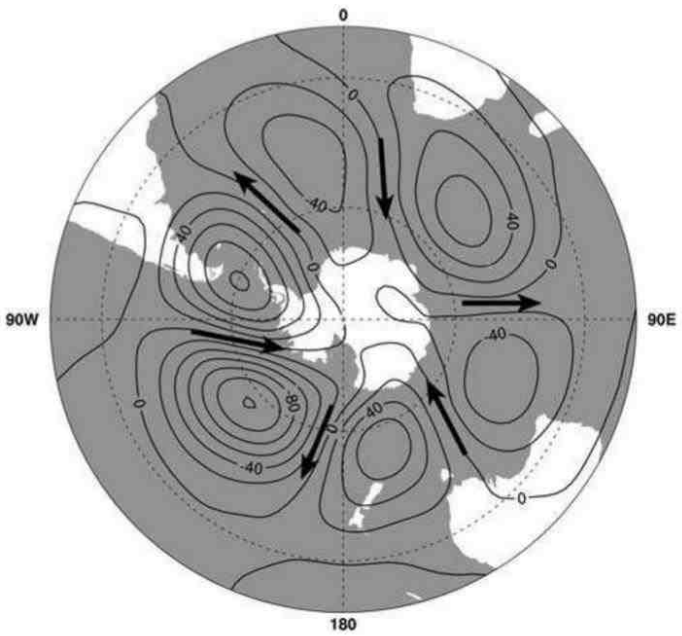

Figure 6.2: Zonal wave 3 circulation (Raphael et al., 2007). Note that Wilkes Land lies in the leeward branch of the circulation cell and is more likely to receive poleward meridional transport than other regions of Antarctica.

A recent study by Mackintosh et al. (2017) has linked the behaviour of mountain glaciers in New Zealand to the climatic conditions in George V Land, East Antarctica (Fig. 2.1). Glacier advance in New Zealand is linked to increased southerly airflow from George V Land, whereas retreat is linked to a greater northerly airflow and warming in George V Land. Historic length records indicate that the retreat of mountain glaciers in New Zealand

was initiated ~1940, followed by a brief stabilization in the early 1960s, before rapid retreat until the mid-1980s. From the mid-1980s to ~2000 mountain glaciers went against the overwhelming worldwide trend of retreat and advanced almost continuously. Therefore, historic length changes of New Zealand Glaciers are broadly consistent with the retreat from 1974-1990, and advance of outlet glaciers from 1990-2000 glaciers in George V Land (Chapter 3). Furthermore, the onset of the retreat of Cook West Ice Shelf, which is located within George V Land, coincides with the onset of retreat of New Zealand mountain glaciers. Importantly, the loss of the Cook West Ice Shelf and the rapid retreat of New Zealand outlet glaciers suggest that the climate forcing these changes was exceptional and outside of the boundaries required to keep the glacier in equilibrium. This is supported marine sediment cores which indicate a major glacier retreat at ~1980, which was unprecedented in the context of the Holocene (Crespin et al., 2014).

Evidence of similar unprecedented warming from the 1940-50s and 1970-80s is seen elsewhere in Antarctica. The present-day retreat and thinning of Pine Island Glacier was initiated ~1945 where exceptional climate forcing (e.g. Schneider and Steig, 2008) is thought to have led to the initial un-grounding of its ice shelf from a seafloor ridge; which ultimately lead to its final un-grounding ~1970 (Smith et al., 2017). This is largely responsible for the rapid mass loss observed today at Pine Island Glacier. In addition, ice core precipitation reconstructions from the Law Dome indicate that the meridional flow of warm and moist air towards Wilkes Land was at its highest point in 750 years during the 1970s and 1980s, before abating in the 1990s (Fig. 6.3; van Ommen et al and Vin Morgan, 2010). Furthermore, ice-core based reconstructions of sea ice extent in Wilkes Land from 1840 to 1995 shows a steady and consistent extent from 1840 to ~1965, before retreating throughout the 1970s and 1980s (Curran et al., 2003).

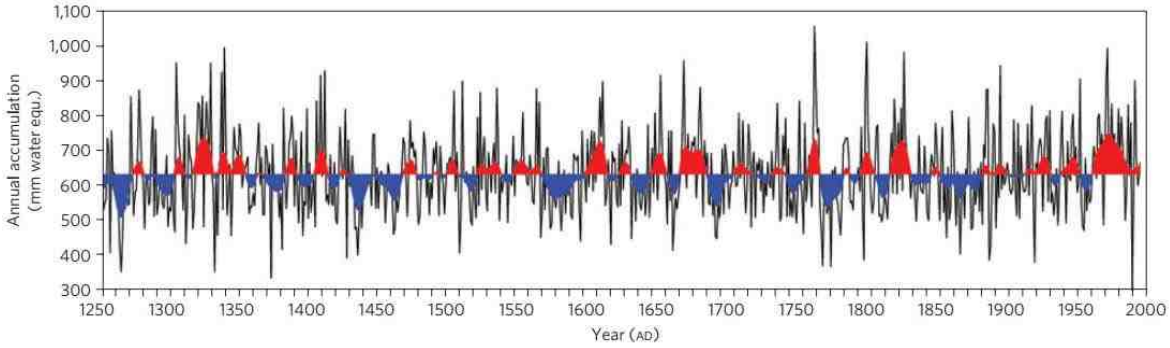

Figure 6.3: Law Dome (Wilkes Land) Precipitation series (van Ommen and Vin Morgan, 2014). The red sectors indicate greater than average precipitation and increased meridional flow. The blue sectors indicate lower than average precipitation and decreased meridional flow. Note the unprecedented increase in precipitation in the 1970s and 1980s.

There have been extreme decadal to multi-decadal variations in the Antarctic climate in the 20th and beginning of the 21st century. In particular, there were distinctive periods of enhanced meridional airflow from ~1940 to ~1950 and from ~1970 to ~1985 (Fig. 6.1). These periods are associated with warming and the results from this thesis (e.g. Chapters 3 and 5), along with other studies (e.g. Smith et al., 2017) hint that these periods where marked with instability in sections of the ice sheet. From 1985 to the 2000s, there was an unprecedented shift towards a prolonged and intense positive period of the SAM (Abram et al., 2014). This is associated with reduced meridional transport and cooler conditions. Outlet glaciers in East Antarctica responded to this by switching from pan-ice retreat to advance in the periods 1990-2000 and 2000-2012 (Chapter 3). The exception to this is Wilkes Land, where the majority of glaciers retreated between 2000 and 2012.

This decadal-scale variability is important in the context of predicting future changes in the East Antarctic Ice Sheet. Most of our understanding of how East Antarctica is currently behaving is based on satellite data which has only been available since the mid-1990s. To further increase our understanding how the EAIS will respond to future changes in climate, clues as to how the ice responded to decadal variations in the 20th century needs to be considered. It is possible that some of these warming periods (e.g. ~1940-1950, ~1970-1985) may represent some of our best analogues for how the EAIS will respond to future warming, at least in the near-future.

Decadal variability in the Antarctic climate should also be considered in the numerical models which predict future sea level contributions. At present some models are forced with global climate models which do not factor in decadal variability and provide a much smoother forcing. An example of the climate forcing extracted from Climate Model

Intercomparison Project phase 5 (CMIP5) model and used to force the Golledge et al. (2015) model is shown in Fig. 6.4. It is notable that there is little variability in comparison to the SAM index displayed in Fig. 6.1c and other reconstructions of climate e.g. Fig. 6.3. Glaciologically, these differences are important because ice shelves respond non-linearly to climate. For example, the current rapid mass loss of Pine Island Glacier can be traced back to its un-grounding in ~1945 (Smith et al., 2017), which subsequently enabled ice dynamics to accelerate its contribution to sea level. This initial ungrounding was forced by exceptional decadal warming in the preceding years; which was far greater than the long term average (Schneider and Steig, 2008; Fig. 6.5). If this warming event between 1935 and 1945 did not happen and climate forcing was smoother (e.g. as in numerical models, Fig. 6.4), it is still highly likely that Pine Island Glacier will have un-grounded because of the underlying warming trend. However, it is plausible this could have occurred at a later date, which could be somewhere in the region of 10, 20, 30+ years later (Fig. 6.6). This, in turn, would have reduced the time available for ice dynamics to accelerate grounding line retreat and would have ultimately resulted in it losing less mass than it is today. Therefore, because of this potential to destabilize glaciers earlier during decadal warmings, the absence of decadal variability in numerical could result in underestimations of sea level contributions. This would have a much greater impact on short-term predictions (e.g. 2100 or 2200) as oppose to millennial predictions. This is because this process operates on decades, which is a significant proportion of 100-200 year predictions, but not 1000-2000 year predictions.

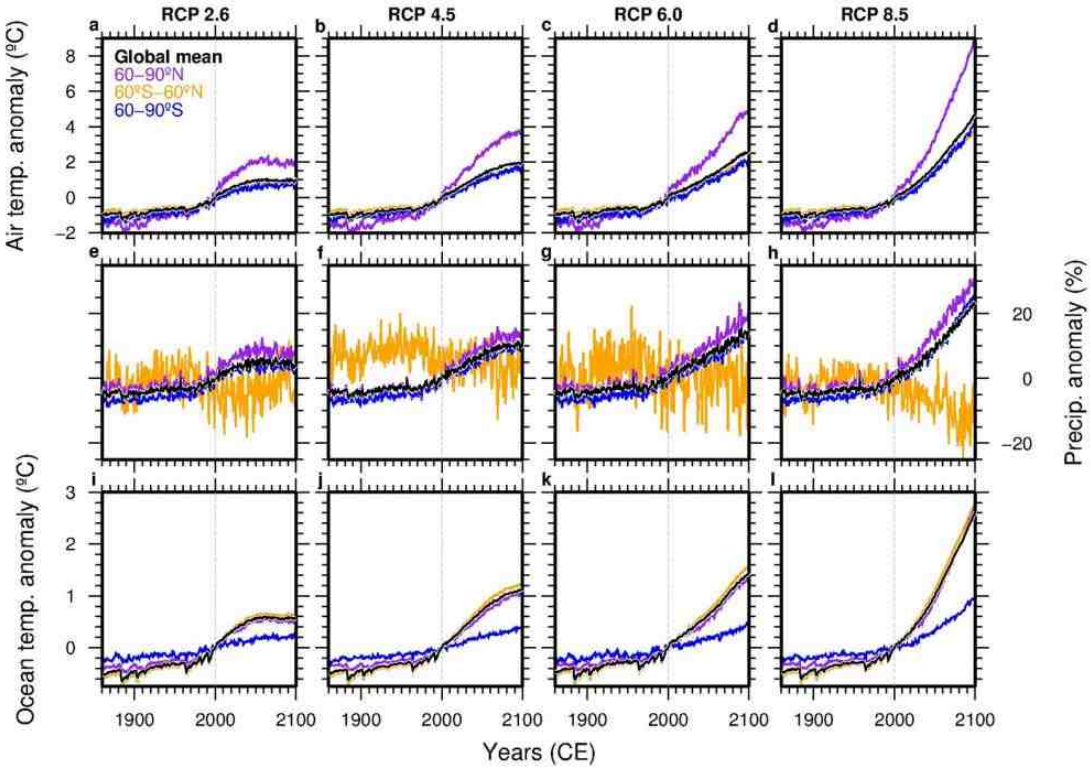

Figure 6.4: CMIP5 multi-model ensemble mean anomaly forcing used in Golledge et al. (2015) based on four RCP scenarios. a-d) Air temperature, e-h) precipitation, i-l) ocean temperature. Note the absence of decadal variations and smooth nature of the climate forcing.

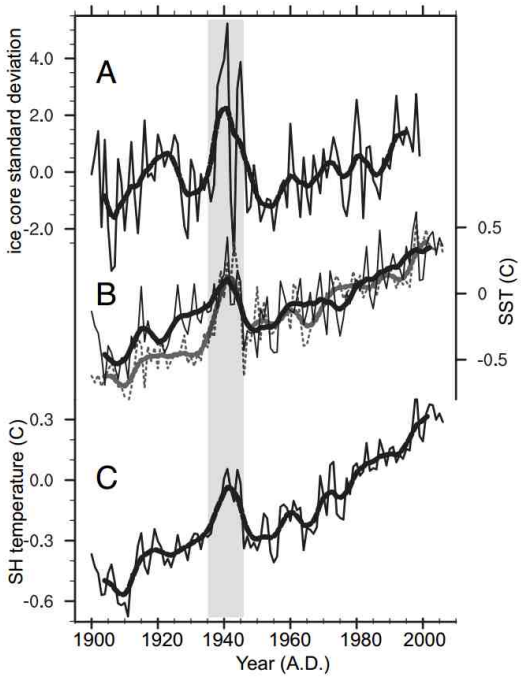

Figure 6.5: West Antarctic ice core composite record (a) compared with SST records for 20S-20N (dark solid lines) and 20S-60S (light dashed lines) (b) and annual mean Southern Hemisphere temperate (c) (Schneider and Steig, 2008). Note the extreme forcing in the 1940s which is associated with the ungrounding of Pine Island Glacier.

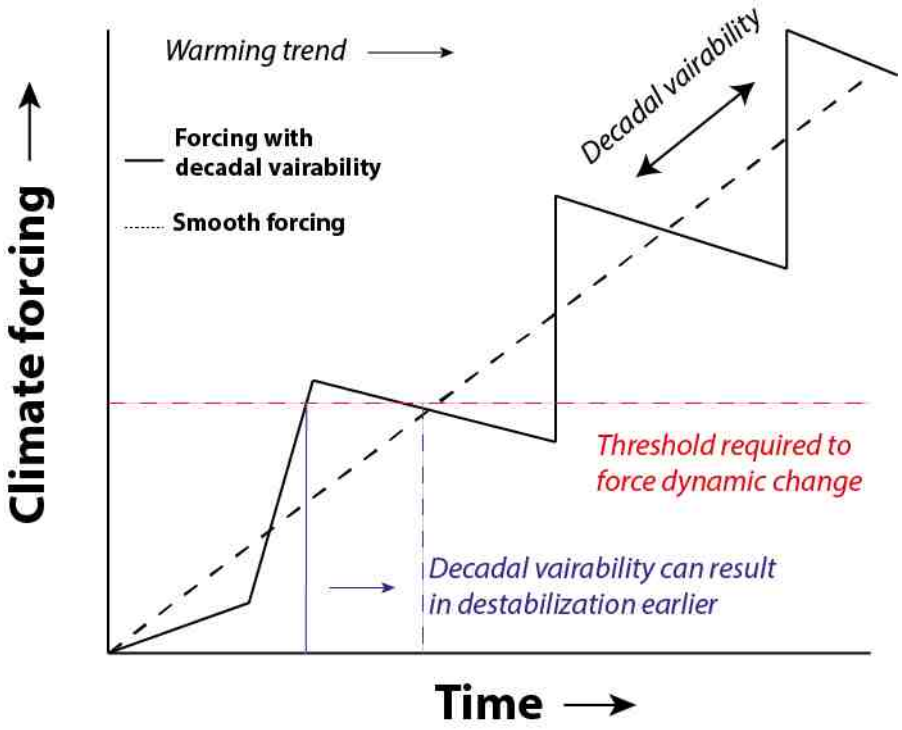

Figure 6.6: Schematic diagram showing the potential for decadal variability (e.g. Fig. 6.1, 6.3 and 6.5) to force a greater glacier response earlier in time in comparison to smooth warming (e.g. Fig. 6.4). This is despite both types of forcing receiving a similar long-term mean warming trend.

1.2 The importance of sea ice on ice-front position change

Chapter 3 (Miles et al., 2016) links decadal trends in ice-front position to trends in the number of sea ice days. In Greenland (e.g. Amundsen et al., 2010; Robel et al., 2017) and some parts of East Antarctica (Chapter 4 and 5) the persistence of ice melange or landfast sea ice at the ice-front can influence the rate of calving. However, in East Antarctica, the ice melange or landfast sea ice does not form in front of the majority of outlet glaciers. This is because most outlet glaciers in East Antarctica are unconstrained and do not terminate in fjords which support ice melange formation at the ice-front. Instead, Chapter 3 links regional decadal trends in terminus position to sea ice inducted changes in ocean stratification. Essentially, large-scale atmospheric forcing has driven changes in the amount of sea ice formed. This, in turn, has driven changes in ocean stratification and the amount of heat reaching glacier termini, ultimately driving the regional trends in terminus position. This is an important observation because it potentially provides a mechanism through which changes in atmospheric circulation can be rapidly reflected in the oceans. It is interesting to note that a similar mechanism has also been recently observed at Pine Island Glacier. Observational records indicate that changes in ocean heat content can be

driven by localised atmospherically forced changes in sea ice production as well as changes to the amount of warm water crossing the continental shelf (Webber et al., 2017).

Chapter 4 links simultaneous large scale calving events of outlet glaciers in Porpoise Bay to landfast sea ice break-out events. Monthly satellite observations between 2002 and 2012 revealed that there had been no calving events when multi-year landfast sea ice was attached to glacier termini. However, in January 2007 and March 2016, the break-out of this multi-year sea ice resulted in rapid disintegration of glacier tongues, leading to 2,900 and 2,200 km^2 of floating ice being lost, respectively. These are some of the largest calving events to ever be recorded. Chapter 4 links these landfast sea ice break-up events to different drivers. The January 2007 break-up event was driven by exceptional conditions in the previous austral summer (2005/06) weakening the landfast sea ice, before its eventual break-out in the following austral summer. The weakening in the 2005/06 summer was driven by the exceptionally warm December 2005 driving enhanced surface melt of the landfast sea ice and negative regional pack-ice anomalies making the landfast sea ice more vulnerable to oceanic swell. On the other hand, the 2016 break-out event was not linked to climate forcing. Instead, this was driven by the gradual advance of the largest glacier in Porpoise Bay (Holmes West) forcing the band of multi-year sea ice out of the more sheltered Porpoise Bay, into the open ocean where it becomes more vulnerable to ocean induced swell.

A similar relationship between landfast sea ice and glacier calving was observed at Cook West Glacier (Chapter 5). The removal of Cook West Ice Shelf created an embayment, which allowed multi-year landfast sea ice to form. This band of landfast sea ice has appeared to have stabilised Cook West Glacier. This is because the glacier can only calve during sea ice break-out events, which are becoming less frequent as the embayment becomes more confined as the neighbouring Cook East Ice Shelf advances. Thus, formation/removal of landfast sea ice is an important stabilising/destabilising mechanism.

In a wider context, the relationship between sea ice and oceanic heat transport to ice shelves is important, but is not fully understood. If the hypothesis that sea ice formation provides a direct role in determining oceanic heat transport to ice shelves is correct (Miles et al., 2016: Chapter 3), it emphasises a great importance on how sea ice in Antarctica will change in the future. On the whole, sea ice extent in Antarctica has been increasing slightly since the late 1970s (Parkinson and Cavalieri, 2012). Some of this overall increase is likely to have been driven by increased offshore winds (Turner et al., 2009), driven by the same large scale atmospheric circulation changes described in Section 1.1. However, freshwater

input from the ice sheet may have also contributed to the observed increase in sea ice through freshening surface ocean layers and increasing their freezing point (e.g. Bintanja et al., 2013). Additionally, changes in the local 'ice-scape' plays a prominent role in determining regional annual to multi-decadal patterns in sea ice (Massom et al., 2013). This because grounded icebergs and outlet glacier tongues play a prominent role in sea ice formation. For example, since the calving of the Metz Glacier Tongue in 2010 there has been a 14-20% decrease in sea ice production in the region (Tamura et al., 2012). Therefore, sea ice conditions in Antarctica are driven by a complex and changing system, which is not only driven by changes in atmospheric circulation. How it responds to future climate change could be important in determining East Antarctica's future sea level contribution.

In Porpoise Bay, landfast sea ice controls the calving rate of outlet glaciers and, ultimately, plays an important role in determining glacier dynamics. Landfast sea ice is thought to be highly sensitive to climate warming (Mahoney et al., 2007). Therefore, an important question is how would these glaciers respond if future warming drives the loss of the semi-permanent band of landfast sea ice? At present, there are large uncertainties and there has yet to be a quantitative assessment of the role landfast sea ice can play in glacier dynamics. Its potential role is an important consideration because there are other regions in East Antarctica where landfast might be important in controlling the stability of glacier tongues e.g. Lutzow-Holm Bay (Aoki, 2017), along with sections of Oates, Enderby and George V Land. Many of these regions are not typically considered to be vulnerable to modest future warming (e.g. Golledge et al., 2015; Ritz et al., 2015; DeConto and Pollard, 2016). However, this assessment does not consider the potential response of glaciers if bands of semi-permanent landfast sea ice are lost. Conversely, the formation of new bands of semi-permanent landfast sea ice onto glacier termini could play an important role in stabilising glaciers in the future. This was observed at Cook West Glacier, where the retreat of its ice shelf leads to the formation of an embayment, which promoted landfast sea ice formation. It is difficult to quantify the absolute impact of this negative feedback mechanism on glacier dynamics, but observations indicate that the newly formed landfast sea ice plays an important role in calving. This negative feedback mechanism could play an important role in the future if ice shelf retreat leads to the formation of similar embayments.

1.3 Cook Glacier: Another potential future sea level contributor from the EAIS?

Chapter 5 reports on the recent instabilities of the Cook Glacier which drains a large proportion of the Wilkes Subglacial Basin. Despite there being little evidence for any changes in ice dynamics over the past 15 years, analysis of a longer-term observational record from 1947-2017 reveals three distinct periods of instability: 1947-1963, 1974-1989 and 1998-2002. Cook West Ice Shelf retreated in two stages, with initial retreat occurring between 1947 and 1963, followed by a period of relative stability between 1963 and 1973, before retreating onto or close to its current grounding line position between 1973 and 1989. The loss of buttressing following this retreat at some point between 1974 and 1989 resulted in a doubling of the glacier's velocity. The Cook East Ice Shelf rapidly thinned at 7.5 m yr^{-1} between 1998 and 2002, this was resulted in a ~10% increase in glacier velocity.

It is notable that the two periods of retreat of the Cook West Ice Shelf coincided with prolonged periods of the negative phases of the SAM (Section 6.1), which promoted warmer conditions, on average, across Antarctica. The initial retreat of Cook West Glacier coincides with the negative phase of the SAM in the 1940s and the initial un-grounding of Pine Island Glacier (Fig. 6.1c). The second retreat phase of Cook West coincides with the negative SAM phase between ~1970 and 1985 and the pan-ice sheet retreat of outlet glaciers (Chapter 3). However, since the availability of satellite altimetry and InSAR in the mid-1990s there has been very little change on Cook West and East Glaciers. The only exception to this is the rapid thinning of Cook East Ice Shelf between 1998 and 2002. Thus, the analogy of Cook Glacier shows that relative stability in the satellite era (e.g. mid-1990s to present day) does not necessarily equate to stability over the preceding decades (see section 6.1).

The remaining Cook East Ice Shelf has a low steady state basal melt rate of 3 m yr^{-1} (Rignot et al., 2013). This means that the ice shelf will thin if its basal melt rate is greater than 3 m yr^{-1}. Between 1998 and 2002 estimates from satellite altimetry suggest its basal melt rate was ~10 m yr^{-1}, which implies that warm mCDW is capable of reaching the glacier. The nature of a low steady state basal melt rate means that in the context of the long-term average, warm water intrusions must be unusual otherwise the ice shelf would not exist. The fact that the Cook West Ice Shelf was completely lost between 1947 and 1989, implies that warm water intrusions must have increased over the past few decades. Given the close proximity of Cook East Ice Shelf to Cook West, it is plausible that the forcing which lead to the retreat of Cook West Ice Shelf also weakened the larger Cook East Ice Shelf during the same time period.

In a wider context, the contrasting behaviour between ice shelves with high steady-state basal melt rates (e.g. Totten and Pine Island) to glaciers with low steady-state basal melt rates (e.g. Cook Glacier) needs to be considered in the debate about the future stability of East Antarctica. High steady-state basal melt rate ice shelves thin through the increases in the mean temperature of the oceanic water which is delivered to the ice shelf, or an increase in the amount of warm water delivered to the ice shelf. On the other hand, low steady-state basal melt rate glaciers require a change in the type of water mass (e.g. shelf water to mCDW) in order to drive rapid instability. However, when warmer water does reach these ice shelves they have the potential to thin at a much greater rate than high steady-state basal melt rate ice shelves. Essentially, it means low steady-state basal rate ice shelves are only a decade or so of warm water forcing away from significantly altering their buttressing potential. Thus, there is an urgent need to establish what causes these periodic intrusions of warm water and how likely they are to occur in the future, without doing so it impossible to accurately predict their future evolution.

6.4 Future work

6.4.1 Incorporate decadal and extreme event climate forcing into numerical models

Decadal variations have been present in the Antarctic climate throughout the 20th century, and warm periods of these variations can be linked to glacier retreat (Section 6.1). Ultimately, these variations in climate forcing impact on the timing of changes in glacier dynamics and, subsequently, the timing of sea level contributions from Antarctica. Moreover, one of the hallmarks of global warming is the increase in extreme climate events, which can also have an impact on outlet glaciers. For example, the warmest December on record (2005) in Porpoise Bay (1979-2016) is linked to the break-up of sea-ice and calving of 2,900 km^2 of ice from outlet glaciers (Chapter 4). Neither decadal variability nor extreme climate events are currently represented in numerical models predicting future sea level contributions from Antarctica. Thus, there is a clear need to test the importance of these factors in numerical models.

6.4.2 Establish an ice sheet wide relationship between landfast sea-ice and ice-front stability.

This thesis has shown that landfast sea-ice can play an important role in ice-front stability and ultimately ice dynamics. However, outside of Porpoise Bay and Cook West Glacier and a few other regions (e.g. Mertz Glacier; Massom et al., 2010 and Lutzow-Holm Bay; Aoki et al., 2017) it is not known which glaciers rely on landfast sea ice for their current stability. Thus, there is a clear need for an ice sheet wide dataset which uses all historical satellite imagery to establish the wider importance of landfast sea ice. Following this, there is a need for a quantitative assessment (e.g. Todd and Christoffersen, 2014) on the importance of landfast sea ice in outlet glacier dynamics for glaciers with Antarctic based geometries as oppose to Greenland fjords. Ultimately, this information could be incorporated into numerical models which forecast future sea level contributions from the ice sheet.

6.4.3 Data-calibrated modelling of the future behaviour of Cook Glacier

The combination of the potential vulnerability of the Wilkes Subglacial Basin to marine ice sheet instability and the observed recent instabilities of Cook Glacier in the recent past, highlight the potential for Cook Glacier to contribute to sea level in the future. Subsequently, there is a need to use numerical modelling to ascertain the likely range of near-future mass loss. Any such model could be constrained with the velocity and ice-front positon data presented in Chapter 5. A similar approach could be used to examine the recent and future behaviour of several of the major glaciers in East Antarctica (e.g. Denman, Totten, Holmes and Moscow University), much like has been carried out for Greenland (Nick et al., 2013) and West Antarctica (Joughin et al., 2014).

Chapter 7: Conclusion

The results from this thesis demonstrate widespread decadal variability in outlet glacier dynamics across the East Antarctic Ice Sheet. The majority of outlet glaciers retreated between 1974 and 1990, before switching to advance between 1990 and 2000, and from 2000-2012. The only exception to this was Wilkes Land, where 74% of glaciers retreated between 2000 and 2012. This anomalous retreat indicates that Wilkes Land is the only region in East Antarctica where outlet glaciers are retreating and losing mass (e.g. King et al., 2012). It is hypothesized that this trend was driven by a reduction in sea ice and the associated impacts on ocean stratification, which increases the incursions of warm deep water towards glacier termini. The results from this study also highlight the importance of decadal variability in determining the behaviour of the EAIS.

This thesis has also highlighted the importance of landfast sea ice. Analysis of satellite imagery over the past 15 years has shown that outlet glaciers in Porpoise Bay only calve when landfast sea ice is removed from glacier termini. In 2007 and 2016 sea ice break-up events resulted in large (2-3,000 km^2) and simultaneous calving events. However, these events were driven by different forcing mechanisms. The 2007 break-up event was forced by an exceptionally warm austral summer in the year prior to its eventual break-up (2005-2006). In contrast, the 2016 break-out event to glacier advance pushing the landfast sea ice further into the open ocean making it more vulnerable to oceanic swell. Observations of Cook West Glacier indicate that landfast sea ice also has the potential to also play an important role in glacier stability if the retreat of ice shelves leads to the formation of an embayment, which creates preferential conditions for landfast sea ice formation.

Despite apparent stability over the past decade, there have been dynamic instabilities of the Cook Glacier in the recent past, which was initiated in the late 1940s. This resulted in the retreat of the Cook West Ice Shelf to its grounding line at some point between 1974 and 1990 and a subsequent doubling of its velocity. The remaining Cook East Ice Shelf has been advancing since it last calving event in the early 1970s. However, it thinned rapidly between 1998 and 2002, which has driven a ~10% increase in the velocity over the same time period. The rate of thinning between 1998 and 2002 is consistent with intrusions of warm mCDW. This is important because Cook Glacier drains a large proportion of the Wilkes Subglacial Basin and is therefore vulnerable to marine ice sheet instability. If these intrusions of warm mCDW become more regular in the future there is a potential for Cook Glacier to lose mass rapidly.

Taken together, these results demonstrate that the EAIS is highly sensitive to changes in climate and vulnerable to future climate warming. They also highlight the importance of decadal variations in climate, which satellite-altimetry and InSAR observation of the EAIS since the mid-1990s do not capture. Importantly, for many outlet glaciers this time period represents a period of modest climatic forcing, in comparison to warmer periods in the 20th century e.g. 1970s and 1980s. Therefore, it is possible that the satellite altimetry and InSAR observations of the EAIS do not capture its full potential to respond to predicted future climate warming. Given that all predictions infer that the EAIS will get warmer by the end of this century, it is inconceivable that it will not contribute to future sea level rise. However, whilst the overall trend in warming is important, the non-linear response of ice shelves to climate forcing means that it is plausible that the magnitude of decadal warmings and extreme climate events, will determine the EAIS future sea level contributions in the short to medium-term.

References

Abram, N. J., et al. 2014. Evolution of the Southern Annular Mode during the past millennium. *Nature Climate Change,* 4**,** 564-569.

Aitken, A. R. A., Roberts, J. L., van Ommen, T. D., Young, D. A., Golledge, N. R., Greenbaum, J. S., Blankenship, D. D., and Siegert, M. J. 2016. Repeated large-scale retreat and advance of Totten Glacier indicated by inland bed erosion, Nature, 533, 385-+, 10.1038/nature17447.

Alley, R. B., Anandakrishnan, S., Bentley, C. R. & Lord, N. 1994. A Water-Piracy Hypothesis for the Stagnation of Ice Stream-C, Antarctica. *Annals of Glaciology, Vol 20, 1994,* 20**,** 187-194.

Amundson, J. M., Fahnestock, M., Truffer, M., Brown, J., Luthi, M. P., and Motyka, R. J. 2010. Ice melange dynamics and implications for terminus stability, Jakobshavn Isbrae Greenland, J Geophys Res-Earth, 115, Artn F01005 Doi 10.1029/2009jf001405.

Aoki, S. 2017. Breakup of land-fast sea ice in Lutzow-Holm Bay, East Antarctica, and its teleconnection to tropical Pacific sea surface temperatures. *Geophysical Research Letters,* 44**,** 3219-3227.

Aoki, S., et al. 2013. Widespread freshening in the Seasonal Ice Zone near 140 degrees E off the Adelie Land Coast, Antarctica, from 1994 to. *Journal of Geophysical Research-Oceans,* 118**,** 6046-6063.

Arntsen, A. E., Song, A. J., Perovich, D. K., and Richter-Menge, J. A. 2015. Observations of the summer breakup of an Arctic sea ice cover, Geophys Res Lett, 42, 8057-8063, 10.1002/2015GL065224.

Astrom, J. A., Vallot, D., Schafer, M., Welty, E. Z., O'Neel, S., Bartholomaus, T. C., Liu, Y., Riikila, T. I., Zwinger, T., Timonen, J., and Moore, J. C. 2014. Termini of calving glaciers as self-organized critical systems, Nat Geosci, 7, 874-878, 10.1038/NGEO2290.

Bamber, J. L., et al. 2013. A new bed elevation dataset for Greenland. Cryosphere, 7, 499-510.

Banwell, A. F., MacAyeal, D. R., and Sergienko, O. V. 2013. Breakup of the Larsen B Ice Shelf triggered by chain reaction drainage of supraglacial lakes, Geophys Res Lett, 40, 5872-5876, 10.1002/2013GL057694.

Barrett, P. J. 2013. Resolving views on Antarctic Neogene glacial history - the Sirius debate. *Earth and Environmental Science Transactions of the Royal Society of Edinburgh,* 104**,** 31-53.

Bassis, J. N., and Jacobs, S. 2013. Diverse calving patterns linked to glacier geometry, Nat Geosci, 6, 833-836, 10.1038/NGEO1887.

Benn, D. I., Warren, C. R. & Mottram, R. H. 2007. Calving processes and the dynamics of calving glaciers. *Earth-Science Reviews,* 82**,** 143-179.

Benn, D. I., Warren, C. R., and Mottram, R. H. 2007. Calving processes and the dynamics of calving glaciers, Earth-Sci Rev, 82, 143-179, 10.1016/j.earscirev.2007.02.002.

Berger, S., et al. 2017. Detecting high spatial variability of ice-shelf basal mass balance (Roi Baudouin ice shelf, Antarctica). The Cryosphere Discuss., 2017, 1-22.

Bintanja, R., et al. 2013. Important role for ocean warming and increased ice-shelf melt in Antarctic sea-ice expansion. *Nature Geoscience,* 6**,** 376-379.

Carr, J. R., Vieli, A. & Stokes, C. 2013. Influence of sea ice decline, atmospheric warming, and glacier width on marine-terminating outlet glacier behavior in northwest Greenland at seasonal to interannual timescales. *Journal of Geophysical Research-Earth Surface,* 118**,** 1210-1226.

Cassotto, R., Fahnestock, M., Amundson, J. M., Truffer, M., and Joughin, I. 2015. Seasonal and interannual variations in ice melange and its impact on terminus stability, Jakobshavn Isbrae, Greenland, J Glaciol, 61, 76-88, 10.3189/2015JoG13J235.

Chapuis, A., and Tetzlaff, T. 2014. The variability of tidewater-glacier calving: origin of event-size and interval distributions, J Glaciol, 60, 622-634, 10.3189/2014JoG13J215.

Comiso, J. C. 2014. 'Bootstrap Sea Ice Concentrations from Nimbus-7 SMMR and DMSP SSM/I-SSMIS. Version 2', *Boulder, Colorado USA: NASA National Snow and Ice Data Center Distributed Active Archive Center.*

Cook, A. J., Fox, A. J., Vaughan, D. G. and Ferrigno, J. G. 2005. 'Retreating Glacier Fronts on the Antarctic Peninsula over the Past Half-Century', *Science*, 308(5721), 541-544.

Cook, C. P., et al. 2013. Dynamic behaviour of the East Antarctic ice sheet during Pliocene warmth. Nature Geoscience, 6, 765-769.

Cook, C. P., Hill, D. J., van de Flierdt, T., Williams, T., Hemming, S. R., Dolan, A. M., Pierce, E. L., Escutia, C., Harwood, D., Cortese, G., and Gonzales, J. J. 2014. Sea surface temperature control on the distribution of far-traveled Southern Ocean ice-rafted detritus during the Pliocene, Paleoceanography, 29, 533-548, Doi 10.1002/2014pa002625.

Crespin, J., et al. 2014. Holocene glacial discharge fluctuations and recent instability in East Antarctica. *Earth and Planetary Science Letters,* 394**,** 38-47.

Curran, M. A. J., et al. 2003. Ice core evidence for Antarctic sea ice decline since the 1950s. *Science,* 302**,** 1203-1206.

Davis, C. H., et al. 2005. Snowfall-driven growth in East Antarctic ice sheet mitigates recent sea-level rise. *Science,* 308**,** 1898-1901.

De Angelis, H. & Skvarca, P. 2003. Glacier surge after ice shelf collapse. *Science,* 299**,** 1560-1562.

De Angelis, H., and Skvarca, P. 2003. Glacier surge after ice shelf collapse, Science, 299, 1560-1562, DOI 10.1126/science.1077987.

DeConto, R. M., and Pollard, D. 2016. Contribution of Antarctica to past and future sea-level rise, Nature, 531, 591-+, 10.1038/nature17145.

Dee, D. P., Uppala, S. M., Simmons, A. J., Berrisford, P., Poli, P., Kobayashi, S., Andrae, U., Balmaseda, M. A., Balsamo, G., Bauer, P., Bechtold, P., Beljaars, A. C. M., van de Berg, L.,

Bidlot, J., Bormann, N., Delsol, C., Dragani, R., Fuentes, M., Geer, A. J., Haimberger, L., Healy, S. B., Hersbach, H., Holm, E. V., Isaksen, L., Kallberg, P., Kohler, M., Matricardi, M., McNally, A. P., Monge-Sanz, B. M., Morcrette, J. J., Park, B. K., Peubey, C., de Rosnay, P., Tavolato, C., Thepaut, J. N. and Vitart, F. 2011. 'The ERA-Interim reanalysis: configuration and performance of the data assimilation system', *Quarterly Journal of the Royal Meteorological Society*, 137(656), 553-597.

Denton, G., Sugden, D., Marchant, D., Hall, B., & Wilch, T. 1993. East Antarctic Ice Sheet Sensitivity to Pliocene Climatic Change from a Dry Valleys Perspective. *Geografiska Annaler. Series A, Physical Geography*, *75*(4), 155-204. doi:10.2307/521200

Depoorter, M. A., Bamber, J. L., Griggs, J. A., Lenaerts, J. T. M., Ligtenberg, S. R. M., van den Broeke, M. R., and Moholdt, G. 2013. Calving fluxes and basal melt rates of Antarctic ice shelves, Nature, 502, 89-+, Doi 10.1038/Nature12567.

Dowsett, H. J. & Cronin, T. M. 1990. High Eustatic Sea-Level during the Middle Pliocene - Evidence from the Southeastern United-States Atlantic Coastal-Plain. Geology, 18, 435-438.

Dupont, T. K. and Alley, R. B. 2005. 'Assessment of the importance of ice-shelf buttressing to ice-sheet flow', *Geophysical Research Letters*, 32(4).

Dutrieux, P., De Rydt, J., Jenkins, A., Holland, P. R., Ha, H. K., Lee, S. H., Steig, E. J., Ding, Q. H., Abrahamsen, E. P. and Schroder, M. 2014. 'Strong Sensitivity of Pine Island Ice-Shelf Melting to Climatic Variability', *Science*, 343(6167), 174-178.

Dutrieux, P., et al. 2013. Pine Island glacier ice shelf melt distributed at kilometre scales. Cryosphere, 7, 1543-1555.

Dutton, A., Carlson, A. E., Long, A. J., Milne, G. A., Clark, P. U., DeConto, R., Horton, B. P., Rahmstorf, S. and Raymo, M. E. 2015. 'Sea-level rise due to polar ice-sheet mass loss during past warm periods', *Science*, 349(6244), 153-+.

Ehn, J. K., Mundy, C. J., Barber, D. G., Hop, H., Rossnagel, A., and Stewart, J. 2011. Impact of horizontal spreading on light propagation in melt pond covered seasonal sea ice in the Canadian Arctic, J Geophys Res-Oceans, 116, Artn C00g02 10.1029/2010jc006908.

Favier, L., et al. 2014. Retreat of Pine Island Glacier controlled by marine ice-sheet instability. Nature Climate Change, 4, 117-121.

Flament, T. & Remy, F. 2012. Dynamic thinning of Antarctic glaciers from along-track repeat radar altimetry. *Journal of Glaciology*, 58**,** 830-840.

Flament, T., Berthier, E. & Remy, F. 2014. Cascading water underneath Wilkes Land, East Antarctic ice sheet, observed using altimetry and digital elevation models. *Cryosphere*, 8**,** 673-687.

Flocco, D., Feltham, D. L., Bailey, E., and Schroeder, D. 2015. The refreezing of melt ponds on Arctic sea ice, J Geophys Res-Oceans, 120, 647-659, 10.1002/2014JC010140.

Fogt, R. L., et al. 2009. Historical SAM Variability. Part II: Twentieth-Century Variability and Trends from Reconstructions, Observations, and the IPCC AR4 Models. *Journal of Climate*, 22**,** 5346-5365.

Fraser, A. D., Massom, R. A., Michael, K. J., Galton-Fenzi, B. K., and Lieser, J. L. 2012. East Antarctic Landfast Sea Ice Distribution and Variability, 2000-08, J Climate, 25, 1137-1156, 10.1175/Jcli-D-10-05032.1.

Fretwell, P., et al. 2013. Bedmap2: improved ice bed, surface and thickness datasets for Antarctica. *Cryosphere,* 7**,** 375-393.

Frezzotti, M. 1997. Ice front fluctuation, iceberg calving flux and mass balance of Victoria Land glaciers. *Antarctic Science,* 9**,** 61-73.

Frezzotti, M., and Polizzi, M. 2002. 50 years of ice-front changes between the Ade´lie and Banzare Coasts, East Antarctica, Ann Glaciol, 34, 235-240, 10.3189/172756402781817897.

Frezzotti, M., Cimbelli, A. & Ferrigno, J. G. 1998. Ice-front change and iceberg behaviour along Oates and George V Coasts, Antarctica, 1912-96. *Annals of Glaciology, Vol 27, 1998,* 27**,** 643-650.

Fürst, J.J., Durand, G., Gillet-Chaulet, F., Tavard, L., Rankl, M., Braun, M., and Gagliardini, O. 2016. The safety band of Antarctic ice shelves. Nature. Clim. Chan., 6, 479-481

Gagliardini, O., et al. 2010. Coupling of ice-shelf melting and buttressing is a key process in ice-sheets dynamics. *Geophysical Research Letters,* 37.

Golledge, N. R., et al. 2015. The multi-millennial Antarctic commitment to future sea-level rise. *Nature,* 526**,** 421-+.

Good, S. A., Martin, M. J. and Rayner, N. A. 2013. 'EN4: Quality controlled ocean temperature and salinity profiles and monthly objective analyses with uncertainty estimates', *Journal of Geophysical Research-Oceans,* 118(12), 6704-6716.

Greenbaum, J. S., Blankenship, D. D., Young, D. A., Richter, T. G., Roberts, J. L., Aitken, A. R. A., Legresy, B., Schroeder, D. M., Warner, R. C., van Ommen, T. D., and Siegert, M. J. 2015. Ocean access to a cavity beneath Totten Glacier in East Antarctica, Nat Geosci, 8, 294-298, 10.1038/NGEO2388.

Gwyther, D. E., Galton-Fenzi, B. K., Hunter, J. R. and Roberts, J. L. 2014. 'Simulated melt rates for the Totten and Dalton ice shelves', *Ocean Science,* 10(3), 267-279.

Harwood, D.M. and Webb, P.N., 1998. Glacial transport of diatoms in the Antarctic Sirius Group: Pliocene refrigerator. GSA Today, 8(4), pp.1-8.

Haywood, A. M., et al. 2013. Large-scale features of Pliocene climate: results from the Pliocene Model Intercomparison Project. Climate of the Past, 9, 191-209.

Heid, T. & Kaab, A. 2012. Evaluation of existing image matching methods for deriving glacier surface displacements globally from optical satellite imagery. *Remote Sensing of Environment,* 118**,** 339-355.

Heil, P. 2006. Atmospheric conditions and fast ice at Davis, East Antarctica: A case study, J Geophys Res-Oceans, 111, Artn C05009 10.1029/2005jc002904.

Hellmer, H. H., et al. 2012. Twenty-first-century warming of a large Antarctic ice-shelf cavity by a redirected coastal current. Nature, 485, 225-228.

Helm, V., Humbert, A. & Miller, H. 2014. Elevation and elevation change of Greenland and Antarctica derived from CryoSat-2. *Cryosphere,* 8**,** 1539-1559.

Herraiz-Borreguero, L., et al. 2016. Basal melt, seasonal water mass transformation, ocean current variability, and deep convection processes along the Amery Ice Shelf calving front, East Antarctica. *Journal of Geophysical Research-Oceans,* 121**,** 4946-4965.

Holland, P. R., Jenkins, A. and Holland, D. M. 2010. 'Ice and ocean processes in the Bellingshausen Sea, Antarctica', *Journal of Geophysical Research: Oceans,* 115(C5), C05020.

Howat, I. M., Joughin, I. & Scambos, T. A. 2007. Rapid changes in ice discharge from Greenland outlet glaciers. *Science,* 315**,** 1559-1561.

Hughes, T. J. 1981. The Weak Underbelly of the West Antarctic Ice-Sheet. *Journal of Glaciology,* 27**,** 518-525.

Huybrechts, P. 2002. Sea-level changes at the LGM from ice-dynamic reconstructions of the Greenland and Antarctic ice sheets during the glacial cycles. Quaternary Science Reviews, 21, 203-231.

Huybrechts, P., 1993. Glaciological modelling of the Late Cenozoic East Antarctic ice sheet: stability or dynamism?. Geografiska Annaler. Series A. Physical Geography, pp.221-238.

Intergovernmental Panel on Climate Change, 1991. *Climate change: The IPCC response strategies*. Island Press.

IPCC, 2013: climate change 2013: the physical science basis. Contribution of working group I to the fifth assessment report of the intergovernmental panel on climate change.

Jamieson, S. S. R., et al. 2012. Ice-stream stability on a reverse bed slope. Nature Geoscience, 5, 799-802.

Jamieson, S. S. R., et al. 2016. An extensive subglacial lake and canyon system in Princess Elizabeth Land, East Antarctica. Geology, 44, 87-90.

Jenkins, A., et al. 2010. Observations beneath Pine Island Glacier in West Antarctica and implications for its retreat. *Nature Geoscience,* 3**,** 468-472.

Jones, R. S., et al. 2015. Rapid Holocene thinning of an East Antarctic outlet glacier driven by marine ice sheet instability. Nature Communications, 6.

Joughin, I. & Padman, L. 2003. Melting and freezing beneath Filchner-Ronne Ice Shelf, Antarctica. *Geophysical Research Letters,* 30.

Joughin, I. and Alley, R. B. 2011. 'Stability of the West Antarctic ice sheet in a warming world', *Nature Geoscience,* 4(8), 506-513.

Joughin, I., Alley, R. B. & Holland, D. M. 2012. Ice-Sheet Response to Oceanic Forcing. *Science,* 338**,** 1172-1176.

Joughin, I., Smith, B. E. & Medley, B. 2014. Marine Ice Sheet Collapse Potentially Under Way for the Thwaites Glacier Basin, West Antarctica. *Science,* 344**,** 735-738.

Kellogg, D. E. & Kellogg, T. B. 1996. Diatoms in South Pole ice: Implications for eolian contamination of Sirius Group deposits. Geology, 24, 115-118.

Khazendar, A., Rignot, E., and Larour, E. 2009. Roles of marine ice, rheology, and fracture in the flow and stability of the Brunt/Stancomb-Wills Ice Shelf, J Geophys Res-Earth, 114, Artn F04007 10.1029/2008jf001124.

Khazendar, A., Schodlok, M. P., Fenty, I., Ligtenberg, S. R. M., Rignot, E. and van den Broeke, M. R. 2013. 'Observed thinning of Totten Glacier is linked to coastal polynya variability', *Nature Communications*, 4.

Kim, K., Jezek, K. C., and Liu, H. 2007. Orthorectified image mosaic of Antarctica from 1963 Argon satellite photography: image processing and glaciological applications, Int J Remote Sens, 28, 5357-5373.

King, M. A., Bingham, R. J., Moore, P., Whitehouse, P. L., Bentley, M. J., and Milne, G. A. 2012. Lower satellite-gravimetry estimates of Antarctic sea-level contribution, Nature, 491, 586-+, Doi 10.1038/Nature11621.

Kingslake, J., Ng, F., and Sole, A. 2015. Modelling channelized surface drainage of supraglacial lakes. J. Glaciol., 61 (225), 185-199.

Kitade, Y., Shimada, K., Tamura, T., Williams, G. D., Aoki, S., Fukamachi, Y., Roquet, F., Hindell, M., Ushio, S. and Ohshima, K. I. 2014. 'Antarctic Bottom Water production from the Vincennes Bay Polynya, East Antarctica', *Geophysical Research Letters*, 41(10), 3528-3534.

Krantz, D. E. 1991. A Chronology of Pliocene Sea-Level Fluctuations - the United-States Middle Atlantic Coastal-Plain Record. Quaternary Science Reviews, 10, 163-174.

Kusahara, K., Hasumi, H. and Tamura, T. 2010. 'Modeling sea ice production and dense shelf water formation in coastal polynyas around East Antarctica', *Journal of Geophysical Research-Oceans*, 115.

Landy, J., Ehn, J., Shields, M., and Barber, D. 2014. Surface and melt pond evolution on landfast first-year sea ice in the Canadian Arctic Archipelago, J Geophys Res-Oceans, 119, 3054-3075, 10.1002/2013JC009617

Langhorne, P. J., Squire, V. A., Fox, C., and Haskell, T. G. 2001. Lifetime estimation for a land-fast ice sheet subjected to ocean swell, Annals of Glaciology, Vol 33, 33, 333-338, Doi 10.3189/172756401781818419.

Langlais, C. E., Rintoul, S. R., and Zika, J. D. 2015. Sensitivity of Antarctic Circumpolar Current Transport and Eddy Activity to Wind Patterns in the Southern Ocean, J Phys Oceanogr, 45, 1051-1067, 10.1175/Jpo-D-14-0053.1.

Langley, E.S., Leeson, A.A., Stokes, C.R., and Jamieson, S.S.R. 2016. Seasonal evolution of supraglacial lakes on an East Antarctic outlet glacier. Geophys. Res. Lett., 43, doi:10.1002/2016GL069511,

Lei, R. B., Li, Z. J., Cheng, B., Zhang, Z. H., and Heil, P. 2010. Annual cycle of landfast sea ice in Prydz Bay, east Antarctica, J Geophys Res-Oceans, 115, Artn C02006 10.1029/2008jc005223.

Lenaerts, J. T. M., et al. 2013. Recent snowfall anomalies in Dronning Maud Land, East Antarctica, in a historical and future climate perspective. *Geophysical Research Letters,* 40**,** 2684-2688.

Leprince, S., Ayoub, F., Klinger, Y. & Avouac, J. P. 2007. Co-Registration of Optically Sensed Images and Correlation (COSI-Corr): an operational methodology for ground deformation measurements. *Igarss: 2007 Ieee International Geoscience and Remote Sensing Symposium, Vols 1-12***,** 1943-+.

Li, X., et al. 2015. Grounding line retreat of Totten Glacier, East Antarctica, 1996 to 2013. Geophysical Research Letters, 42, 8049-8056.

Li, X., Rignot, E. & Mouginot, J. 2016. Ice flow dynamics and mass loss of Totten Glacier, East Antarctica, from 1989 to 2015. *Geophysical Research Letters,* 43**,** 6366-6373.

Liu, H. X., and Jezek, K. C. 2004. A complete high-resolution coastline of antarctica extracted from orthorectified Radarsat SAR imagery, Photogramm Eng Rem S, 70, 605-616.

Liu, Y., Moore, J. C., Cheng, X., Gladstone, R. M., Bassis, J. N., Liu, H., Wen, J. and Hui, F. 2015. 'Ocean-driven thinning enhances iceberg calving and retreat of Antarctic ice shelves', *Proceedings of the National Academy of Sciences,* 112(11), 3263-3268.

Lovell, A., Stokes, C., & Jamieson, S. 2017. Sub-decadal variations in outlet glacier terminus positions in Victoria Land, Oates Land and George V Land, East Antarctica (1972–2013). Antarctic Science, 1-16. doi:10.1017/S0954102017000074

MacGregor, J. A., Catania, G. A., Markowski, M. S. and Andrews, A. G. 2012. 'Widespread rifting and retreat of ice-shelf margins in the eastern Amundsen Sea Embayment between 1972 and 2011', *Journal of Glaciology,* 58(209), 458-466.

Mackintosh, A. N., et al. 2017. Regional cooling caused recent New Zealand glacier advances in a period of global warming. *Nature Communications,* 8.

Mahoney, A., Eicken, H., Gaylord, A. G., and Shapiro, L. 2007. Alaska landfast sea ice: Links with bathymetry and atmospheric circulation, J Geophys Res-Oceans, 112, Artn C02001 10.1029/2006jc003559

Makinson, K. & Nicholls, K. W. 1999. Modeling tidal currents beneath Filchner-Ronne Ice Shelf and on the adjacent continental shelf: their effect on mixing and transport. *Journal of Geophysical Research-Oceans,* 104**,** 13449-13465.

Maqueda, M. A. M., Willmott, A. J. and Biggs, N. R. T. 2004. 'Polynya dynamics: A review of observations and modeling', *Reviews of Geophysics,* 42(1).

Marshall, G. J., Orr, A. & Turner, J. 2013. A Predominant Reversal in the Relationship between the SAM and East Antarctic Temperatures during the Twenty-First Century. Journal of Climate, 26, 5196-5204.

Marshall, G. J. 2007. Half-century seasonal relationships between the Southern Annular Mode and Antarctic temperatures, Int J Climatol, 27, 373-383, 10.1002/joc.1407.

Marshall, G. J. 2003. Trends in the southern annular mode from observations and reanalyses, J Climate, 16, 4134-4143, Doi 10.1175/1520-0442(2003)016<4134:Titsam>2.0.Co;2.

Martin-Espanol, A., Bamber, J. L. & Zammit-Mangion, A. 2017. Constraining the mass balance of East Antarctica. *Geophysical Research Letters,* 44**,** 4168-4175.

Massom, R. A., Giles, A. B., Warner, R. C., Fricker, H. A., Legresy, B., Hyland, G., Lescarmontier, L., and Young, N. 2015. External influences on the Mertz Glacier Tongue (East Antarctica) in the decade leading up to its calving in 2010, J Geophys Res-Earth, 120, 490-506, 10.1002/2014JF003223.

Massom, R., et al. 2013. Change and Variability in East Antarctic Sea Ice Seasonality, 1979/80–2009/10. *PLoS ONE,* 8**,** e64756.

Mayewski, P. A., et al. 2015. Potential for Southern Hemisphere climate surprises. *Journal of Quaternary Science,* 30**,** 391-395.

McMillan, M., et al. 2013. Three-dimensional mapping by CryoSat-2 of subglacial lake volume changes. *Geophysical Research Letters,* 40**,** 4321-4327.

McMillan, M., Shepherd, A., Sundal, A., Briggs, K., Muir, A., Ridout, A., Hogg, A., and Wingham, D. 2014. Increased ice losses from Antarctica detected by CryoSat-2, Geophys Res Lett, 41, 3899-3905, Doi 10.1002/2014gl060111.

Meehl, G. A., et al. 2016. Antarctic sea-ice expansion between 2000 and 2014 driven by tropical Pacific decadal climate variability. *Nature Geoscience,* 9**,** 590-+.

Mengel, M. & Levermann, A. 2014. Ice plug prevents irreversible discharge from East Antarctica. Nature Climate Change, 4, 451-455.

Mercer, J. H. 1978. West Antarctic Ice Sheet and Co2 Greenhouse Effect - Threat of Disaster. Nature, 271, 321-325.

Miles, B. W. J., Stokes, C. R. & Jamieson, S. S. R. 2017. Simultaneous disintegration of outlet glaciers in Porpoise Bay (Wilkes Land), East Antarctica, driven by sea ice break-up. *The Cryosphere,* 11**,** 427-442.

Miles, B. W. J., Stokes, C. R., and Jamieson, S. S. R. 2016. Pan–ice-sheet glacier terminus change in East Antarctica reveals sensitivity of Wilkes Land to sea ice changes, Science Advances, 2, 10.1126/sciadv.1501350.

Miles, B. W. J., Stokes, C. R., Vieli, A., and Cox, N. J. 2013. Rapid, climate-driven changes in outlet glaciers on the Pacific coast of East Antarctica, Nature, 500, 563-+, Doi 10.1038/Nature12382.

Miller, K. G., et al. 2012. High tide of the warm Pliocene: Implications of global sea level for Antarctic deglaciation. Geology, 40, 407-410.

Miller, M.F. and Mabin, M.C.G., 1998. Antarctic Neogene landscapes—in the refrigerator or in the deep freeze. *GSA Today*, *8*(4), pp.1-3.

Moon, T. and Joughin, I. (2008) 'Changes in ice front position on Greenland's outlet glaciers from 1992 to 2007', *Journal of Geophysical Research-Earth Surface,* 113(F2).

Moon, T., and Joughin, I. 2008. Changes in ice front position on Greenland's outlet glaciers from 1992 to 2007, J Geophys Res-Earth, 113, Artn F02022 Doi 10.1029/2007jf000927..

Moon, T., et al. 2014. Distinct patterns of seasonal Greenland glacier velocity. Geophysical Research Letters, 41, 7209-7216.

Neumann, B., Vafeidis, A. T., Zimmermann, J. & Nicholls, R. J. 2015. Future Coastal Population Growth and Exposure to Sea-Level Rise and Coastal Flooding - A Global Assessment (vol 10, e0118571, 2015). *Plos One,* 10.

Nick, F. M., et al. 2013. Future sea-level rise from Greenland's main outlet glaciers in a warming climate. *Nature,* 497**,** 235-238.

Nick, F. M., Vieli, A., Howat, I. M. & Joughin, I. 2009. Large-scale changes in Greenland outlet glacier dynamics triggered at the terminus. *Nature Geoscience,* 2**,** 110-114.

Paolo, F. S., Fricker, H. A. & Padman, L. 2015. Volume loss from Antarctic ice shelves is accelerating. *Science*.

Parkinson, C. L. & Cavalieri, D. J. 2012. Antarctic sea ice variability and trends, 1979-2010. *Cryosphere,* 6**,** 871-880.

Parkinson, C. L., J. C. Comiso, and H. J. Zwally. 1999, updated 2004. *Nimbus-5 ESMR Polar Gridded Sea Ice Concentrations*. Edited by W. Meier and J. Stroeve. Boulder, Colorado USA: National Snow and Ice Data Center. Digital media.

Payne, A. J., et al. 2004. Recent dramatic thinning of largest West Antarctic ice stream triggered by oceans. *Geophysical Research Letters,* 31.

Petrich, C., Eicken, H., Polashenski, C. M., Sturm, M., Harbeck, J. P., Perovich, D. K., and Finnegan, D. C. 2012. Snow dunes: A controlling factor of melt pond distribution on Arctic sea ice, J Geophys Res-Oceans, 117, Artn C0902910.1029/2012jc008192

Petty, A. A., Holland, P. R. and Feltham, D. L. 2014 'Sea ice and the ocean mixed layer over the Antarctic shelf seas', *Cryosphere,* 8(2), 761-783.

Phillips, H. A. 1998. Surface meltstreams on the Amery Ice Shelf, East Antarctica. Annals of Glaciology, Vol 27, 1998, 27, 177-181.

Pollard, D., DeConto, R. M. & Alley, R. B. 2015. Potential Antarctic Ice Sheet retreat driven by hydrofracturing and ice cliff failure. Earth and Planetary Science Letters, 412, 112-121.

Pollard, D., DeConto, R. M. & Nyblade, A. A. 2005. Sensitivity of Cenozoic Antarctic ice sheet variations to geothermal heat flux. Global and Planetary Change, 49, 63-74.

Pollard, D., DeConto, R. M. and Alley, R. B. 2015 'Potential Antarctic Ice Sheet retreat driven by hydrofracturing and ice cliff failure', *Earth and Planetary Science Letters,* 412, 112-121.

Pritchard, H. D., Arthern, R. J., Vaughan, D. G. & Edwards, L. A. 2009. Extensive dynamic thinning on the margins of the Greenland and Antarctic ice sheets. Nature, 461, 971-975.

Pritchard, H. D., et al. 2012. Antarctic ice-sheet loss driven by basal melting of ice shelves. *Nature,* 484**,** 502-505.

Raphael, M. N. 2004. A zonal wave 3 index for the Southern Hemisphere. *Geophysical Research Letters,* 31.

Raymo, M. E., et al. 2011. Departures from eustasy in Pliocene sea-level records. Nature Geoscience, 4, 328-332.

Rignot, E. & Kanagaratnam, P. 2006. Changes in the velocity structure of the Greenland ice sheet. *Science,* 311**,** 986-990.

Rignot, E. 2006. Changes in ice dynamics and mass balance of the Antarctic ice sheet. *Philosophical Transactions of the Royal Society a-Mathematical Physical and Engineering Sciences,* 364**,** 1637-1655.

Rignot, E., Casassa, G., Gogineni, P., Krabill, W., Rivera, A., and Thomas, R. 2004. Accelerated ice discharge from the Antarctic Peninsula following the collapse of Larsen B ice shelf, Geophys Res Lett, 31, Artn L1840110.1029/2004gl020697.

Rignot, E., et al. 2011a. Acceleration of the contribution of the Greenland and Antarctic ice sheets to sea level rise. *Geophysical Research Letters,* 38.

Rignot, E., Jacobs, S., Mouginot, J., and Scheuchl, B. 2013. Ice-Shelf Melting Around Antarctica, Science, 341, 266-270, DOI 10.1126/science.1235798.

Rignot, E., Mouginot, J. & Scheuchl, B. 2011c. Antarctic grounding line mapping from differential satellite radar interferometry. *Geophysical Research Letters,* 38.

Rignot, E., Mouginot, J., and Scheuchl, B. 2011b. Ice Flow of the Antarctic Ice Sheet, Science, 333, 1427-1430, 10.1126/science.1208336..

Rintoul, S. R., et al. 2016. Ocean heat drives rapid basal melt of the Totten Ice Shelf. Science Advances, 2.

Ritz, C., et al. 2015. Potential sea-level rise from Antarctic ice-sheet instability constrained by observations. *Nature,* 528**,** 115-+.

Ritz, C., Rommelaere, V. & Dumas, C. 2001. Modeling the evolution of Antarctic ice sheet over the last 420,000 years: Implications for altitude changes in the Vostok region. Journal of Geophysical Research-Atmospheres, 106, 31943-31964.

Robel, A. A. 2017. Thinning sea ice weakens buttressing force of iceberg melange and promotes calving. Nature Communications, 8.

Rott, H., Rack, W., Skvarca, P., and De Angelis, H. 2002. Northern Larsen Ice Shelf, Antarctica: further retreat after collapse, Annals of Glaciology, Vol 34, 2002, 34, 277-282, Doi 10.3189/172756402781817716.

Rott, H., Skvarca, P., and Nagler, T. 1996. Rapid collapse of northern Larsen Ice Shelf, Antarctica, Science, 271, 788-792, DOI 10.1126/science.271.5250.788.

Sasgen, I., Konrad, H., Ivins, E. R., Van den Broeke, M. R., Bamber, J. L., Martinec, Z., and Klemann, V. 2013. Antarctic ice-mass balance 2003 to 2012: regional reanalysis of GRACE satellite gravimetry measurements with improved estimate of glacial-isostatic adjustment based on GPS uplift rates, Cryosphere, 7, 1499-1512, DOI 10.5194/tc-7-1499-2013.

Scambos, T. A., Berthier, E. & Shuman, C. A. 2011. The triggering of subglacial lake drainage during rapid glacier drawdown: Crane Glacier, Antarctic Peninsula. *Annals of Glaciology*, 52**,** 74-82.

Scambos, T. A., Bohlander, J. A., Shuman, C. A. & Skvarca, P. 2004. Glacier acceleration and thinning after ice shelf collapse in the Larsen B embayment, Antarctica. *Geophysical Research Letters,* 31.

Scambos, T., Fricker, H. A., Liu, C. C., Bohlander, J., Fastook, J., Sargent, A., Massom, R., and Wu, A. M. 2009. Ice shelf disintegration by plate bending and hydro-fracture: Satellite observations and model results of the 2008 Wilkins ice shelf break-ups, Earth Planet Sc Lett, 280, 51-60, 10.1016/j.epsl.2008.12.027.

Scambos, T., Hulbe, C., and Fahnestock, M. 2003. Climate-induced ice shelf disintegration in the Antarctic Peninsula, Antarct Res Ser, 79, 79-92.

Scherler, D., Leprince, S. & Strecker, M. R. 2008. Glacier-surface velocities in alpine terrain from optical satellite imagery - Accuracy improvement and quality assessment. *Remote Sensing of Environment*, 112**,** 3806-3819.

Schneider, D. P. & Steig, E. J. 2008. Ice cores record significant 1940s Antarctic warmth related to tropical climate variability. *Proceedings of the National Academy of Sciences of the United States of America,* 105**,** 12154-12158.

Schoof, C. 2007. Ice sheet grounding line dynamics: Steady states, stability, and hysteresis. Journal of Geophysical Research-Earth Surface, 112.

Schroder, D., Feltham, D. L., Flocco, D., and Tsamados, M. 2014. September Arctic sea ice minimum predicted by spring melt-pond fraction, Nat Clim Change, 4, 353-357, 10.1038/Nclimate2203

Shepherd, A. & Wingham, D. 2007. Recent sea-level contributions of the Antarctic and Greenland ice sheets. *Science,* 315**,** 1529-1532.

Shepherd, A. & Wingham, D. 2008. Antarctic glacier thinning, 1992-2003. *Scottish Geographical Journal,* 124**,** 154-164.

Shepherd, A., et al. 2012. A Reconciled Estimate of Ice-Sheet Mass Balance. *Science,* 338**,** 1183-1189.

Siegfried, M. R., Fricker, H. A., Carter, S. P. & Tulaczyk, S. 2016. Episodic ice velocity fluctuations triggered by a subglacial flood in West Antarctica. *Geophysical Research Letters,* 43**,** 2640-2648.

Silvano, A., Rintoul, S. R. & Herraiz-Borreguero, L. 2016. Ocean-Ice Shelf Interaction in East Antarctica. *Oceanography,* 29**,** 130-143.

Silvano, A., Rintoul, S. R., Pena-Molino, B. & Williams, G. D. 2017. Distribution of water masses and meltwater on the continental shelf near the Totten and Moscow University ice shelves. *Journal of Geophysical Research-Oceans,* 122**,** 2050-2068.

Smith, J. A., et al. 2017. Sub-ice-shelf sediments record history of twentieth-century retreat of Pine Island Glacier. *Nature,* 541**,** 77-+.

Spreen, G., Kaleschke, L., and Heygster, G. 2008. Sea ice remote sensing using AMSR-E 89-GHz channels, J Geophys Res-Oceans, 113, Artn C02s0310.1029/2005jc003384

Stearns, L. A., Smith, B. E. & Hamilton, G. S. 2008. Increased flow speed on a large East Antarctic outlet glacier caused by subglacial floods. Nature Geoscience, 1, 827-831.

Stroeven, A. P., Prentice, M. L. & Kleman, J. 1996. On marine microfossil transport and pathways in Antarctica during the late Neogene: Evidence from the Sirius group at Mount Fleming. Geology, 24, 727-730.

Stroeven, A.P., Burckle, L.H., Kleman, J. and Prentice, M.L., 1998. Atmospheric transport of diatoms in the Antarctic Sirius Group: Pliocene deep freeze. GSA Today, 8(4), pp.1-5.

Sugden, D., Marchant, D., & Denton, G. 1993. The Case for a Stable East Antarctic Ice Sheet: The Background. *Geografiska Annaler. Series A, Physical Geography, 75*(4), 151-154. doi:10.2307/521199

Sugimoto, F., Tamura, T., Shimoda, H., Uto, S., Simizu, D., Tateyama, K., Hoshino, S., Ozeki, T., Fukamachi, Y., Ushio, S., and Ohshima, K. I. 2016. Interannual variability in sea ice thickness in the pack-ice zone off Lutzow-Holm Bay, East Antarctica, Polar Sci, 10, 43-51, 10.1016/j.polar.2015.10.003.

Tamura, T., Ohshima, K. I. and Nihashi, S. 2008 'Mapping of sea ice production for Antarctic coastal polynyas', *Geophysical Research Letters,* 35(7).

Tamura, T., Williams, G. D., Fraser, A. D. & Ohshima, K. I. 2012. Potential regime shift in decreased sea ice production after the Mertz Glacier calving. *Nature Communications,* 3.

Tedstone, A. J., et al. 2015. Decadal slowdown of a land-terminating sector of the Greenland Ice Sheet despite warming. Nature, 526, 692-695.

Thoma, M., Jenkins, A., Holland, D. and Jacobs, S. 2008 'Modelling Circumpolar Deep Water intrusions on the Amundsen Sea continental shelf, Antarctica', *Geophysical Research Letters,* 35(18).

Thompson, D. W. J. & Solomon, S. 2002. Interpretation of recent Southern Hemisphere climate change. *Science,* 296**,** 895-899.

Thompson, D. W. J., et al. 2011. Signatures of the Antarctic ozone hole in Southern Hemisphere surface climate change. *Nature Geoscience,* 4**,** 741-749.

Timmermann, R. & Hellmer, H. H. 2013. Southern Ocean warming and increased ice shelf basal melting in the twenty-first and twenty-second centuries based on coupled ice-ocean finite-element modelling. Ocean Dynamics, 63, 1011-1026.

Todd, J., and Christoffersen, P. 2014. Are seasonal calving dynamics forced by buttressing from ice melange or undercutting by melting? Outcomes from full-Stokes simulations of Store Glacier, West Greenland, Cryosphere, 8, 2353-2365, 10.5194/tc-8-2353-2014.

Trusel, L. D., et al. 2015. Divergent trajectories of Antarctic surface melt under two twenty-first-century climate scenarios. Nature Geoscience, 8, 927-U56.

Turner, J. 2004. The El Nino-southern oscillation and Antarctica. *International Journal of Climatology,* 24**,** 1-31.

Turner, J., et al. 2009. Non-annular atmospheric circulation change induced by stratospheric ozone depletion and its role in the recent increase of Antarctic sea ice extent. *Geophysical Research Letters,* 36.

Ushio, S. 2006. Factors affecting fast-ice break-up frequency in Lutzow-Holm bay, Antarctica, Annals of Glaciology, Vol 44, 2006, 44, 177-182, Doi 10.3189/172756406781811835

Van de Berg, W. J., Van den Broeke, M. R., Reijmer, C. H. & Van Meijgaard, E. 2005. Characteristics of the Antarctic surface mass balance, 1958-2002, using a regional atmospheric climate model. *Annals of Glaciology, Vol 41 2005,* 41**,** 97-104.

van den Broeke, M., et al. 2009. Partitioning Recent Greenland Mass Loss. Science, 326, 984-986.

van der Veen, C. J. 2002. Calving glaciers, Prog Phys Geog, 26, 96-122, 10.1191/0309133302pp327ra

van Ommen, T. D. & Morgan, V. 2010. Snowfall increase in coastal East Antarctica linked with southwest Western Australian drought. *Nature Geoscience,* 3**,** 267-272.

van Wessem, J. M., Reijmer, C. H., Morlighem, M., Mouginot, J., Rignot, E., Medley, B., Joughin, I., Wouters, B., Depoorter, M. A., Bamber, J. L., Lenaerts, J. T. M., van de Berg, W. J., van den Broeke, M. R., and van Meijgaard, E. 2014. Improved representation of East Antarctic surface mass balance in a regional atmospheric climate model, J Glaciol, 60, 761-770, 10.3189/2014JoG14J051

Vaughan, D. G. 2008. West Antarctic Ice Sheet collapse - the fall and rise of a paradigm. *Climatic Change,* 91**,** 65-79.

Wang, X., Holland, D. M., Cheng, X., and Gong, P. 2016. Grounding and Calving Cycle of Mertz Ice Tongue Revealed by Shallow Mertz Bank, The Cryosphere Discuss., 2016, 1-37, 10.5194/tc-2016-3

Webb, P. N. & Harwood, D. M. 1991. Late Cenozoic Glacial History of the Ross Embayment, Antarctica. Quaternary Science Reviews, 10, 215-223.

Webb, P. N., et al. 1984. Cenozoic Marine Sedimentation and Ice-Volume Variation on the East Antarctic Craton. Geology, 12, 287-291.

Webber, B. G. M., et al. 2017. Mechanisms driving variability in the ocean forcing of Pine Island Glacier. *Nature Communications,* 8.

Weertman, J. 1974. Stability of the Junction of an Ice Sheet and an Ice Shelf. *Journal of Glaciology, 13*(67), 3-11. doi:10.1017/S0022143000023327

Williams, S. D. P., Moore, P., King, M. A. & Whitehouse, P. L. 2014. Revisiting GRACE Antarctic ice mass trends and accelerations considering autocorrelation. *Earth and Planetary Science Letters,* 385**,** 12-21.

Williams, T., et al. 2010. Evidence for iceberg armadas from East Antarctica in the Southern Ocean during the late Miocene and early Pliocene. Earth and Planetary Science Letters, 290, 351-361.

Wuite, J., Rott, H., Hetzenecker, M., Floricioiu, D., De Rydt, J., Gudmundsson, G. H., Nagler, T., and Kern, M. 2015.: Evolution of surface velocities and ice discharge of Larsen B outlet glaciers from 1995 to 2013, Cryosphere, 9, 957-969, 10.5194/tc-9-957-2015

Yang, Y., Li, Z. J., Leppazranta, M., Cheng, B., Shi, L. Q., and Lei, R. B. 2016.: Modelling the thickness of landfast sea ice in Prydz Bay, East Antarctica, Antarct Sci, 28, 59-70, 10.1017/S0954102015000449

Young, D. A., Wright, A. P., Roberts, J. L., Warner, R. C., Young, N. W., Greenbaum, J. S., Schroeder, D. M., Holt, J. W., Sugden, D. E., Blankenship, D. D., van Ommen, T. D., and Siegert, M. J. 2011: A dynamic early East Antarctic Ice Sheet suggested by ice-covered fjord landscapes, Nature, 474, 72-75, 10.1038/nature10114.

Zwally, H. J. and Giovinetto, M. B. 2011. 'Overview and Assessment of Antarctic Ice-Sheet Mass Balance Estimates: 1992-2009', *Surveys in Geophysics,* 32(4-5), 351-376.

Zwally, H. J., et al. 2015. Mass gains of the Antarctic ice sheet exceed losses. *Journal of Glaciology,* 61**,** 1019-1036.